PREVENTING ELECTROMAGNETIC INTERFERENCE FROM INTEGRATED CIRCUITS AND PRINTED CIRCUIT BOARDS USING COMPUTER SIMULATION.

Author: Frank B.J. Leferink.
Report number: EL-BSC-92N138

Stud. nr.	:	8608113
Student	:	Frank B.J. Leferink
Period	:	December 1991 - July 1992
University	:	University of Twente
Faculty	:	Faculty of Electrical Engineering, Laboratory for Network Theory
Committee	:	Prof. Dr.-Ing. O.E. Herrmann Dr. Ir. A.C. Brombacher Dr. Ir. C.H. Slump Ir. M.J.C.M. van Doorn Ir. F.J.K. Buesink

ABSTRACT.

This report describes a simple but accurate method to calculate the electromagnetic radiation of a product in its development stage.
A main source of radiation is caused by the so called common mode currents. Another source of radiation, but in modern circuits smaller than the former one, is caused by differential mode current. Nearly all existing electromagnetic interference computer aided design programs are using only the differential mode currents which leads to awkward results.
In this report new models are developed to determine the ground lift voltage and the resulting common mode current.
Using these models it is possible to predict whether the product can fulfil the (legislative) requirements. Also quantitative choices are possible to fundate a specific technology such as multi-layer printed circuit boards.
Furthermore some new design rules for measures to prevent EMI are developed.

TABLE OF CONTENTS.

APPENDICES.

PREFACE.

This research is carried out in coöperation with Philips Consumer Electronics and the University of Twente. Furthermore my employer, Hollandse Signaalapparaten, is involved.

First of all I would like to thank my collegeas of Hollandse Signaalapparaten B.V. and especially my collegeas of the Laboratory for Physical Measurements for their support during my studying period as a working student. Without their help it would have been impossible to complete my study and this research. I would like to thank my manager Ben Puylaert for the interesting and open discussions, my collegeas Wim van Lenthe and Karel Ringenoldus and my former collegea Peter Suringa for the commitment they showed.
I would like to thank Dick Schuuring for the first impulses and Jan Raatgerink for the very constructive and pleasant discussions during my study. I would like to thank Rikus Eising for the approval to finish my study with a research project at another company although the sublect is supplementary to my daily work.

Furthermore I would like to thank Marcel van Doorn for the interesting discussions, the coöperation and all the correction and steering activities during this research.

Finally, but in the first place, I want to thank Anne-Marie for all those hours she was alone but never complained.

'...The first process therefore in the effectual study of the science, must be one of simplification and reduction of the results of previous investigations to a form in which the mind can grasp them. The results of this simplification may take the form of a purely mathematical formula or of a physical hypothesis. In the first case we entirely lose light of the phenomena to be explained; and though we may trace out the consequences of given laws, we never obtain more extended views of the connexions of the subject. If, on the other hand, we adopt a physical hypothesis, we see the phenomena only through a medium, and are liable to that blindness to facts and rashness in assumption which a partial explanation encourages.'
James Clerk Maxwell

'My neighbour has had a new heart pacemaker fitted.
Every time he makes love my garage doors open.'
Bob Hope
(both from Chatterton, 1992)

Models are to be used,
but not to be believed.
Henri Thiel.

Everything must be made as simple as possible,
but not simpler.
Albert Einstein.

1. INTRODUCTION.

Electromagnetic compatibility (EMC) is the ability of an electronic system to function properly in its intended environment without adding new disturbing signals to that environment.
For the description the term electromagnetic interference (EMI) is used because EMI describes the behaviour of the product itself while the often used term EMC describes the behaviour of the product with respect to its neighbour.

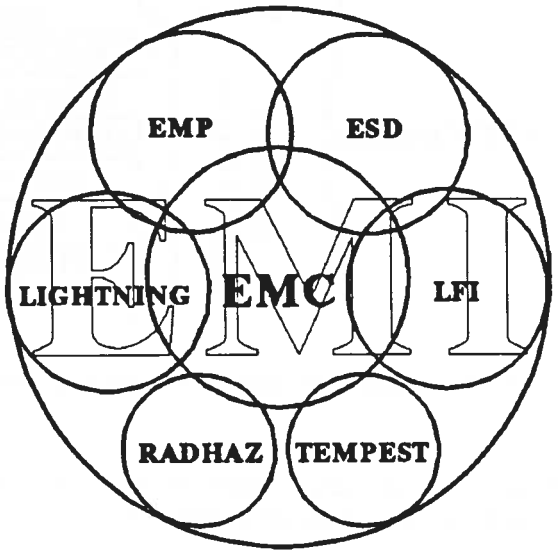

Figure 1.1: The electromagnetic environmental phenomena.

In general EMI describes several environmental effects such as:

* lightning,
* ESD (electro-static discharge),
* EMP (electromagnetic pulse),
* LFI (low frequency interference),
* RadHaz (radiation hazards, biological),
* Tempest (eavesdropping via EM radiation),

as drawn in Figure 1.1.
We are only interested in the EMI effects with respect to EMC, so the effects when one ore more electronic devices are concerned.

EMI can be divided into two parts: intra-EMI and inter-EMI.

* When a circuit does not function according to its specifications due to small disturbing voltages and currents developed by itself then we call this intra-EMI. Intra-EMI will be discussed in Chapter 3. Intra-EMI is the main cause of electromagnetic reliability problems in the design stage of a product.
* When a circuit radiates more electromagnetic energy than is allowed, via cables or directly by an electromagnetic field then we call this inter-EMI, which is discussed in Chapter 4.

To be cost-effective, EMI should be considered early in the design. A well known graph is given as Figure 1.2.

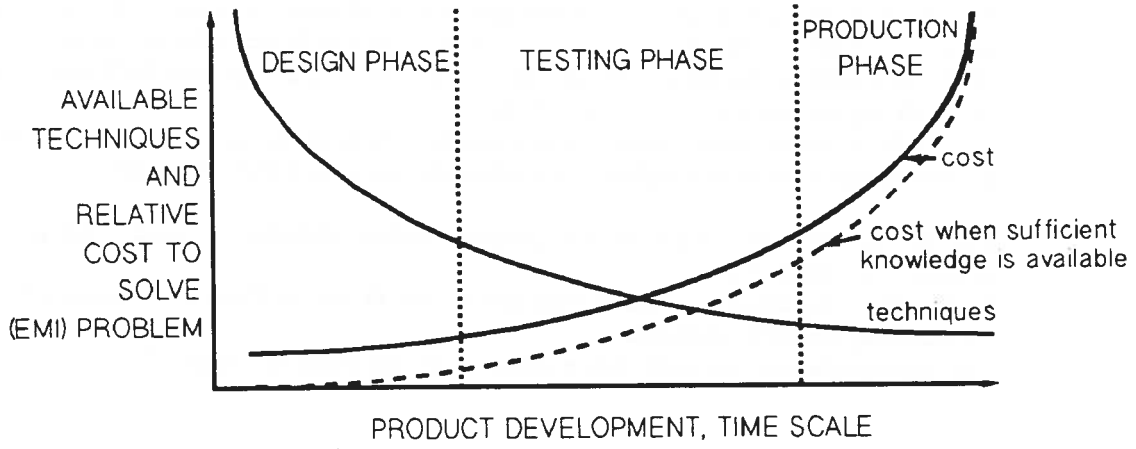

Figure 1.2: Cost effective design.

Contrarily to populair belief, EMI precautions can lower the total product cost when sufficient knowledge is available to tackle EMI problems in a very early stage, see Figure 1.2.

EMI is one of the additional requirements of a product, see Figure 1.3.
The order of the requirements in Figure 1.3. are subjective. in the last decade more and more legislative requirements are demanded.

Because the legislative requirements are tight for modern digital equipment we will use those requirements in this report as our starting-point.

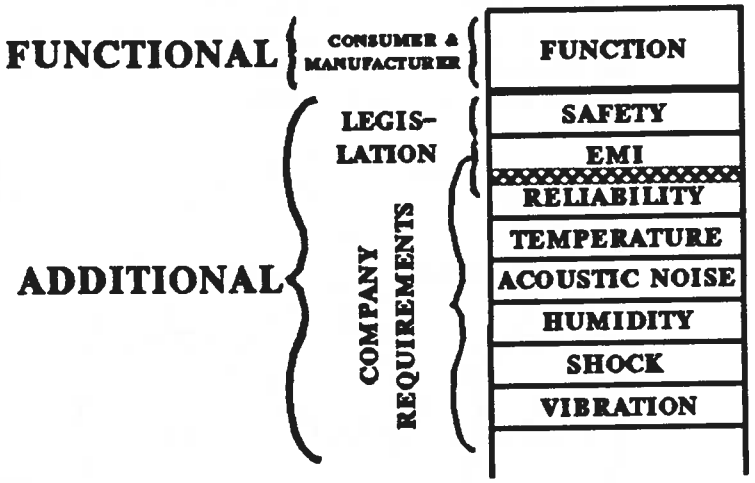

Figure 1.3: The functional and additional requirements of a product.

For the correct answer to the question of how any electric circuit behaves, Maxwell's equations must be solved. Solutions for any but the simplest problems are usually very complex. To avoid this complexity, an approximate circuit analysis technique is used during most design procedures.

Circuit analysis assumes the following:
- All electric fields are confined to the interiors of capacitors.
- All magnetic fields are confined to the interiors of inductors.
- Dimensions of the circuits are small compared to the wavelength under consideration.

For the circuit analysis we use models to simulate the actual circuit. When proper models are available then it is possible to predict the EMI behaviour already in the design stage of a new product. Until now there are no simple and accurate models to calculate the radiated emission. Only design rules, obtained from experience, are available. In Chapter 4 a new, simple but accurate, model is given.
This new model is the core of this research.

The above mentioned design rules cannot give any 'EMI value' or 'EMI performance' which can be used to fundate the choice for specific IC packages and PCB technologies (monolayer, multilayer). With the results of this study a choice can be made for IC packages and PCB technologies to meet the EMI requirements in a cost effective way.
Especially at this moment (1992) where legislative requirements are introduced in 1993 and digital IC technology tends to use higher frequencies, this research is very important.

For the calculations a sophisticated program, called MINNIE, is used. This program will be described in Chapter 2.
In Chapter 5 the theory is verified using several test PCB's. In Chapter 6 a general method is given for handling practical situations.
The conclusions and points for future research are described in Chapter 7.

2. THE SOFTWARE PROGRAM MINNIE.

The software program MINNIE[1] is an interactive tool for simulation of electronic circuits. It consists of three parts:

* An interactive schematic capture part with the possibility to define subcircuits.
* An analysis part, where the signals to be studied can be defined. The simulation then is carried out by another program.
* A result part. In this part it is possible to process the data using mathematical methods, and to display it in various graphical forms.

Furthermore, MINNIE has some special features. One feature is design centering. It is possible to perform Monte Carlo analysis with the goal to optimize a circuit towards its maximum performance. MINNIE provides a design centering algorithm for this optimization by comparing the simulation results with a given requirement.

The simulator used is the Philips Pstar[2] circuit simulator. This simulator uses a standard netlist as an input similar to programs as SPICE do. Pstar allows equations to be used as relationships between any node voltage and branch current in the circuit. This feature makes it very easy for the user to define so-called behavioural models.
The simulator offers three different analysis types: DC, AC(frequency domain) and Transient(time domain) analysis.

When a circuit is non-linear, simulation in the time domain is recommended. Later on the results can be transformed from the time-domain to the frequency domain. The program MATLAB[3] is used for this Fourier transform.

---

[1] MINNIE: Interactive Solutions Limited, London.

[2] Pstar is a program developed by Philips, Eindhoven.

[3] MATLAB is developed by Mathworks Inc, USA.

3. INTRA-EMI.

In this chapter we will discuss in bird's eye view some intra-EMI effects. This discussion is intended to enhance this report with some important aspects. Nearly all intra-EMI effects are well known, but only some of them are modeled in the right manner.
We will discuss shortly:

- reflections in transmission lines,
- input and output impedance of digital circuits,
- crosstalk between transmission lines,
- power supply decoupling,
- ground-bounce effects.

3.1. REFLECTIONS IN TRANSMISSION LINES.

Transmission line effects exist in all interconnections. However, with the advent of devices posessing extremely fast rise and fall times, these effects are more pronounced. The results of these effects, delays and reflections along an interconnection, can cause unexpected behaviour.

Two key elements to consider in transmission lines analyisis are the characteristic impedance Z and the propagation delay τ.

Z The characteristic impedance is the ratio of the voltage to the current in a circuit. Mismatches in impedance between segments of a trace and devices connected to the trace cause reflections, which result in performance-limiting ringing and delays.

τ The propagation delay is important because it predicts whether or not the effects of these reflections will be hidden during the rise and fall times of a circuit. Furthermore, in circuits where skew, which is the difference in time of arrival of a signal, is very important, propagation delay must be taken into account.

Transmission line effects need to be examined prior to final PCB design. Not all scenarios can be improved by adding termination. Therefore, circuit simulation and optimalisation is strongly recommended.

Figure 3.1 shows a transmission line modeled in lumped, constant elements, using the intrinsic resistance, inductance, capacitance and conductance of a trace. This representation can be used to determine the characteristic impedance Z and the propagation delay τ. In Chapter 4 we will discuss the transmission line parameters extensively.

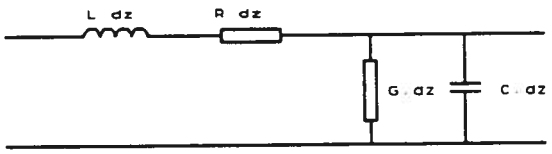

Figure 3.1: Transmission line of length *dz*.

When a trace is loaded with devices, inductance and capacitance from the devices add to the trace's inductance and capacitance. This loading alters the propagation delay and characteristic impedance values.

To remove the undesired effects of unmatched traces and loads, termination of traces may be utilized. There is no standard termination that can be universally applied due to the complexities of layout geometries, power considerations, component count, etc. Five of the most frequently used terminations are as follows:

1. Series termination resistor.
2. Parallel termination resistor.
3. Thevenin network.
4. RC network.
5. Diode network.

These networks are drawn in Figure 3.2.
The 'output impedance correction' (series termination) must be nearby the driver.
The 'input impedance correction' (the other terminations) must be nearby the receiver.

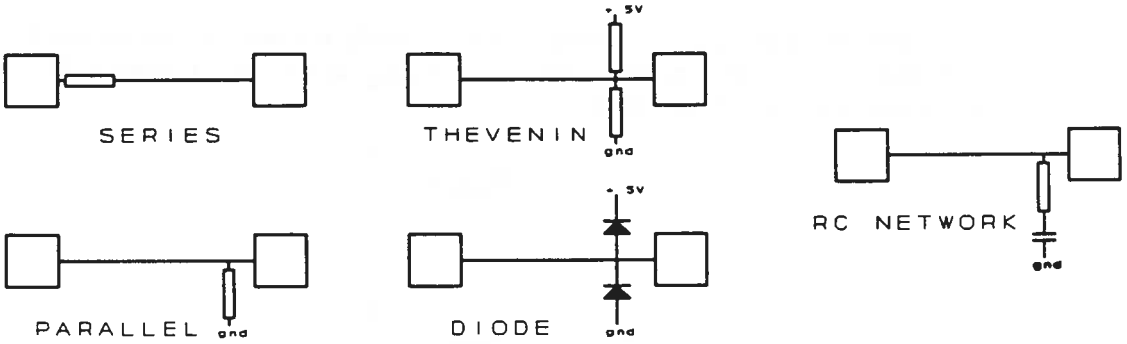

Figure 3.2: Termination types.

In Table 3.1 the properties of the termination types are given.

Termination type	Added parts	Delay added	Power required	Parts values	Comments
series	1	yes	low	R = Z-R(driv.)	Good DC noise margin, reduced drive cap.
parallel	1	small	high	R = Z	Power consumption is a problem
thevenin	2	small	high	R = 2 * Z	High power for CMOS
rc-netw.	2	small	medium	R=Z, C= 300 p	Check bandwidth and added capacitance
diode	2	small	low	-	Limits undershoots; ringing at diodes

Table 3.1: Termination types and their properties.

3.2. INPUT AND OUTPUT IMPEDANCE OF DIGITAL CIRCUITS.

Knowing the input and output impedance of a digital device is important when trying to predict the reflection and crosstalk performance (see Paragraph 3.3). Unfortunately, a logic device has a strongly nonlinear V-I characteristic because of its two-state nature. Its impedance cannot be modeled by one simple resistance. However, we can approximate the input and output impedance. For input impedance, the fully saturated situation does not present much interest. The critical conditions begin when a gate is leaving either a 'low' or a 'high' state. So the knowledge of the V_{in}-I_{in} curve during the narrow transition zone of the transfer function allows a dynamic resistance to be approximately defined during the transfer:

$$R_{in(dyn)} = \frac{\Delta V_{in}}{\Delta I_{in}}$$

For output resistance, since the device's output generally is a more or less saturated transistor plus a limiting resistor and a clamping diode, the V_{out},I_{out} curves can be plotted. The corresponding output resistance can be derived by:

$$R_{out(high)} = \frac{\Delta V_h}{\Delta I_h}$$

$$R_{out(low)} = \frac{\Delta V_l}{\Delta I_l}$$

Figure 3.3 shows the impedances for several digital families. This figure is taken from Mardiguian [Mardiguian, 1988].

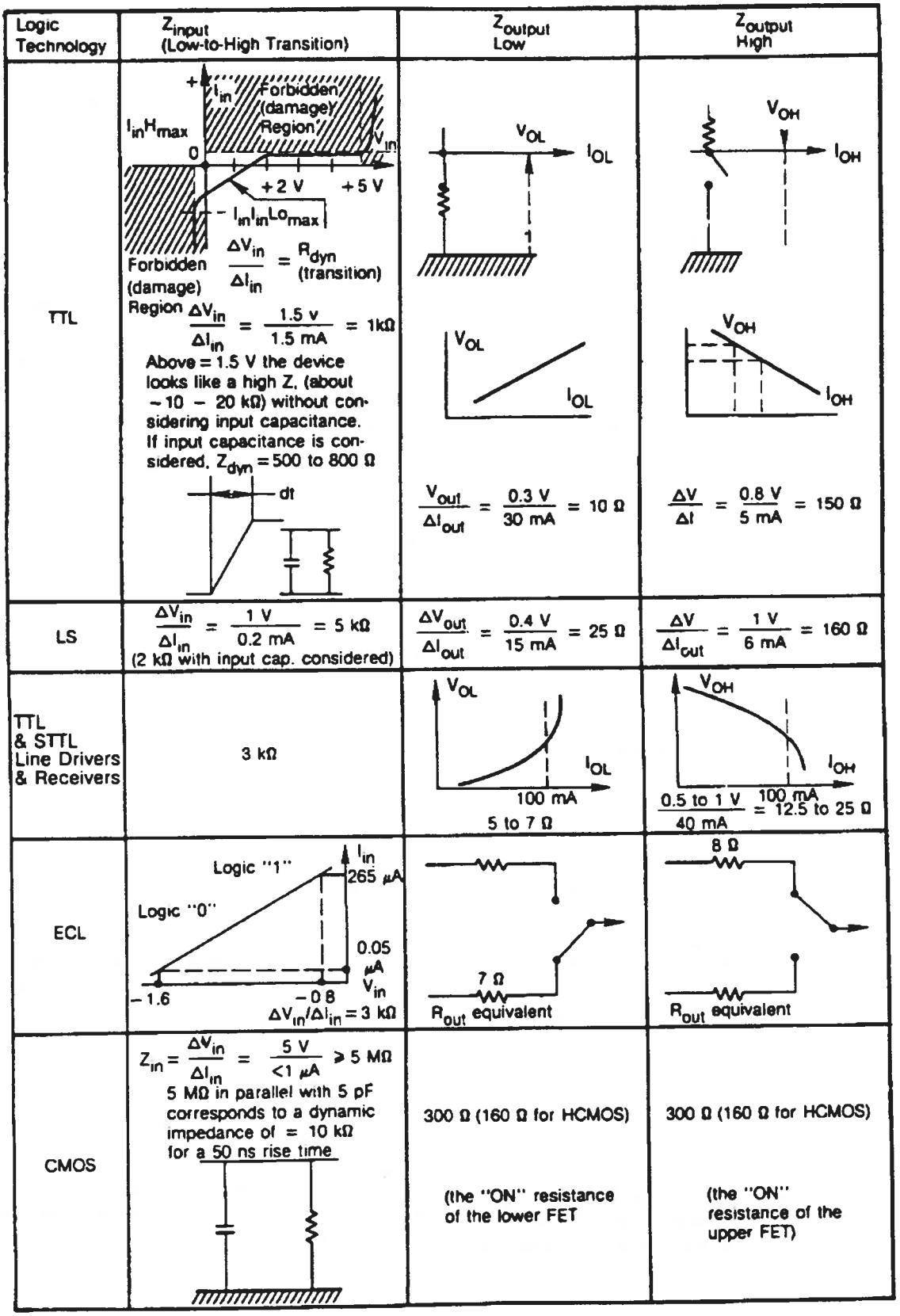

Figure 3.3: Impedances for several digital families.

3.3. CROSSTALK BETWEEN TRANSMISSION LINES.

In Figure 3.4 the three basic elements in interference, source - coupling path - sink, are drawn. In this paragraph we will only discuss the conductive coupling path. When we are interested in the influence of the conductive coupling on the functional behaviour then these effects are called crosstalk, or Xtalk.

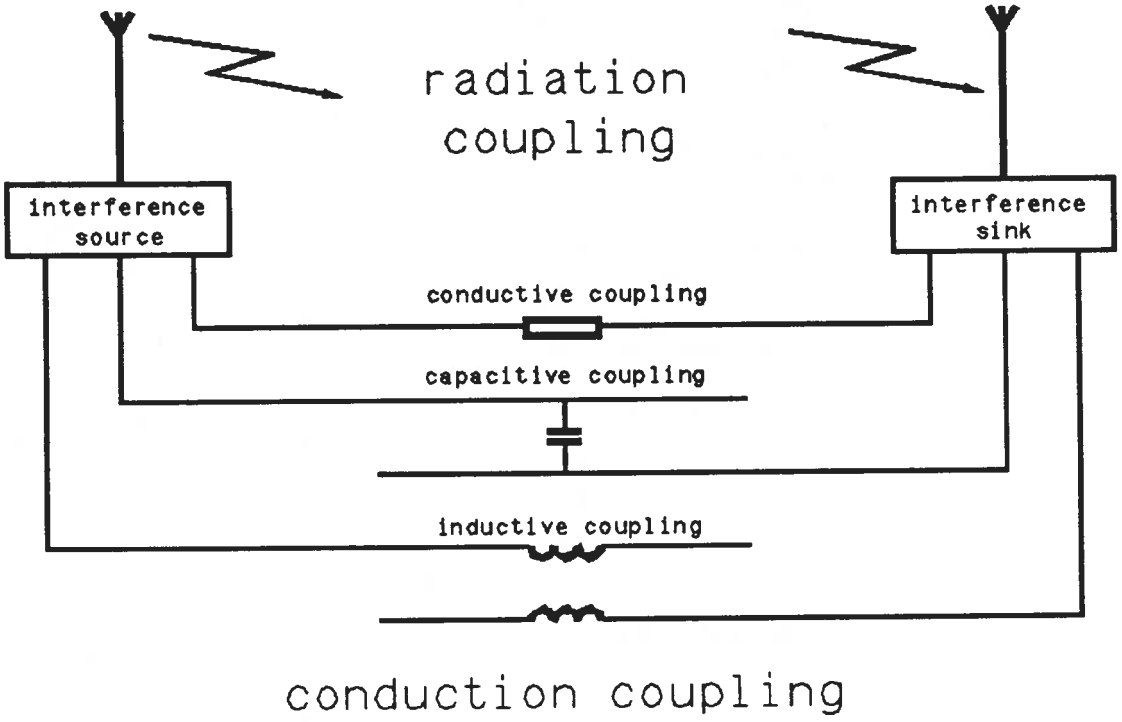

Figure 3.4: Coupling mechanisms between source and receptor.

There are three kinds of coupling, see Figure 3.4:

R Conductive or common impedance coupling. This is a phenomen by which a common impedance (generally return or power bus) is shared between the emission source and the victim, or sink. The I.R or I.ωL drop in this path will affect the victim by creating a common mode voltage in series with the circuit loop.

C Wire-to-wire capacitive coupling occurs when two different circuits having a parallel run exhibit a mutual capacitance *C*. Therefore, if the source circuit carries a voltage *V* the victim circuit will see a current capacitively coupled via

$$I_{Xtalk} = C\frac{dV_{source}}{dt}$$

L Wire-to-wire inductive coupling occurs when two different circuits having a parallel run exhibit a mutual inductance *M*. Therefore, if the source circuit carries a current *I* the victim circuit will see a voltage inductively coupled via

$$V_{Xtalk} = M\frac{dI_{source}}{dt}$$

3.4. POWER SUPPLY DECOUPLING.

The best PCB layout is to use large ground (='reference') planes or grids. For the supply small tracks (with respect to the ground plane) must be used, and each logic IC, and preferably, each power supply pin, must be decoupled using a suitable decoupling capacitor. This decoupling capacitor can be regarded as a reservoir which provides the inrush currents that the logic device needs to switch in the specified time. The value of the decoupling capacitor close to the logic elements requiring the switching current I is:

$$C = \frac{dI\ dt}{dU} \qquad [F]$$

Wherein: C = value for the capacitor, in [F],
dI = current transient, demanded by the logic device, in [A],
dt = logic switching time, in [s],
dU = maximal allowed supply voltage drop, in [V].

It is extremely important to minimize the inductance of the conductors between the IC and the decoupling capacitor. This inductance consists of three components:

* the inductance of the capacitor itself,
* the inductance of the traces connecting the capacitor to the IC,
* the inductance of the lead frame within the IC.

These parasitic inductances in combination with the capacitance results in a resonating L-C circuit. Above this resonance frequency the circuit becomes inductive and it performs poorly as a decoupling capacitor. A decoupling capacitor larger than necessary should not be used because it will have a lower resonant frequency. On the other hand, if the capacitor is too small in value, it will not have sufficient charge storage to supply the transient current needed by the IC without an excessive drop in voltage. Therefore an optimum value capacitor exists for every application.

The decoupling capacitor must be placed as close to the IC as possible to prevent large track-inductance. For large IC's it is often difficult to find a way to mount a capacitor close enough to the IC to be effective. In these cases some alternatives are available:

+ use of different IC packages, e.g. a leadless chip carrier,
+ use of on-chip capacitors,
+ use of a capacitor molded into the IC package,
+ use of an IC socket mounted capacitor,
+ use of a surface mounted capacitor on the non-component side of the board.

To prevent HF currents in the supply circuit a ferrite bead or μ-choke, see Figure 3.5, can be used in series with the supply lines, but not in the ground line. The ferrite bead is effective in three manners:

- it prevents HF-currents in the supply circuit, which can influence other IC's,
- it forces the signal current through the ground plane instead of a supply lead, and therefore only 1 transmission line/characteristic impedance exist [Coenen, 1989],
- it improves the common mode radiation behaviour, see Chapter 4.

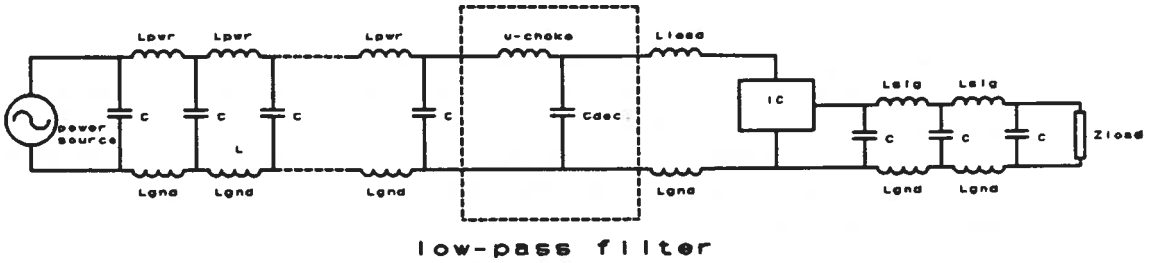

Figure 3.5: Ciruit around an IC, with supply transmission line, signal transmission line, and the power supply decoupling ciruit via a µ-choke and a decoupling capacitor.

3.5. GROUND-BOUNCE EFFECTS.

Transient switching current results in a voltage drop over the supply leads when several output ports are using the same power supply, see Figure 3.6. This effect is called 'ground-bounce'. Especially in IC's with several driver outputs, which are not switching simultaneously, this can influence the signals of the non-switching outputs in such a manner that these signal levels are 'undefined'.

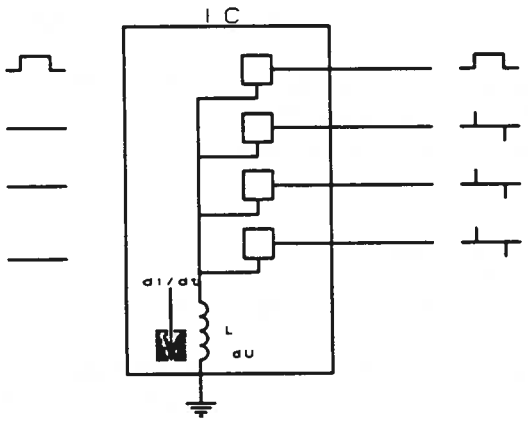

Figure 3.6: Ground bounce effect in an IC.

The solution for these problems is to use low-inductive IC packages.

In larger circuits ground bounce effects can also be a problem. In general this is a 'common-impedance' crosstalk effect.
The best solution is to apply the power supply in the *'chinese'* fashion: In general, the western way of designing, reading and drawing is from left to right. This results in applying the power supply at the left side, or the input side, of the circuit, while the most energy is needed at the output side!. Therefore we should apply the power supply at the output of an circuit, i.e. at the right side of the drawing. The Chineze are writing from right to the left, so, use of a 'chinese power supply scheme' results in less ground bounce effects or common impedance coupling.

Of course, this latter problem is an example of 'human conditioning' where the layout of the circuit diagram is copied to the circuit board. Proper knowledge of basic electromagnetic principles can help overcome this bad habit.

4. INTER-EMI.

4.1. DIFFERENT KINDS OF ELECTROMAGNETIC RADIATION.

(Inter) EMI can be separated such as given in Figure 4.1. The conducted and radiated parts are additive.

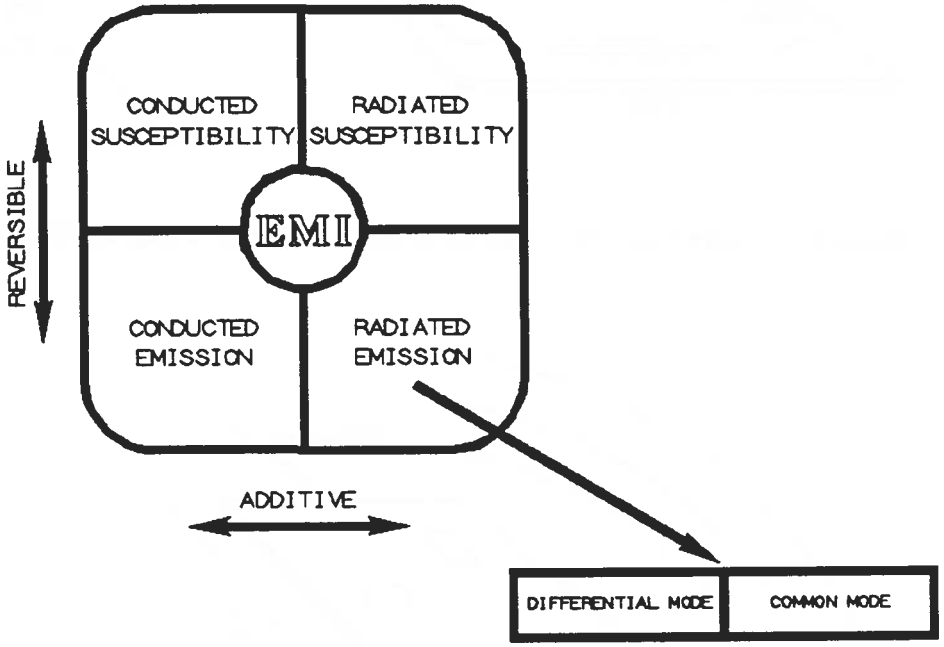

Figure 4.1: Separation of inter-EMI aspects.

When we consider the four parts of EMI with respect to the legislative requirements such as the European Norm EN 55000 series and FCC part 15 then for integrated circuits (IC's), printed circuit boards (PCB's) and the wiring the most severe EMI effect is the radiated emission (RE).
This chapter models the radiation process and outlines the parameters on which radiation depends. It also provides a method for predicting the radiated emission as a function of the electrical characteristics of the signals and the physical properties of the system. Knowing the parameters that affect radiation helps to develop techniques to minimize it.

Radiation from digital electronics can occur as either differential mode or common mode radiation. Differential mode radiation (REdm = Radiated Emission Differential Mode) is the result of current flowing in loops formed by the conductors of the circuit. These loops act as small radiating magnetic dipoles, see Figure 4.2. Although these *desired* signal current loops are necessary for circuit operation, their size must be controlled during the design process (of the layout), in order to limit the radiation.

Common mode radiation (REcm = Radiated Emission Common Mode), on the other hand, is the result of *undesired* voltage drops in the circuit that cause some parts of the system to be at a common mode voltage above some ground. Often this is the result of voltage drops in the digital ground system or reference so we call this the 'ground lift voltage' U_{gl}. When external cables are subsequentially connected to the system, they are driven at this common mode ground lift voltage, forming antennas which radiate electric fields, see Figure 4.3.

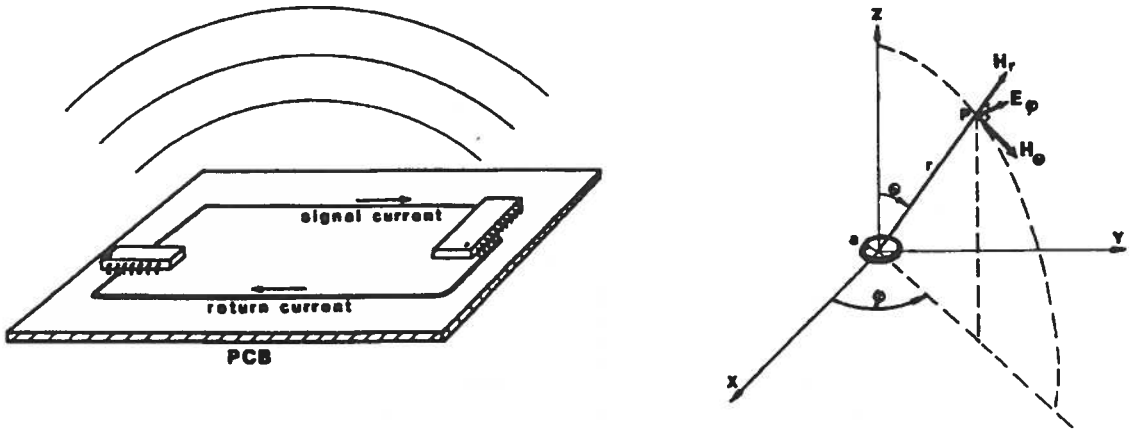

Figure 4.2: A current loop on a practical circuit as source for a magnetic loop antenna.

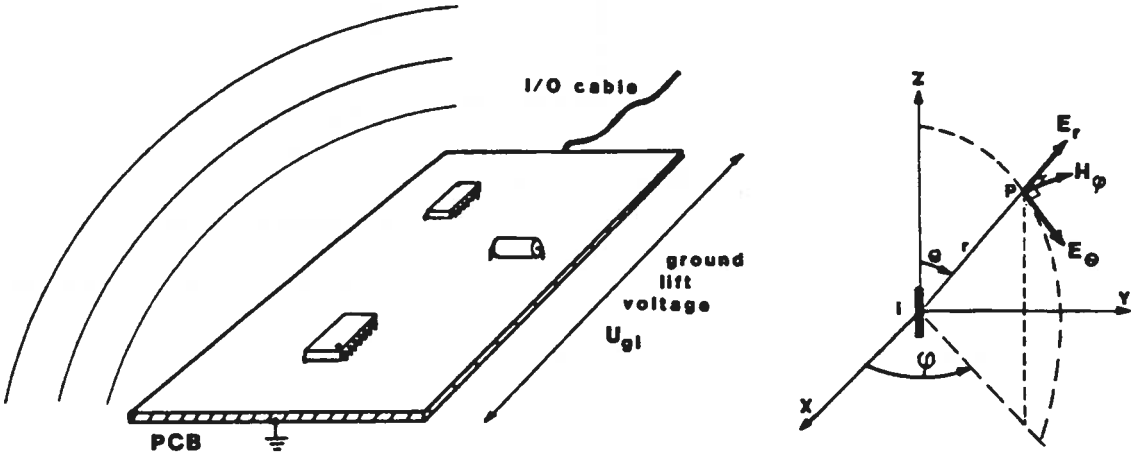

Figure 4.3: A ground lift voltage as source for a electric dipole antenna.

Since this undesired ground lift voltage is not intentionally designed into the system, common-mode radiation is harder to control than differential mode radiation. Furthermore there are no adequate models available to calculate the ground lift voltages. Therefore new models are developed.

In Figure 4.4. the differential mode and common mode currents are given for a simple circuit.

The differential mode current (Idm) is the logic current while common mode current (Icm) is the undesired current. It can often be seen as only a displacement current (see Appendix 2) or as an antenna current but has no influence on the desired differential mode signal.

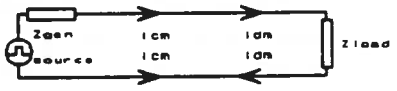

Figure 4.4: Differential and common mode currents in a transmission line.

The differential mode current can easily be obtained from the circuit diagram. The common mode current is very difficult to determine. Until now the common mode current could only be measured at the prototype stage or even later! Using the common mode models developed in Paragraph 4.3. it is possible to predict the radiated emission in a simple and accurate manner!

A note about symmetric and asymmetric ciruits.
First of all, in practice it is impossible to create a 100% symmetric circuit over the whole frequency range.
Some authors state that the common mode current results from asymmetry in the circuit [Hardin 1991]. When considering a circuit diagram without radiation models taken into account, this is true. However, when calculating the electromagnetic fields descended from a magnetic dipole, the differential mode current is used in this calculation. When calculating the electromagnetic fields descended from an electric dipole, the common mode current is used. In general, this common mode current is the antenna current and is not similar to the common mode current which results from circuit asymmetry! It is custom in the EMI world to use the term common mode for both applications, but nearly anyone is aware of this fundamental distinction.
We are using only the definition wherein the common mode current is the same as the electric dipole antenna current.
In Paragraph 4.3. we will show that a symmetric circuit (→ no common mode according to [Hardin 1991]) still produces more electromagnetic radiation than calculated from the differential mode models.

In this chapter we will discuss an asymmetry factor which is responsible for less common mode radiation. This asymmetry factor must not be compared with the symmetry-note mentioned above. The asymmetry factor we will use is only the ratio: inductance of ground conductor with respect to the total inductance of the circuit.

Wheeler [Wheeler, 1975] states that all radiation is basically either magnetic/inductive or electric/capacitive. Without any further comment I state that the differential mode radiation is based on magnetic radiation and the common mode radiation is based on electric radiation. However in the far field it does not matter which electromagnetic field type is radiated by the source. Be aware of the fact that in the far field the ratio of the electric and magnetic fields has a constant value, which is called the wave impedance, of Z = 377 Ω. In [Leferink 1989] the distance between radiating source and the observer where the far field starts is obtained and found to be

$$r = 7\,\frac{\lambda}{2\,\pi} \quad [m] \tag{4.1}$$

and

$$\lambda = \frac{c}{f} \quad [m] \tag{4.2}$$

Wherein:
- r = distance radiator-receiver in [m]
- λ = wavelength in [m]
- f = frequency in [Hz]
- c = speed of light, in vacuum 3.10^8, in [m/s].

Between $r=0.7\lambda/2\pi$ and $r=7\lambda/2\pi$ there is a transition region between the near field and the far field and the wave impedance Z is $250\ \Omega < Z < 500\ \Omega$. Therefore in several publications a multiplication factor 1 is chosen.

Now we can obtain the frequency where the far field formulas are valid, when we know the measuring distance. In most legislative requirements the measuring distance r is either 3 m or 10 m. Then the far field region, with a multiplication factor equal to 1, is valid from 16 MHz and 4.7 MHz upward respectively.

In Paragraph 4.2 we will discuss the properties of differential mode while in Paragraph 4.3 common mode will be discussed.

Note: In the formulas in this chapter all currents and voltages are a function of the frequency!

4.2. DIFFERENTIAL MODE RADIATION.

4.2.1.BASIC FORMULA WITH RESTRICTIONS.

Differential mode radiation can be modeled as occuring from a small loop antenna, see Figure 4.2. In [Leferink 1989] the electric field component of a small loop of radius a carrying a uniform current I_{dm} is given as:

$$E_\phi = Z_0 \frac{(\beta\ a)^2\ I_{dm} \sin(\theta)}{4\ r}[1 + \frac{1}{j\ \beta\ r}]e^{-j\ \beta\ r} \quad [V/m] \tag{4.3}$$

Wherein:
- E_ϕ = electric fieldstrength in [V/m]
- Z_0 = far field wave impedance, 377 Ω ($\sqrt{(\mu/e)}$),
- μ = permeability in [H/m]
- e = permittivity in [F/m]
- β = $2\ \pi/\lambda$
- a = radius loop in [m]
- I_{dm} = differential mode current in [A]
- r = measuring distance in [m]
- θ = angle with respect to the normal of the loop.

From equation 4.3. the time averaged expression for the far field (i.e. where terms in $1/r$ dominate over those in $1/r^2$) electric component of a small loop antenna of area $A = \pi a^2$ assuming a uniform current without any voltage drop due to finite impedance and for $\theta = 90^o$ (i.e. in the plane of the loop), and using $Z_0 = 377\ \Omega$ can be written as

$$E_{dm} = \frac{13.2\ 10^{-15}\ (f^2\ A\ I_{dm})}{r} \quad [V/m] \tag{4.4}$$

Wherein:
- E_{dm} = electric fieldstrength due to differential mode current, in [V/m],
- A = area of loop, in [m^2],
- f = frequency, in [Hz].

Although the above mentioned formula is derived for a circular loop, it can be used for any planar loop because, for small loops, the maximum radiation is insensitive to the shape of the loop and depends only on its area.

Several restrictions must be taken into account.

I First of all the direction of maximum radiation differs as a function of the frequency. For low frequencies, where the circumference of the loop is small with respect to the wavelength, the maximum radiation is from the sides of the loop and in the plane of the loop. When the perimeter of the loop equals a wavelength then the maximum radiation occurs in the direction normal to the loop. The above mentioned formula gives the maximum radiation without the angle taken into account.

II Furthermore the current is thougth to be distributed uniformly over the loop. This is called the quasi-static approximation.

III Also the area of the loop must be small with respect to the measuring distance.

IV The last restriction is that the above mentioned formula is valid in free space. When large conductive objects are nearby the fieldstrength will be lower.

The first restriction is practically of no influence because when measuring the electric fieldstrength according to the legislative requirements the product or equipment under test (EUT) must be positioned in such a manner that the maximum fieldstrength is measured.

The second restriction is more important. Practically the frequencies of interest are high so the loop can act as a resonant antenna ($\lambda/4$ etc.). However the radiator is less efficient due to internal impedance at these frequencies and the above mentioned formula can be used.
The third restriction can often be neglected because we are measuring at 3 m or 10 m distances, which is for most EUT's larger than the loop radius.
The fourth restriction can be used by the designer. When an infinite conducting surface or metal sheet (or even a grid) is placed nearby the loop then currents will flow in the surface which tend to cancel the field.
This can be represented by an image of the loop. The total magnetic fieldstrength at a distance r caused by a loop conducting a current I and its image current is given as:

$$H = \frac{I\,a^2}{2\,r^3} - \frac{I\,a^2}{2\,(r+2\,d)^3} \quad [A/m] \tag{4.5}$$

Wherein:
- H = magnetic fieldstrength in [A/m]
- I = current in wire [A]
- r = distance to wire in [m]
- a = radius of loop in [m]
- d = distance between wire and plane in [m].

Now the attenuation of the radiated field due to the image surface can be calculated:

$$Attenuation = 1 - \frac{r^3}{(r + 2d)^3} \tag{4.6}$$

or:

$$Attenuation_{dB} = -20 \log\left(1 - \frac{r^3}{(r + 2d)^3}\right) \quad [dB] \tag{4.7}$$

This attenuation is called the quasi active shielding (QAS) because the conducting surface is not an electromagnetic shield but it results however in a lower fieldstrength. In practice we are not using infinite conducting surfaces but a finite printed circuit board with power plane grids. Also the QAS is lower for off-axis angles.
The QAS is calculated for a loop but can also be calculated for a wire. The QAS of a wire above a grid gives comparable results.

Furthermore, this deduction of the QAS is for near fields, so for a distance r which is less than $0.7\lambda/2\pi$, see Formula 4.1. In practical situations where r= 3 m, this is for frequencies below 11 MHz.

Another remark must be made. Because of the large conductive surface close to the radiation source the antenna (see Paragraph 4.3.) will be more effective. More common mode radiation, especially in the lower frequency range (below $\lambda/4$) will be the result.... Therefore the conductive plane must be connected to the reference of the circuit. This will 'kill' the effectiveness of the antenna.

In Figure 4.5. the attenuation (in dB) of the radiated field is given for $r=3\ m$ as a function of the distance d (in mm), when an infinite surface is used.

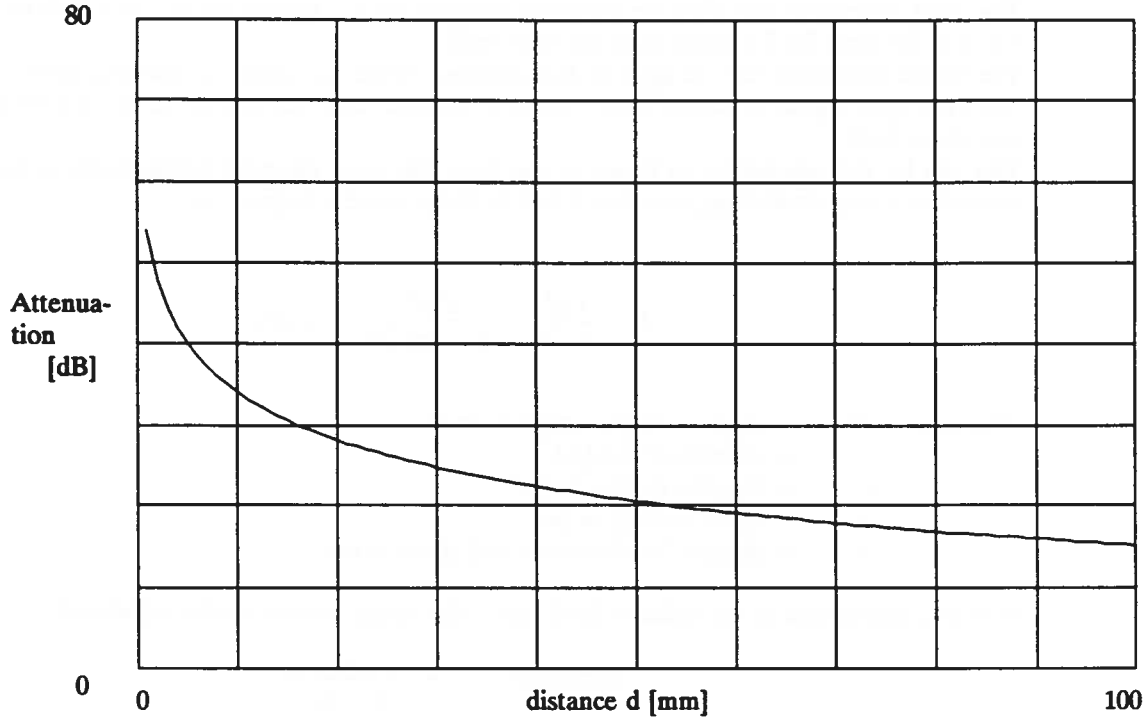

Figure 4.5. Attenuation of radiated field at 3 meter distance due to Quasi Active Shielding.

An experiment is carried out to verify the theory of QAS. Therefore two magnetic antennas are placed at 200 mm distance away from eachother. One antenna was used as a source and the other was used as a receiver.
Two measurements were carried out in the frequency range 100 kHz to 3 MHz because for higher frequencies the antennas are resonant. The first measurement was made with no conducting planes nearby. The second measurement was made when a brass plate of 300 x 300 x 3 mm^3 was placed approximately 4 mm behind the transmitting antenna (the source antenna would give the same results). The difference in transmitted (magnetic) fieldstrength was approximately 21 dB, see Figure 4.6. while the theoretical attenuation is, using equation 4.7, equal to 19 dB.
This small difference is negligable.

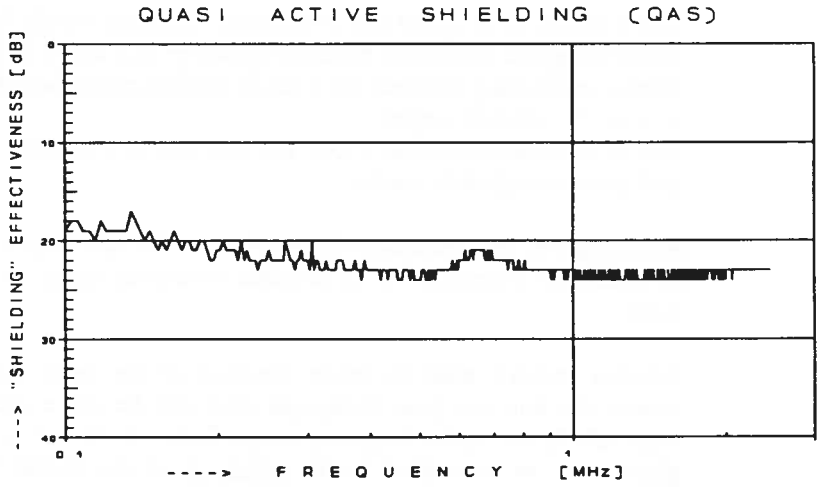

Figure 4.6: Measured QAS for distance $d=$ *4 mm* and measuring distance $r=$ *200 mm*.

4.2.2.MODELING THE DIFFERENTIAL MODE RADIATION.

The differential mode radiation can be modelled very simple because the differential mode current is the logic current in a circuit. It is very important to include all parasitic elements in this simulation because these elements can have a large influence on the results.
It is possible to simulate a circuit in two domains, the time domain or the frequency domain. However, most digital circuits are non-linear so frequency domain simulations cannot be carried out. Therefore time domain simulations must be used and the simulated Idm must be transformed using (Fast) Fourier Transformations (FFT).
In the simulation environment described in Chapter 2 this process is carried out by using MINNIE for the simulations and MATLAB for the FFT of the Idm.
In Chapter 5 a simulation and electric field calculation is carried out for several test PCB's.

Equation 4.4. is for a small loop in free space. Most measurements of radiation from electronic products, however, are made in an open field over a ground plane and not in free space. The extra ground reflection can increase the measured emission by as much as 6 dB. To account for this equation 4.4. must be multiplied by a factor of two. Empirically it is maximal a factor 1.83 (according to B. Danker and M. van Doorn, Philips CE). Then equation 4.4. can be corrected to:

$$E_{dm} = \frac{24.16\ 10^{-15}\ (f^2\ A\ I_{dm})}{r} \quad [V/m] \tag{4.8}$$

All legislative requirements and all measurements are carried out using logarithms (the electric fieldstrength unit is dBμV/m), we can transform formula 4.8. into:

$$E_{dm[dB]} = 20\ \log\left(\frac{24.16\ 10^{-15}\ f^2\ A\ I_{dm}}{r}\right) + 120 \quad [dB\mu V/m] \tag{4.9}$$

or:

$$E_{dm[dB]} = -152+20\log(A)-20\log(r)+20\log(I_{dm})+20\log(f^2) \quad [dB\mu V/m] \tag{4.10}$$

wherein the constant terms and the frequency dependant terms are splitted.

In EMI research we are always searching the weakest link. Therefore it is unneccesary to look at all loops in a circuit but one has to search the most dangerous parts because these define the radiated emission behaviour of the product. Based on experience the parts in the circuit which are the main contributors to REdm are, in order of importance:

* The power supply decoupling loop, because in this loop the largest currents with a large bandwidth are flowing.
* The clock signal loop, because a clock signal is a coherent signal. Then several radiating loops in a circuit are coherent sources and the resulting fieldstrengths will add.
* Signal lines with a large bandwidth. With respect to the clocksignals these signals are less coherent and the resulting fieldstrength is broadening in the frequency spectrum with a smaller amplitude.

In Chapter 5 some practical circuits will be described and step-by-step analysed.

4.2.3.DESIGNABLE PARAMETERS.

Equation 4.4. shows that the radiation is proportional to the current *Idm*, the loop area *A* and the square of the frequency *f*. Therefore radiation can be controlled by:

1. reducing the magnitude of the current,
2. reducing the frequency or harmonic content (see Appendix 3) of the current,
3. reducing the loop area.

Because the Idm is the logic current and its frequency is already predetermined by the application and IC family selection, the only free designable parameter is the loop area. Rewriting Formula 4.4.:

$$A = \frac{41.410^{12}\ E_{dm}\ r}{f^2\ I_{dm}} \quad [m^2] \tag{4.11}$$

A specific legislative requirement will not be used in this report because several different limits do exist. For our examples we use the requirement:

$$E < 100\ \mu V/m \tag{4.12}$$

for a measuring distance of $r=3m$.
Then the maximal allowed loop area is:

$$A < \frac{1.24\ 10^{10}}{f^2\ I_{dm}} \quad [m^2] \tag{4.13}$$

When *f* in MHz, *Idm* in milliamperes and *A* in square millimeters:

$$A < \frac{12.4}{f^2\ I_{dm}} \quad [mm^2] \tag{4.14}$$

This area *A* is the designable, or controllable, parameter.
Because Idm is frequency dependant and the frequency *f* is present in the formula, the designable parameter is frequency dependant, see Appendix 3.

4.3. COMMON MODE RADIATION.

4.3.1.BASIC FORMULA WITH RESTRICTIONS.

Differential mode radiation is 'easily' controlled in the design and layout of a product. On the other hand, common mode radiation is harder to control and normally determines the overall emission performance of a product ([Paul 1988,1989],[Schibuya 1987,1991]).
Common mode radiation can be modeled as occuring from a small monopole antenna, see Figure 4.3. In [Leferink 1989] the electric field component of a small monopole of length l carrying a uniform current I_{cm} is given as:

$$E_\theta = Z_0\, j\, \frac{\beta\, I_{cm}\, l \sin(\theta)}{4\,\pi\, r}\left[1 + \frac{1}{j\,\beta\, r} - \frac{1}{(\beta\, r)^2}\right] e^{-j\,\beta\, r} \quad [V/m] \qquad (4.15)$$

Wherein:
- E_θ = electric fieldstrength in [V/m]
- Z_0 = far field wave impedance, 377 Ω ($\sqrt{(\mu/\epsilon)}$),
- μ = permeability in [H/m]
- ϵ = permittivity in [F/m]
- β = $2\,\pi/\lambda$
- l = length wire in [m]
- I_{cm} = common mode current in [A]
- r = measuring distance in [m]
- θ = angle with respect to the direction of the wire.

From Formula 4.15. the time averaged expression for the far field (i.e. where terms in $1/r$ dominate over those in $1/r^2$) electric component of a small monopole antenna assuming a uniform current without any voltage drop due to finite impedance and for $\theta = 90°$ (i.e. in the plane normal to the wire), and using $Z_0 = 377\ \Omega$ can be written as

$$E_{cm} = \frac{0.63\ 10^{-6}\, f\, I_{cm}\, l}{r} \quad [V/m] \qquad (4.16)$$

Wherein: E_{cm} = electric fieldstrength due to common mode current, in [V/m].

Several restrictions, as for the differential mode radiation, must be taken into account.

I The above mentioned formula gives the maximum radiation, i.e. without the angle θ taken into account.

II Furthermore the current is thought to be distributed uniformly over the wire. This is called the quasi-static approximation.

III Also the length of the monopole must be small with respect to the measuring distance.

IV The last restriction is that the above mentioned formula is valid in free space. When large conductive objects are nearby the fieldstrength can be lower or even higher.

The first restriction is practically of no influence because when measuring the electric fieldstrength according to the legislative requirements the product or equipment under test (EUT) must be positioned in such a manner that the maximum fieldstrength is measured.
The second restriction is more important. Practically the frequencies of interest are high so the wire can act as a resonant antenna ($\lambda/4$ etc.). Later in this chapter, when we derive the antenna impedance formula, it will be shown that this restriction is of no interest.
The third restriction can often be neglected because we are measuring at 3 m or 10 m distances, which is for most EUT's or cables larger than the wire length.

4.3.2.MODELING THE COMMON MODE RADIATION.

As discussed in Paragraph 4.1. the common mode current is an unwanted signal. Furthermore its amplitude is some orders of magnitude smaller than the differential mode current. Therefore it is usually neglected by the circuit designer. Until now no appropriate simple and accurate models for calculating the common mode current are available. In this paragraph we will develop such a model.

It is known that the common mode current can be controlled by lowering the ground lift voltage U_{gl} [Ott 1988].
Consider the transmission lines in Figure 4.7.

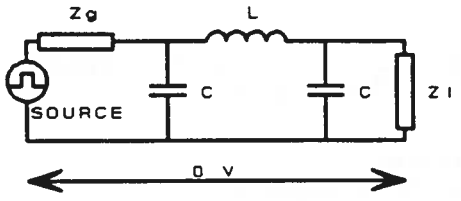

Figure 4.7a: One-wire transmission line.

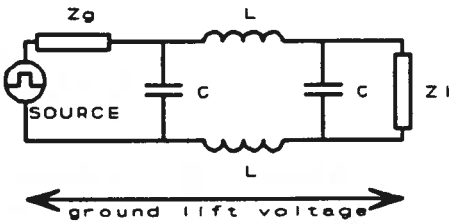

Figure 4.7b: Two-wire transmission line.

For the desired signal at the end of the line the placement of the line inductance in the model is indifferent as long as the total effective inductance is not changed. This has resulted in the habit to concentrate the line inductance in <u>one</u> inductance. Using such ideal transmission line model will never yield any ground lift voltage, see Figure 4.7a.
For our calculations it is neccesary to use a transmission line with inductances in the signal- <u>and</u> in the return line, see Figure 4.7b. This two-inductance transmission line is called a two-wire transmission line. In Paragraph 4.3.4. some transmission lines will be considered.

The normal logic current Idm will cause a voltage drop over the return inductance. Because the return lead is often thought to be the 'ground' lead and in most circuits the interconnection cables are connected to the 'ground', any voltage drop over the ground lead will cause a ground lift voltage U_{gl} which is the driving force for the common mode current.

It is obvious that the Ugl depends on the ground inductance. This inductance is a <u>designable parameter</u> which means that by controlling this ground inductance the electromagnetic radiation can be controlled. All authors found upto know state that the inductance of a massive PCB ground plane <u>can be neglected</u>. The ground inductance was thought to be negligible or small due to the holes for the component pins. One paper describes the ground inductance of a power grid on a PCB [Smith 1991 (&Paul)] but still the inductance of the (massive) plane is neglected. Furthermore there is hardly no research into inductance carried out in the last 30 years. This has lead to several (small) mistakes in modern EMI research, see Appendix 4. In Paragraph 4.3.6. and Appendix 4 some investigation into inductances is described.

At first sight the ground lift voltage seems to be a strong function of the differential mode current. This is true for low frequencies (where the length of the wire is much smaller than the wavelength) but for high frequencies the differential mode current is hardly of interest, i.e. for the common mode radiation it is indifferent whether the load impedance is connected or not. This effect will be described in Paragraph 4.3.5.

Now the ground lift voltage can be determined using the two-wire transmission line model. The ground lift voltage can be seen as a driving antenna voltage. To determine the common mode (or antenna) current from the ground lift voltage an antenna impedance $Z_{\underline{antenna}}$ must be found:

$$I_{common\ mode} = \frac{U_{groundlift}}{Z_{antenna} + Z_{Ugl}} \quad [A] \qquad (4.17)$$

Now the complete circuit for calculating the ground lift voltage and the resulting common mode current is given in Figure 4.8.

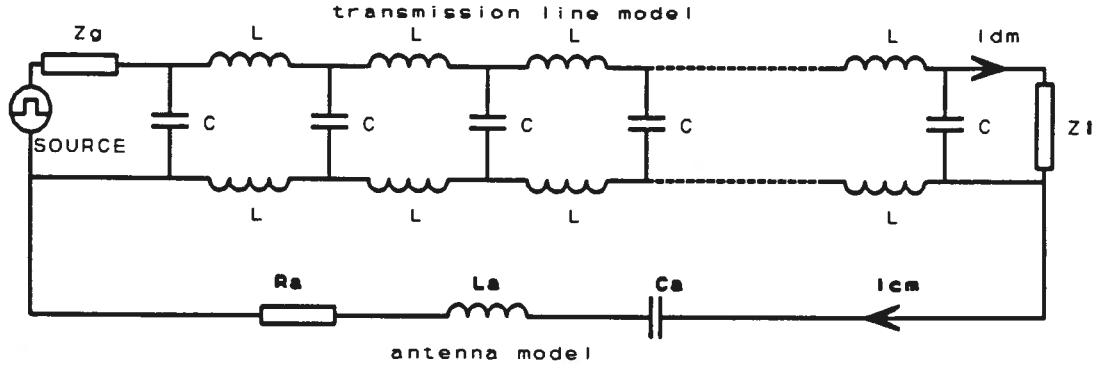

Figure 4.8: Transmission line and antenna model.

The antenna model is described in the next paragraph. The transmission line model is described in Paragraph 4.3.4.

It is possible to simulate a circuit in two domains, the time domain or the frequency domain. In the next paragraph the antenna impedance will be given. This antenna impedance is a function of the frequency so time domain simulations cannot be carried out. Therefore frequency domain simulations must be used. For the (non-linear) source signal the envelope of the Fourier spectrum (see Appendix 3) will be used.

Equation 4.16. is for a small monopole wire in free space. Most measurements of radiation from electronic products, however, are made in an open field over a ground plane and not in free space. The extra ground reflection can increase the measured emission by as much as 6 dB. To account for this equation 4.16. must be multiplied by a factor of two. Empirically it is maximal a factor 1.83 (according to B. Danker and M. van Doorn, Philips CE). Then equation 4.16. can be corrected to:

$$E_{cm} = \frac{1.15\ 10^{-6} f I_{cm} l}{r} \quad [V/m] \tag{4.18}$$

In EMI research we are always searching the weakest link. Therefore it is unneccesary to look at all wires in a circuit but one has to search the most dangerous parts because these determine the radiated emission behaviour of the product. Based on experience (see also Paragraph 4.2) the parts in the circuit which are the main contributors to REcm are, in order of importance:

* The power supply path, because in this path large currents with a large bandwidth are flowing so these can develop a relative large ground lift voltage.
* The clock signal return paths, because a clock signal is a coherent signal. Then several radiating parts in a circuit are coherent sources and the resulting fieldstrength will add.
* Signal lines with a large bandwidth. In contrast to the clocksignals these signals are less coherent and the resulting fieldstrength is broadening in the frequency spectrum with a smaller amplitude.

In Chapter 5 some practical circuits will be described and analysed step-by-step.

4.3.3.THE ANTENNA MODEL.

A formula which gives the capacitance of a wire with respect to 'Mother Earth' was already known in 1914 [Jasik 1961]:

$$C_a = \frac{2\,\pi\,e\,l}{\ln(\frac{l}{a})-1} \quad [F] \tag{4.19}$$

Wherein: l = length antenna in [m]
a = radius antenna in [m]
e = permitivity in [F/m]

We can use this same formula for the low-frequency impedance when 'Mother Earth' is replaced by the *reference* of our product. Be aware of the fact that for example a satellite can radiate without 'Mother Earth' in the neighbourhood!
Note that the value for the antenna capacitance is for ideal situations with no metallic objects nearby.

Several textbooks (here [Meinke&Gundlach 1986]) give the radiation resistance of a short antenna above its reference as:

$$R_a = 40\,(\frac{\pi\,l}{\lambda})^2 \quad [\Omega] \tag{4.20}$$

Wherein: λ = wavelength in [m]
l = length antenna in [m]

This impedance is for a lossless antenna which, four our purpose, is the worst case situation.
The loss of an antenna can be calculated using [Stutzman 1981]:

$$R_{loss} \approx \frac{l}{2\,\pi\,a}\sqrt{\frac{\omega\,\mu}{2\sigma}} \quad [\Omega] \tag{4.21}$$

Wherein: ω = 2πf in [rad/s]
σ = conductivity in [S/m].
In our case this loss is small and can be neglected.

At the resonance frequency of the wire, that is when $l=\lambda/4$ and $l=\lambda/2$ and so on, the impedance of the wire is purely resistive. A model with only capacitance and resistance does not resonate, so, to account for this effect, we will have to add an 'antenna inductance' L_{ant} to our model and tune its value to exhibit the resonance effect.
At the resonance frequency a RLC series network is purely resistive.
(For HF freaks: at λ/4 -> RLC series, λ/2 -> RLC parallel. We are using a simplified model).

The resonance frequencies can be determined via:

$$f_{res} = n\,\frac{c}{4\,l} \quad [Hz] \tag{4.22}$$

Wherein: c = speed of light, 3.10^8 [m/s]
n = integer, [1,2,3,...]

Now the total antenna impedance is:

$$Z_a = R_a + j(\omega L_a - \frac{1}{\omega C_a}) \quad [\Omega] \tag{4.23}$$

Wherein:

$$L_a = \frac{1}{C_a\,(\omega_{res})^2} \quad [H] \tag{4.24}$$

For $\lambda/4$ and $\lambda/2$ the impedance of an antenna with length $l = 1m$ and radius $a = 1mm$ is given in Figure 4.9.
For each frequency the lowest antenna impedance must be used in the calculations.

Note:
As a matter of fact this consideration is not complete. Because the resistor is a function of the frequency the antenna impedance has not a minimum at exactly the resonance frequency. This effect is more pronounced for high frequencies. A correction can be made by determining the zeros of:

$$\frac{d|Z_{ant}|}{df} = 0$$

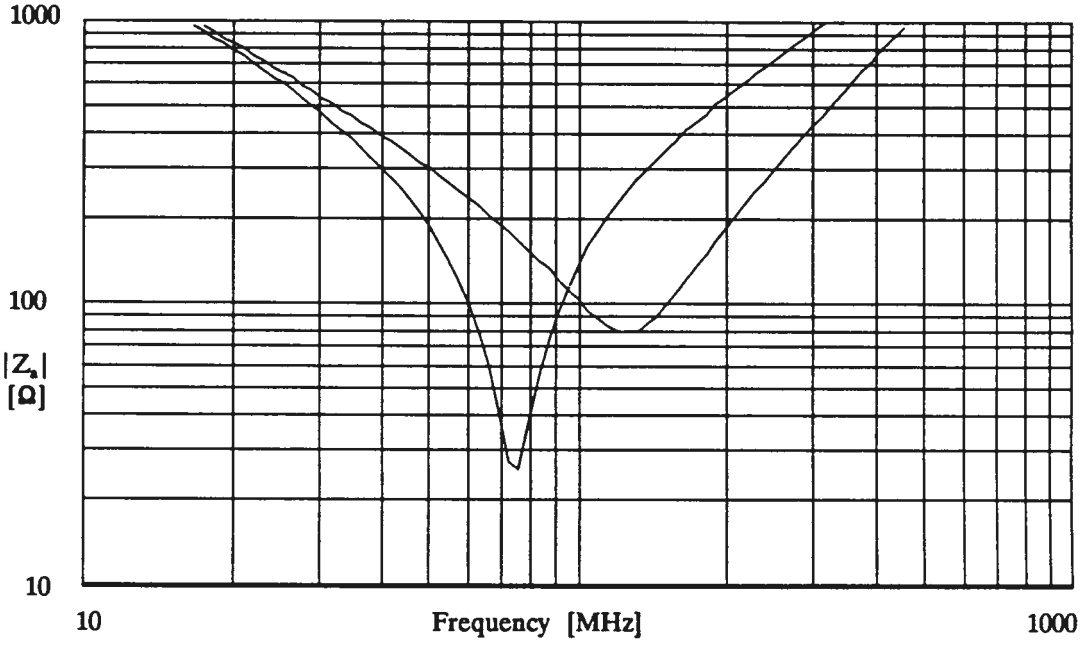

Figure 4.9: Impedance of antenna of length $l = 1\ m$ and radius $a = 1\ mm$.

Another approach compared to the one mentioned above is to look at the resonance frequencies only. For a wire in resonance at $\lambda/2$ the antenna impedance is 73 Ω. This value is within 3 dB compared to the former method for the lowest resonant modes. The disadvantage of the resonance method is that the antenna impedance is known only at one frequency.

One important remark must be made. The formula for the radiated common mode emission assumes a uniform current (quasi-static approach). Especially at resonance this current is not uniform at all. Still it is possible to calculate the REcm with an accuracy which is satisfactory for EMI applications. Some research could be done for a better and more accurate model. However in our opinion this will be at the expence of the simplicty which is very important for engineers who are not interested in EMI theory but in the EMI performance of their product.
Hence, for electronic engineers who are interested in the EMI performance of their product this approach is accurate enough.

The following remarks must be kept in mind:

- The antenna impedance is accurate for the lower resonant frequencies. In practical situations where the lower resonance frequencies are responsible for the highest radiated emission this antenna impedance can be used. For higher resonance frequencies the forementioned note (derivative of the impedance) describes the method to correct the antenna impedance.
- The antenna impedance formula is accurate for a thin wire, such as an interconnecting lead. A large plane instead of the wire as the radiating antenna will cause a lower level, up to 20 dB. So the forementioned impedance will yield the worst case situation.
- The antenna impedance is determined in free space. When large conducting surfaces are nearby this can result in a lower emission level, when the surface is properly mounted 'over' the ground lift voltage points (and 'shortening' this voltage), or in a higher emission level, when the surface is not connected (floating).

4.3.4.MODELLING A TRANSMISSION LINE.

Electromagnetic energy can propagate in the form of free space electromagnetic waves but also as confined waves along various configurations of conductors called transmission lines. This paragraph will review the basic equations needed as well as their most important properties. The properties of transmission lines depend on the frequency range, the way they are terminated, and their geometric properties.

An equivalent circuit analysis enables the behaviour of current *I* and the voltage *U* to be calculated at any point along the line. If the wavelength of the signal is much less than the length of the line then the lumped circuit approximation is valid and ordinary circuit analysis suffices. Once the dimension of the line becomes comparable to the wavelength, transit time effects become important and transmission line properties must be considered. To discuss the mathematics of transmission lines an equivalent circuit model of basic line types can be constructed, based on the following ideas:

1. The existance of an electric field between the two conductors suggests a parallel capacitance between the conductors --> **C**.
2. Voltage drop down the conductor suggest a series resistance along the line --> **R**.
3. The current indicates that magnetic field exists, so inductive effects occur. This suggests that a series inductance is needed --> **L**.
4. There may be leakage across the diëlectric insulating the space between the two conductors. This can be modelled as a parallel resistor of conductance --> **G**.

Putting these ideas together leads to an equivalent cicuit model for a transmission line shown in Figure 4.10 The values quoted are ohms, henrys, and farads per unit length *dz* of the line.

The L, C, R and G are circuit representations or models for the electromagnetic behaviour of the transmission line. The models can be used in calculations using Kirchhoff laws but the fundamental laws collected by Maxwell give the better description of the behaviour of the line.

As mentioned in Paragraph 4.3.1. the placement of the series resistance and the series inductance is indifferent for the wanted signal at the end of the line as long as the effective impedance is not changed. For our considerations this placement is very important and from now on we will use only two-wire transmission lines (transmission line with a signal and a return inductor). As a matter of fact for digital ciruits the return path is the ground and, when the positive supply lead is not decoupled via a small inductance (micro-choke), then even the positive supply lead is a return path. In the latter case we should use a three-wire transmission line. This would complicate the study in such a manner that our objective, a simple method, is unattainable.

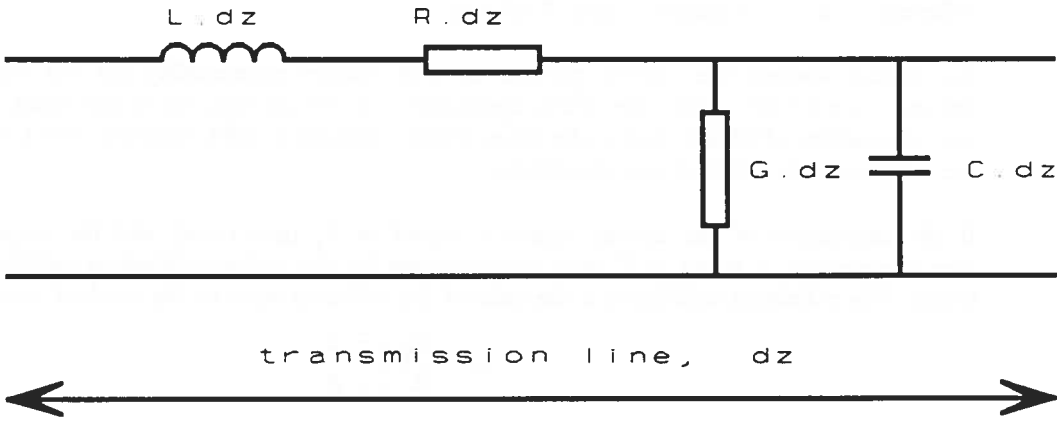

Figure 4.10: General circuit representation of a transmission line of length dz.

Using this complete model for the full lossy transmission line it is possible to determine a general expression for the characteristic impedance ([Chatterton 1992], [Grabinski 1991]):

$$Z = \sqrt{\frac{R + j\,\omega\,L}{G + j\,\omega\,C}} \quad [\Omega] \tag{4.25}$$

Wherein: L, C, R and G as in Figure 4.10,
Z = characteristic impedance.

For a lossless transmission line, wherein $R=0$ and $G=0$, this characteristic impedance is equal to:

$$Z = \sqrt{\frac{L}{C}} \quad [\Omega] \tag{4.25b}$$

and the wave is travelling with velocity:

$$\upsilon = \frac{1}{\sqrt{L\,C}} \quad [m/s] \tag{4.26}$$

Wherein: υ = wave velocity.

When the transmission line is <u>not lossless</u> the velocity can be frequency dependent. This means that the different frequency components in the Fouries expansion of a pulse shape travel at different velocities, so distorting the pulse shape. This effect is called dispersion.

When the transmission line is lossless the L and C are reciprocal functions of each other, so that the product LC, hence the speed of a TEM wave (Transverse ElectroMagnetic, i.e. E and H vector normal with respect to eachother and normal with respect to the transmitting direction), is independent of the line geometry. In fact:

$$L\,C = \mu_0\,\mu_r\,\epsilon_0\,\epsilon_r \tag{4.27}$$

so the wave velocity is:

$$\upsilon = \frac{c}{\sqrt{\mu_r\,\epsilon_r}} \quad [m/s] \tag{4.28}$$

Wherein: c = speed of light, 3.10^8 m/s.

For media wherein the relative permittivity and relative permeability are not equal to 1 (for instance, $\epsilon_r=4.7$ for epoxy) the TEM approximations are actually no longer valid. However, for our applications (PCB's etcetera) the Quasi-TEM approach is valid [Sperling, 1992] and we can use the same formulas without any restrictions.

If the impedance of the driving source is equal to Z_s (generator) and the impedance of the transmission line is equal to Z then an expression for the voltage reflection coëfficient ρ can be found. This reflection coëfficient is the ratio of the reflected wave to the incident wave.

$$\rho = \frac{Z_{load} - Z}{Z_{load} + Z} \tag{4.29}$$

After these general properties I will describe the modelling of the parts which are important for our EMI considerations.

G First of all we can neglect the conductance *G*.

R The series resistance *R* must be separated in a DC and a AC resistance. The DC resistance can be determined via:

$$R_{DC} = \frac{l}{\sigma A} \quad [\Omega] \tag{4.30}$$

Wherein: l = length conductor in [m],
σ = conductivity in [S/m],
A = area of conductor in [m^2].

Durcansky [Durcansky 1991] gives a correction factor for this formula when a large plane, such as a ground plane on a PCB is used. Then this DC resistance must be multiplied with a factor, approximately equal to 5.

For higher frequencies the current flows more and more in the skin of the conductor due to the internal magnetic field produced by the current itself. Consequently, the effective cross section available for the current to flow decreases. This phenomenon is called the 'skin effect'. For any conductor, a fictitious thickness is defined where everything behaves as if the current were concentrated in a skin depth given by:

$$\delta = \frac{66}{\sqrt{\sigma_r \, \mu_r \, f_{[MHz]}}} \quad [\mu m] \tag{4.31}$$

Wherein: δ = skindepth, in [μm],
σ_r = relative conductivity = 1 for copper,
μ_r = relative permeability = 1 for copper,
$f_{[MHz]}$ = frequency in [MHz].

From [Meinke & Gundlach 1986] then the AC resistance for a round wire is:

$$R_{AC} = R_{DC} \left(\frac{d}{4\delta} + \frac{1}{4} \right) \quad [\Omega] \tag{4.32}$$

Wherein: d = wire diameter in same units as the skindepth δ.

C The capacitance represents the electric field between the two conductors of the transmission line. In the tables in Appendix 4 some values for specific constructions are given.

L The inductance in the transmission line represents several effects. First we will consider the internal inductance, then the external inductance, which is influenced by the coupled flux of the return lead due to the mutual inductance.
Internal inductance is due to the effects of magnetic field created by the current within the conductor itself. It, in turn, is closely associated with skin effect since both phenomena are interactive. At frequencies where the current flows through a small skin of the conductor the H-field is leaving the center core and the internal inductance L_i decreases.
At DC and low frequencies, below the skin-effect frequency, i.e. $\delta > d$, the value of L_i for a round conductor is given by [Grover 1945]:

$$L_i = \frac{\mu \, l}{8 \, \pi} \quad [H] \tag{4.33}$$

Wherein: l = length conductor, in [m],
μ = permeability = $4\pi 10^{-7}$ [H/m].

As frequency increases L_i decreases and can be neglected with respect to the external inductance.

For the external inductance we must be aware that the so-called self-inductance must be corrected by the mutual inductance of the return lead. This method is described and applied in the formulas developed by Grover [Grover 1945]. This author is the most referred author with respect to inductance, but most referees are still using the term self-inductance while this is not the meaning of Grover.
Another method of calculating the inductance is by determining the coupled flux as Kaden does [Kaden 1959].
A third method can be found in the microwave area were the capacitance is determined and via Formula 4.27. the inductance.

By definition: 'A change of current in a conductor will induce a voltage due to the changing flux linkage of its self-produced magnetic field'. The conductor is said to have self-inductance. A field produced by another conductor (wherein another current or the return current flows) will also produce a voltage in the first conductor. This coupling is called mutual-inductance.
When two wires are conducting the same current but with opposite direction then the effective inductance can be calculated using:

$$L_{eff} = L_{1self} + L_{2self} - M_{12} - M_{21} \quad [H] \tag{4.34}$$

Wherein: L_{1self} = self inductance of signal conductor, when the return is in infinity,
L_{2self} = self inductance of return conductor,when the return is in infinity,
M_{12} = mutual inductance between signal and return conductor,
M_{21} = mutual inductance between return and signal conductor.

Because $M_{12} = M_{21}$:

$$L_{eff} = L_{1self} + L_{2self} - 2\,M \quad [H] \tag{4.35}$$

Wherein: L_{eff} = inductance as seen by the 'world'.

Because the current must always flow in a loop the self inductance does only exist in theory because somewhere the return lead will conduct the return current which reduces the self inductance with the mutual inductance.
Magnetic fields produced by current in conductors nearby will also influence the inductance. This is an intra-EMI effect and called crosstalk, see Chapter 3.

In Appendix 4 the formulas for inductance found upto now are given. Basically these can be split into the three fundamental approaches such as given in the foregoing discussion:

- the Grover method: $L_{eff} = L_{self} - M$ (typically: the length l in the ln (natural logarithm), but this l can be removed via simplification),
- the Kaden method: $L_{eff} = \phi_k/i$, wherein $\phi_k = \int BdA$, (typically: no l in the ln because edge effects are neglected),
- the capacitance method: $L_{eff} = \epsilon.\mu/C$ (typically: also no l in the ln).

As described in Paragraph 4.3.2. we are interested in the ground or return lead inductance. The effective inductance is the signal line inductance plus the return line inductance. Unfortunately all three methods do not directly yield the return inductance. Only the second method, via the coupled flux can be used, because the first method, developed by Grover, always assumes symmetrical ciruits. Maybe this is the reason why our method of determining the ground lift voltage for asymmetrical circuits, such as PCB's with a ground plane, is not found in literature.
In Paragraph 4.3.6. the inductance of a solid plane conducting the return current of the signal line laid above is determined.

Now all parts of the transmission line are discussed. Summarizing, see also Figure 4.11:

- The conductance G can be neglected.
- The resistance R consists of two parts,
  - \+ the DC resistance R_{DC},
  - \+ and the AC resistance R_{AC}.

  In most calculations this resistance will also be neglected because it has much less influence than the inductance has.
- The capacitance C represents the electric field between the conductors.
- The inductance L represents the magnetic field around the conductors and consists of three parts,
  - \+ $L_{internal}$, which can be neglected in our considerations,
  - \+ $L_{external}$, which consists of
    - L_{self}, the self inductance and
    - L_{mutual}, or M, the mutual inductance.

  We are especially interested in the return lead inductance which is in most cases the ground inductance L_{gnd}.

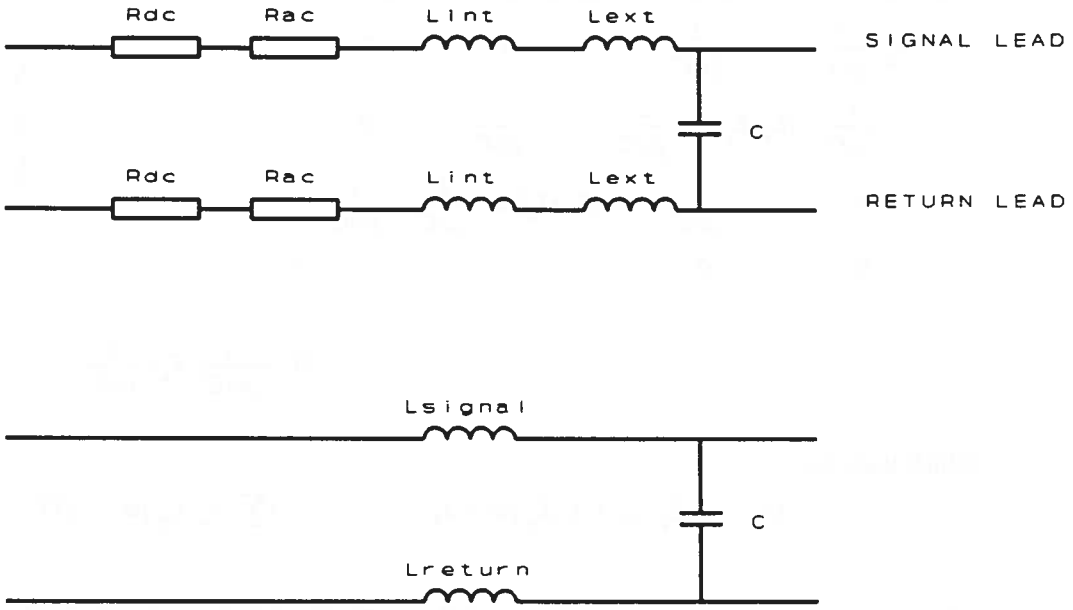

Figure 4.11: Two-wire transmission line, extensive and simplified model.

The transmission line model exists of several two-wire transmission lines in series, the so-called 'lumped circuit' which consists of partial inductances and capacitances. The inductances and capacitances represent the electromagnetic behaviour of a piece Δz of the transmission line. When this piece Δz is very small with respect to the wavelength ($\Delta z << \lambda$) then one L-C section is sufficient. Otherwise the L-C sections must be split into parts where all parts are small with respect to the wavelength.
A rule of thumb is:

$$l_{section} < 5\ \tau_{rise} \quad [cm] \tag{4.36}$$

Wherein: $l_{section}$ = length of section of transmission line.
τ_r = risetime of signal, in [ns].

4.3.5.THE DM TO CM TRANSFORMATION.

In this paragraph we will develop a simple rule which makes it possible to perform manual calculations. Also design rules can developed from this rule.
Consider the two-wire transmission line in Figure 4.12.

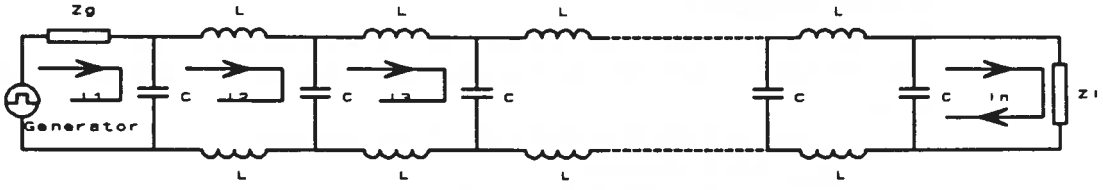

Figure 4.12: Two-wire transmission line with mesh currents.

The equation for the mesh currents in matrix form is:

$$\begin{bmatrix} Z_g+\frac{1}{j\omega C} & -\frac{1}{j\omega C} & 0 & 0 & \cdots & & i_1 & u_{in} \\ -\frac{1}{j\omega C} & (L_s+L_g)j\omega+\frac{2}{j\omega C} & -\frac{1}{j\omega C} & 0 & \cdots & & i_2 & 0 \\ 0 & -\frac{1}{j\omega C} & (L_s+L_g)j\omega+\frac{2}{j\omega C} & -\frac{1}{j\omega C} & \cdots & & i_3 & 0 \\ 0 & 0 & + & * & + & \cdots & \cdot & = \cdot \\ \cdot & \cdot & \cdot & \cdot & \cdot & \cdots & \cdot & \cdot \\ \cdot & \cdot & \cdot & \cdot & 0 & -\frac{1}{j\omega C} \quad Z_L+\frac{1}{j\omega C} & \cdot & \cdot \end{bmatrix}$$

Which leads to:

$$U_{gl} = i_2 L_g j\omega + i_3 L_g j\omega + i_4 \ldots\ldots = \sum i_m L_g j\omega \quad [V] \qquad (4.37)$$

When the load impedance is not connected then still all mesh currents, except the last one, will flow. Therefore it is possible that a common mode current due to the ground lift voltage is created without any differential mode current at the end of the line. We assume here that differential mode current = logic (wanted) current at the end of the line, because the mesh current i_1 is in itself 'differential mode current' but using this name for this mesh current is very confusing.

For developing design rules the above mentioned equations are not very helpfull. The only thing to say is that the ground inductance must be kept as small as possible. However, does the signal line inductance influence the ground lift voltage or is the ground inductance the designable parameter? Therefore, several simulations are carried out. Using the Formula 4.27:

$$L_{eff} C = \mu \epsilon$$

and:

$$Z = \sqrt{\frac{L_{eff}}{C}} \quad [\Omega] \qquad (4.38)$$

as a basis then we can deduct:

$$L_{eff} = \sqrt{\mu\, e}\;\; Z \qquad [H/m] \tag{4.39}$$

$$C = \frac{\mu\, e}{L_{eff}} \qquad [F/m] \tag{4.40}$$

Wherein: Z = characteristic impedance of the transmission line, in [Ω],
L_{eff} = effective inductance (signal + return inductance) per length *l* of the transmission line, in [H/m],
C = capacitance per length *l* between the conductors, in [F/m],
μ = permeability of the medium, $\mu_0.\mu_r$,
e = permittivity of the medium, $e_0.e_r$.

An *asymmetry* factor is added so the signal- and the ground inductance can be split as follows:

$$L_{signal} = (1+asym)\; L_{eff} \qquad L_{ground} = (1-asym)\; L_{eff} \tag{4.41}$$

$$asym = \frac{L_{signal} - L_{ground}}{L_{signal} + L_{ground}} \qquad (1-asym) = \frac{1}{2}\,\frac{L_{ground}}{L_{ground} + L_{signal}} \tag{4.42}$$

Wherein: asym = asymmetry factor, $0 \le asym < 1$,
0 for complete symmetry, 0.9999.. for optimal asymmetry, (only a coax cable can have an asymmetry factor equal to 1.....)

Two two-wire transmission lines as given in Figure 4.13 are simulated several times with several variations of the parameter values.

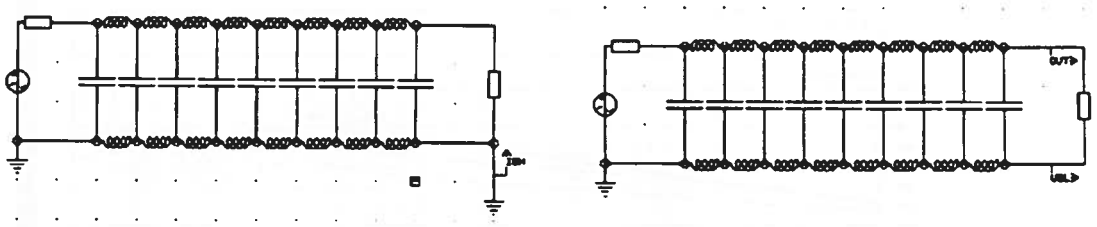

Figure 4.13: Transmission lines for DM-CM conversion.

The starting-point values for the transmission line used in the simulations were:

e	= permittivity	$= e_r.e_0$	$= 8.85\ 10^{-12}$	[F/m],
μ	= permeability	$= \mu_r.\mu_0$	$= 4\ \pi\ 10^{-7}$	[H/m],
l	= length		= 1	[m],
Z	= characteristic impedance		= 100	[Ω],
Z_g	= generator impedance		= 100 + 0j	[Ω],
Z_l	= load impedance		= 100 + 0j	[Ω],
asym	= asymmetry factor		= 0.	

In Figure 4.14 three combined graphs are given. All graphs are drawn as a function of the frequency for Z_l = *100 Ω* with the generator impedance Z_g as a parameter. For the generator impedance the values 1 - 10 - 100 - 1k - 10k Ω are used, which is equal to 0.01 - 0.1 - 1 - 10 - 100 * Z. In Figure 4.15 the same graphs are given, but now the load impedance Z_l is changed from 100 Ω to 10 kΩ.

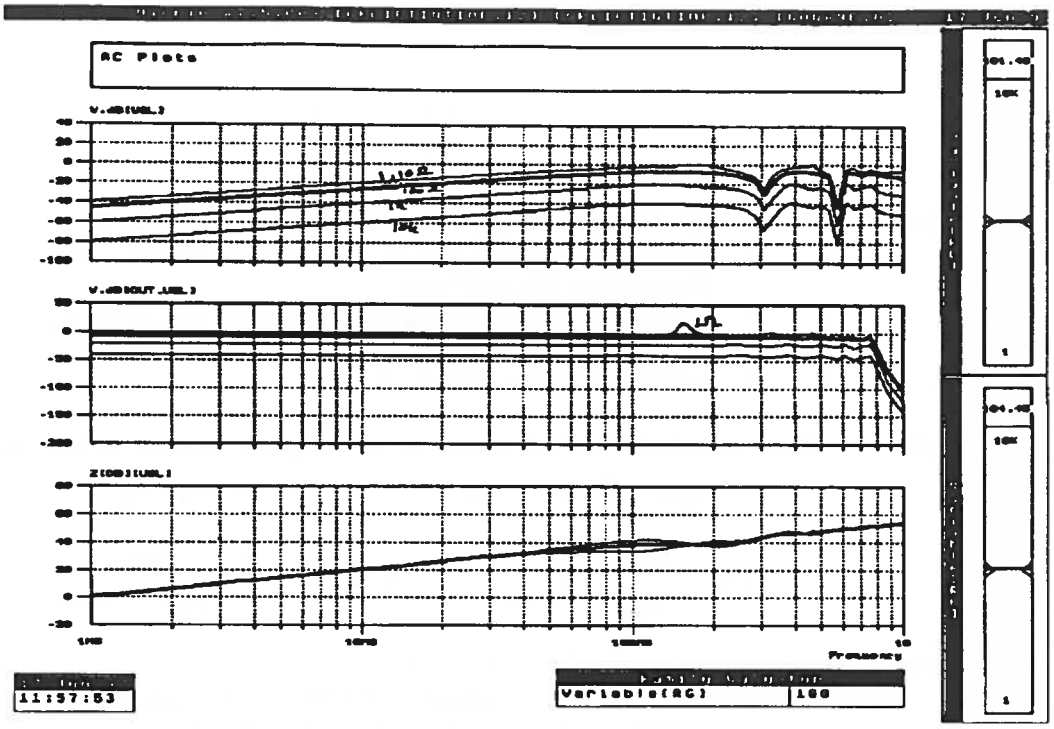

Figure 4.14: The groundlift voltage, the transmitted signal and the internal impedance of the 'ground lift voltage source', for Z_l= *100 Ω* and variable Z_g.

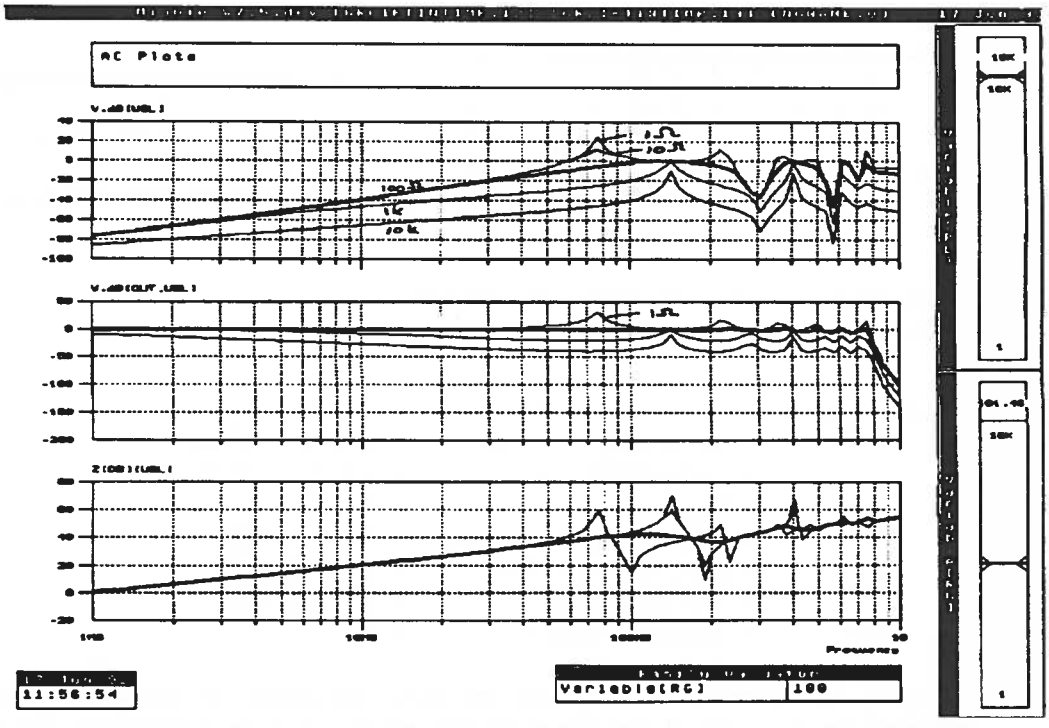

Figure 4.15: The groundlift voltage, the transmitted signal and the internal impedance of the 'ground lift voltage source', for Z_l= *10 kΩ* and variable Z_g.

The first graph in Figures 4.14 and 4.15 gives the ground lift voltage in dB with respect to the generator voltage. The second graph gives the signal voltage at the end of the line with respect to the generator voltage and the third graph gives the internal impedance Z_{Ugl} of the ground lift voltage.

We will discuss the results, starting with the signal voltage at the end of the line, then the ground lift voltage and then the internal impedance.

* The signal voltage (second graph in the figures) is a well known figure. From [Meinke & Gundlach 1986]:

$$\left|\frac{U_{point}}{U_{load}}\right| = \sqrt{\left(\cos\frac{2\pi l}{\lambda}\right)^2 + \left(\frac{Z}{Z_{load}}\sin\frac{2\pi l}{\lambda}\right)^2} \qquad (4.43)$$

which results in the same figure.
The 'low-pass' behaviour at 750 MHz is caused by the finite number of L-C transmission line sections and caused by the simulation, and is of no interest four out considerations. When more sections were used (here 8) this 'low-pass frequency' would be higher.

* The ground lift voltage U_{gl} with respect to the generator voltage is an important figure. Because the generator voltage is the wanted signal, and in our terminology this is the differential mode signal (DM), and the ground lift voltage is the source of a disturbing common mode (CM) signal we will call this figure the DM-CM transformation.
When the line is properly fed and terminated (here 100 Ω) then the DM-CM tranformation is like a first order high-pass filter with the 'cross-over frequency' f_c at:

$$f_c = \frac{\upsilon}{\lambda_c} \quad [Hz] \qquad (4.44)$$

Wherein: f_c = cross-over frequency, in [Hz],
υ = wave velocity, in [m/s],
λ_c = cross-over wavelength, in [m].
and (Formula 4.26):

$$\upsilon = \frac{c}{\sqrt{\mu_r\, e_r}} \quad [m/s] \qquad (4.45)$$

and:

$$\lambda_c = 2\, l_{PCB} \quad [m] \qquad (4.46)$$

Wherein: l_{PCB} = length PCB transmission line.
so:

$$f_c = \frac{c}{2\sqrt{\mu_r\, e_r}}\,\frac{1}{l_{PCB}} \quad [Hz] \qquad (4.47)$$

In practical circuits the relative permeability μ_r equals 1. Then we can conclude that the cross-over frequency f_c is inversaly proportional to the square root of the relative permittivity e_r and inversaly proportional to the length l_{PCB} of the transmission line.

The feeding (Z_g) and termination (Z_l) impedance has also a large influence on the DM-CM transformation. As can be seen in Figure 4.14 feeding with a large impedance will result in lower DM-CM transformation as long as the generator impedance is higher than the transmission line impedance. The ratio is also simple to deduct: 20 dB attenuation per multiplication for the generator impedance by a factor 10.

Comparing Figure 4.14 and 4.15 we see that a large load impedance Z_l results in a steeper slope. For $Z_l = \infty$ this slope is 40 dB/decade instead of the 20 dB/dec when properly terminated. Furthermore, when the line is terminated with a high impedance some resonances occur, see Figure 4.15. For low generator impedance Z_g at:

$$f_{res} = (2n-1)\frac{c}{4l\sqrt{\mu_r e_r}} \quad [Hz] \tag{4.48}$$

wherein: n = integer, range 1..∞.

and for high generator impedance Z_g at:

$$f_{res} = (2n)\frac{c}{4l\sqrt{\mu_r e_r}} \quad [Hz] \tag{4.49}$$

The amplitude at resonance is inversaly proportional to the generator impedance Z_g.

We can see in the figures that the transmission of the differential mode generator signal to the common mode ground lift voltage is equal to -6 dB in the 'pass band', with dips at:

$$f_{dip} = n\frac{c}{l\sqrt{\mu_r e_r}} \quad [Hz] \tag{4.50}$$

The amplitude in the pass band (properly: the whole spectrum...) appears to be controllable (designable) via the asymmetry factor. An asymmetry factor equal to 0 means that the signal- and ground inductance are similar and the DM-CM ratio in the pass band is -6 dB.
An asymmetry factor equal to 0.99 means that the signal- and ground inductance are about a factor 100 in difference and the DM-CM ratio in the pass band is -40 dB.
An asymmetry factor equal to 1 means that the ground inductance equals 0 and the whole effective inductance is found in the signal inductance which results in a DM-CM ratio of -∞!

* The internal impedance of the ground lift voltage is determined via:

$$Z_{Ugl} = \frac{U_{gl}}{I_{short}} \quad [\Omega] \tag{4.51}$$

In Figure 4.15 and Figure 4.16 only the amplitude in dB[Ω] (decibel above 1 ohm) is given and no phase diagram.
We can see in the figures that the internal impedance of U_{gl}, which is the driving source for common mode current, is nearly indifferent to the termination. From the figure we can see that the internal impedance is about 1 Ω at 1 MHz, 10 Ω at 10 MHz, 100 Ω at 100 MHz and so on.

The transmission line we are using in the simulation has a length l = 1m. This transmission line will radiate electromagnetic energy at f = 150 MHz ($\lambda/2$), where it has an impedance of Z_{ant} = 73 Ω (if the transmission line is a thin wire). This impedance is of the same order as the internal impedance of the driving ground lift voltage (ideal matching), see Figure 4.16, so there is a maximum radiation amplitude at this 'dangerous' frequency!

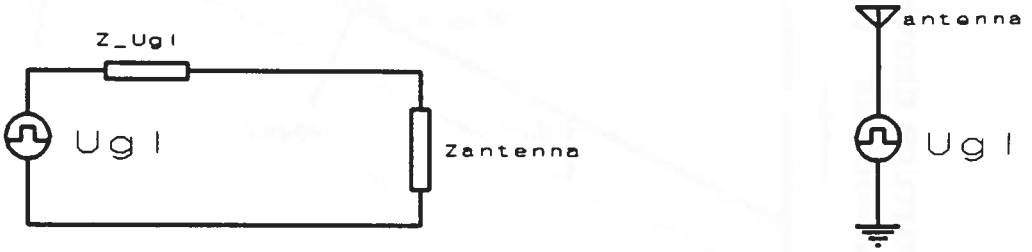

Figure 4.16: The ground lift voltage as a driving antenna source.

Summarizing:

- All conductors are transmission lines which can be a source of radiation.
- The generator signal is transformed to a disturbing signal. This process is called the DM-CM transformation.
- The following general figure can be set up. This Figure 4.17 can be used for manual calculations.

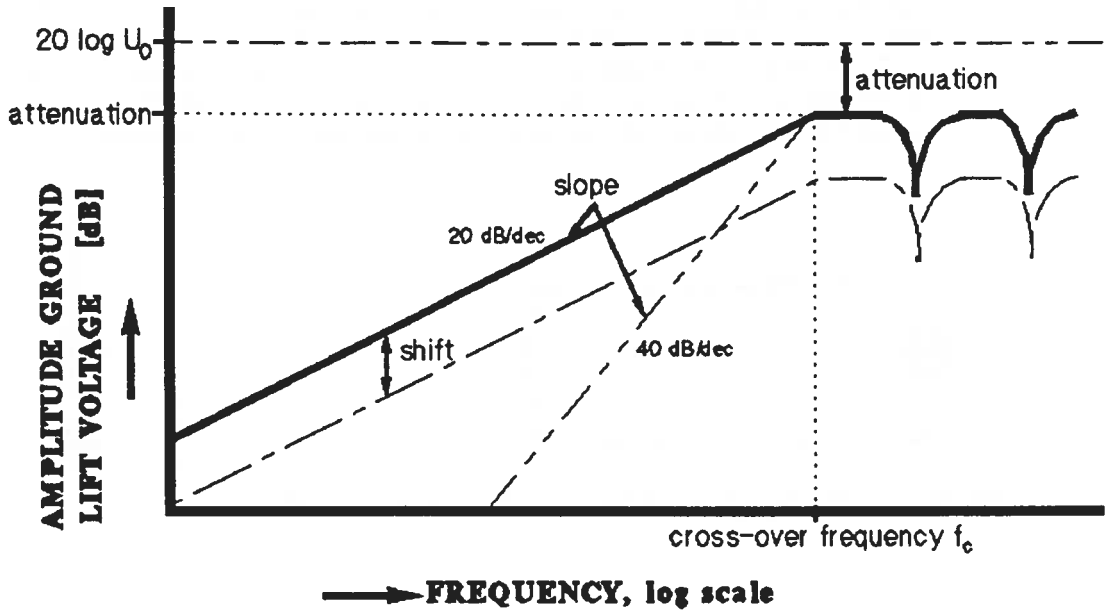

Figure 4.17: General DM-CM conversion.

Herein:

attenuation	=	- 20 log (1-asymmetry) + 6 [dB]
	=	- 20 log ($L_{ground}/(L_{signal}+L_{ground})$) [dB]
	=	- 20 log (L_{gnd}/L_{eff}) [dB],
f_c	=	$c/(2l\sqrt{e_r})$ [Hz],
shift	=	20 log (Z_g/Z) [dB], if $Z_g > Z$,
slope	=	20 dB/dec if $Z_l \approx Z$,
	=	40 dB/dec if $Z_l >> Z$.

When large mismatches exist between the generator-, characteristic- and load-impedance then resonances will occur.

When the transmission line on the PCB is properly terminated then the ground lift voltage U_{gl} is simply determined only by the cross-over frequency f_c and the attenuation in the pass band and:

$$U_{gl[dB]} = 20 \log U_{signal} + 20 \log(1-asym) - 6 - 20 \log(1+\frac{f_c}{f}) \quad [dBV] \qquad (4.52)$$

Wherein the second and third (-6 dB) term represents the attenuation in the pass band and the last term results in a 'high pass' spectrum.

4.3.6.INDUCTANCE AS A DESIGNABLE PARAMETER.

As in the case of differential mode radiation, it is desirable to limit both the rise time and the frequency of the signal to decrease common mode emission.
Cable length is determined by the distance between the components being connected, and is not usually under the designer's control. In addition, when the cable length reaches one-quarter wavelength, the emission no longer continues to increase with cable length, due to the presence of out-of-phase current.
The only parameter that the designer can control to minimize the emission is the common mode current. This can be controlled by:

1. Minimizing the driving source voltage, the ground lift voltage, that drives the 'antenna'.
2. Short-circuiting the ground lift voltage U_{gl} via a large plane (adding asymmetry).
3. Providing a large common mode impedance in series with the cable in the form of a lossy ferrite bead. The attenuation is limited due to crosstalk via the parasitic capacitance of the cable, and the maximum obtainable attenuation is practically 20 dB.
4. Shielding the interconnecting cables.

The third and fourth method are 'crash' methods and must not be used until all other methods are exhausted. The second method is complementary to the first method.
The first method is the best method to control the common mode electromagnetic radiation.

As discussed in the preceding paragraphs the ratio of the ground inductance L_{ground} with respect to the signal inductance L_{signal} is the designable parameter. In this paragraph we will discuss the ground inductance.
In this research, it became clear that the inductance of a solid power plane such as used in multi-layer printed circuit boards is, in contrast to what is accepted in general, not negligible.
As mentioned before, the formulas developed by Grover [Grover 1945] cannot be used because he assumes symmetrical circuits.

We will now deduct the inductance for an asymmetric circuit as drawn below in Figure 4.18.
Inductances taken from literature are given in Appendix 4.

The magnetic field between the signal (narrow) and return (wide) conductor can be determined via

$$\oint H\,dl = I + \iint \frac{\partial D}{\partial t} \qquad (4.53)$$

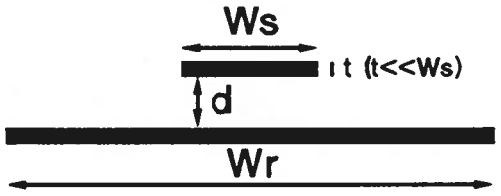

Figure 4.18: Signal track above a wide return track.

Neglecting the displacement current ($\iint \partial D/\partial t$: AC) and assuming the current flowing through a very thin surface due to the skin-effect, this leads to:

$$H_{signal} = \frac{I}{2\pi r + 2w_s} \quad [A/m] \qquad (4.54)$$

and:

$$H_{return} = \frac{I}{2\pi r + 2w_r} \quad [A/m] \qquad (4.55)$$

with opposite directions for H_{signal} and H_{return}.

Because Φ_{tot} is proportional to L_{eff} and $\Phi_{tot} = \Phi_{signal} + \Phi_{return}$ this leads to $L_{eff} = L_{signal} + L_{return}$.
So:

$$L_{return} = \frac{\Phi}{I} = \frac{1}{I}\int \mu H_r \, dA \quad [H] \tag{4.56}$$

and so:

$$L_{return} = \frac{l\,\mu}{2\,\pi} \ln\left(\frac{d\,\pi}{w_r} + 1\right) \quad [H] \tag{4.57}$$

Wherein: l = length track (l>>d), in [m],
d = distance between signal and return track, in [m],
w_r = width return track, in [m].
In most circuits the return inductance is the same as the ground inductance, then $L_{return} = L_{ground}$.
The signal line inductance can be calculated using the same formula wherein w_r is replaced by w_s.

In Figure 4.19 the ground or return inductance L_{return} is given in [nH/cm] as function of the track width *w* in [mm] with the distance *d* in [mm] between signal and return conductor as a parameter.

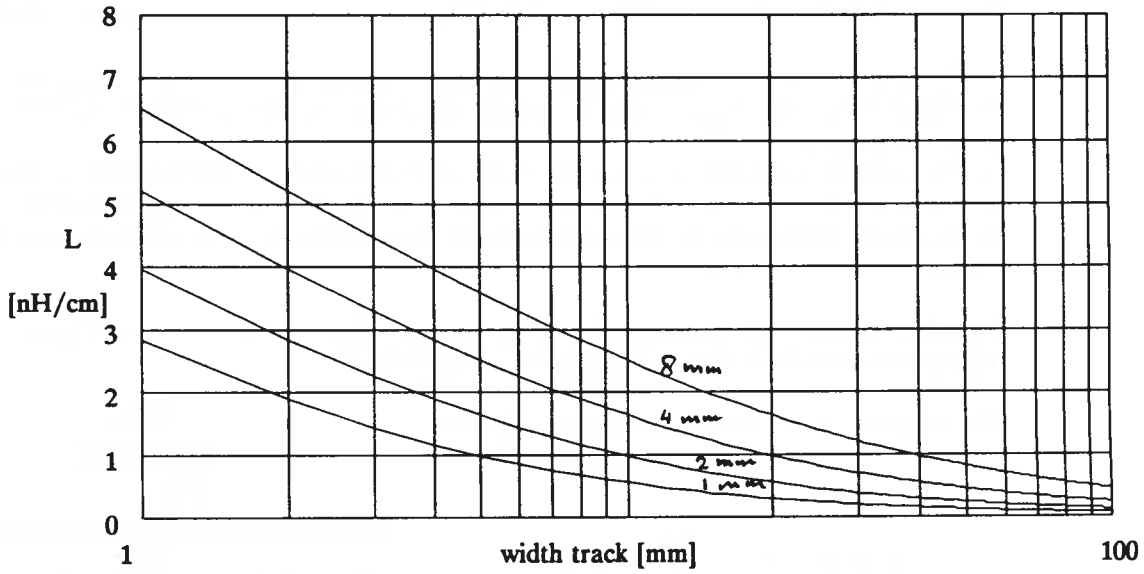

Figure 4.19: The return inductance L_{return} as function of the track width *w* with the distance *d* as a parameter.

In Figure 4.20 the ground or return inductance L_{return} is given in [nH/cm] as function of the distance d between signal and return conductor in [mm] with the width w_t in [mm] as a parameter.

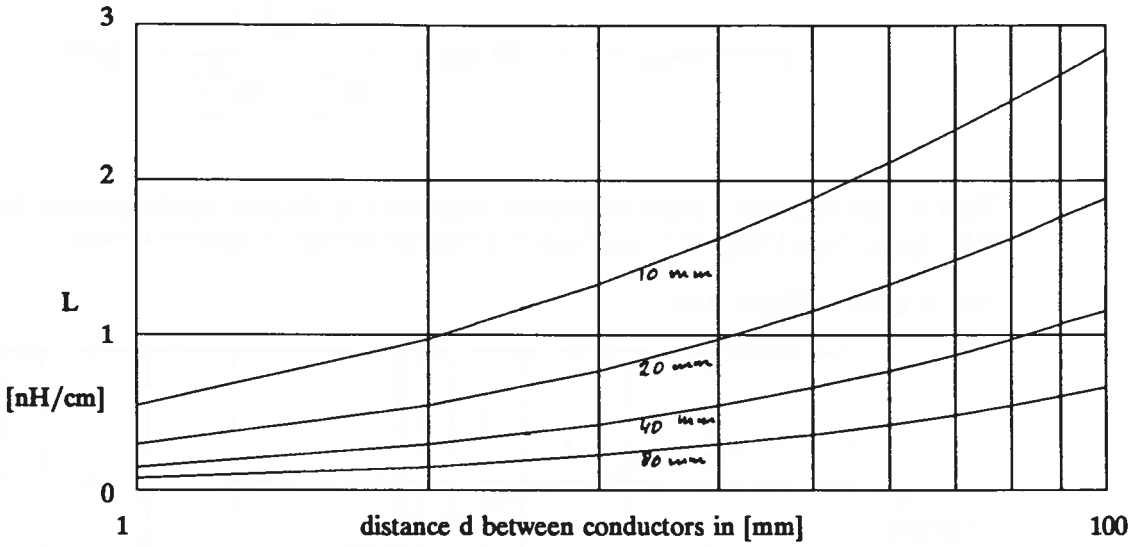

Figure 4.20: The return inductance L_{return} as function of the distance d with the track width w_t as a parameter.

As a conclusion, a better coupling by shortening the distance d between the signal and the return track, or by broadening the return track w_t, will result in a lower ground inductance.

In the preceding paragraph the 'attenuation' of the DM-CM transformed signal is determined by an asymmetry factor. This asymmetry factor is the ratio between the signal and return/ground inductance. Repeating these formulas:

$$L_{eff} = L_{signal} + L_{ground} \quad [H] \tag{4.58}$$

$$L_{signal} = (1 + asym) L_{eff} \quad [H] \tag{4.59}$$

$$L_{ground} = (1 - asym) L_{eff} \quad [H] \tag{4.60}$$

Because the attenuation in the pass band (and for normal termination) is equal to:

$$\frac{L_{ground}}{L_{ground} + L_{signal}} = \frac{1}{2} (1 - asym) \tag{4.61}$$

or in dB's:

$$attenuation_{[dB]} = - 6 + 20 \log(1 - asym) \quad [dB] \tag{4.62}$$

Wherein: asym = asymmetry factor ($0 \leq asymm < 1$) which is equal to:
0 for symmetry and equal to
0.99... for maximal asymmetry (practical, theoritical -> 1).

We can fill in the inductances of a signal and return conductor, determined using Formula 4.57, in Formula 4.61 and 4.62:

$$attenuation_{[dB]} = -6 + 20 \log\left(1 - \frac{\ln\left(\frac{d\,\pi}{w_r} + 1\right)}{\ln\left(\frac{d\,\pi}{w_r}\right) + \ln\left(\frac{d\,\pi}{w_s}\right)}\right) \quad [dB] \qquad (4.63)$$

Then we can construct a graph wherein the attenuation in the pass band is given as function of the ratio w_{ground}/w_{signal} (instead of L_{signal}/L_{eff}) at a constant distance d equal to 1.6 mm.

This is drawn in Figure 4.21.

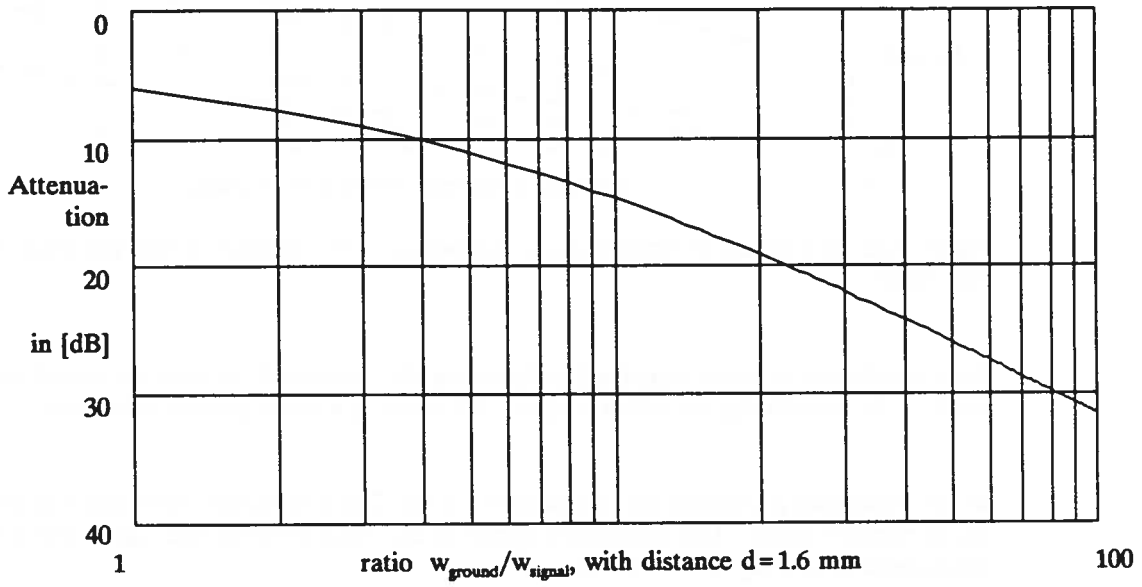

Figure 4.21: Attenuation of the ground lift voltage as function of the ratio width return track/ width signal track.

As we did in Paragraph 4.2.3 for the loop area A we can deduct a required asymmetry value

$$\frac{L_{gnd}}{L_{gnd} + L_{sig}} < \ldots.$$

to meet a certain emission limit.

This is a very complicated formula because several signals are a function of the frequency. Therefore this formula is given in Appendix 3.

4.3.7.APPLICATION AND COMPILATION OF THE COMMON MODE MODEL.

The model to calculate the common mode current and the resulting common mode radiated emission is build up using a two-wire transmission line and an antenna impedance.
In Figure 4.22 a basic circuit is drawn.

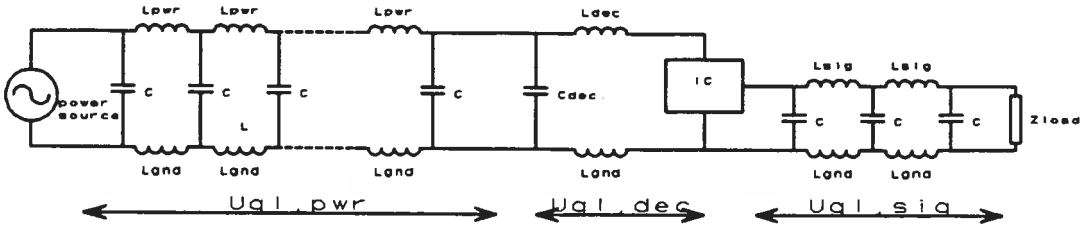

Figure 4.22: Basic circuit.

Three parts can be recognised:

$U_{gl,pwr}$ The ground lift voltage in the power supply circuit.
$U_{gl,dec}$ The ground lift voltage in the power supply decoupling circuit.
$U_{gl,sig}$ The ground lift voltage in the signal circuit.

The antenna impedance is nearly equal for these sources because the voltage drop due to the common mode current is negligible. This voltage drop is very small because it is determined by the (very small) common mode current and the (very small) 'antenna' impedance.
The ground lift voltages can be thought to be situated at the ends of the circuit, see Figure 4.23. Therefore, the length of the antenna l_{ant} in the formulas is always equal to that part in the circuit with the largest length.

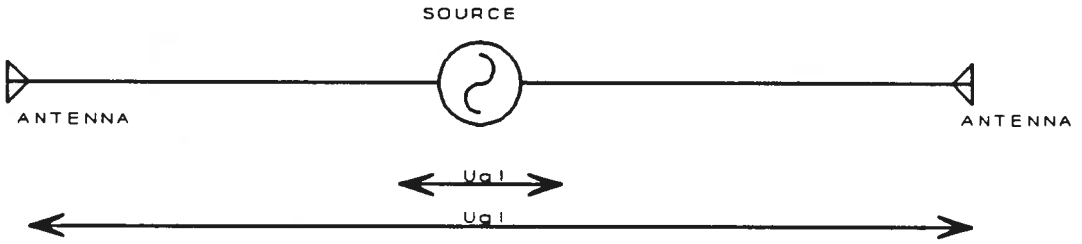

Figure 4.23: The antenna source voltage is situated at the end of the antenna.

As can be seen in Figure 4.22, The decoupling circuit is very important. When the decoupling capacitor was not present, all high frequency supply current would flow through the PCB.
Separated parts in an IC, such as an output buffer, are always consuming power, terminated or not. Therefore each power supply pin must be decoupled, preferably via a ferrite bead in the positive supply lead, and an appropriate capacitor between the supply leads.

Furthermore, as was shown in the preceding paragraphs for the signal transmission line, the power supply line must be made asymmetric too by using large ground (reference) planes and small positive supply leads. Possibly ferrite beads should be used.
The application of ferrite beads is well known, but never given a theoretical basis. Using the theories described in this report the effect of the ferrite beads (or micro-chokes) is obvious!

4.4. APPROXIMATIONS FOR MANUAL CALCULATIONS.

We will develop formulas for the electromagnetic differential and common mode radiation which is specifically for manual calculations. When simulating circuits (using circuit analysis software), the original formulas, Formula 4.8 and Formula 4.18, must be used!
The purpose of this paragraph is to get more insight into radiation problems.

4.4.1.DIFFERENTIAL MODE.

The basis is Formula 4.10, which is repeated here:

$$E_{dm[dB]} = -152+20\log(A)-20\log(r)+20\log(I_{dm})+20\log(f^2) \qquad [dB\mu V/m]$$

The differential mode current I_{dm} is equal to about the signal voltage divided by the load impedance plus the internal impedance of the generator or source:

$$I_{dm} = \frac{U_{sig}}{Z_i + Z_l} \qquad [A] \tag{4.64}$$

Wherein: U_{sig} = signal voltage, in [V],
Z_i = internal impedance of voltage source, in [Ω],
Z_l = load impedance, in [Ω],

It is possible to graphically construct the radiated emission spectrum. Only the factor f^2 and the differential mode current are frequency-dependant.
In Figure 4.24 an example of a current spectrum is given.

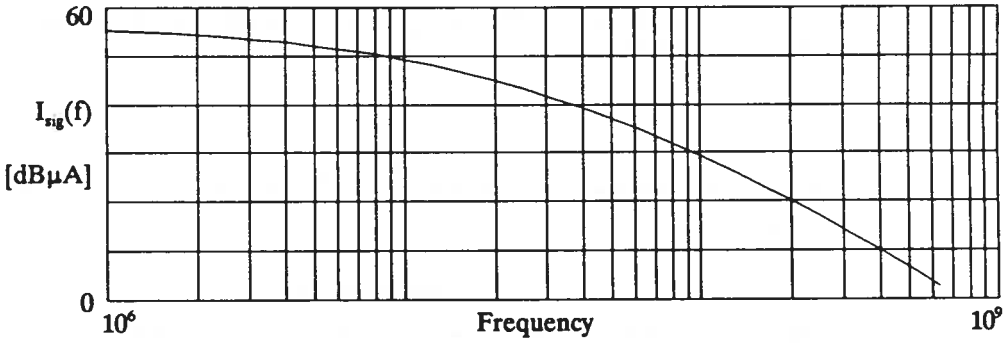

Figure 4.24: Frequency spectrum of the signal current, for I_{sig} = 1 mA, f0 = 10 MHz and f1 = 100MHz (see Appendix 3).

In Figure 4.25 the resulting radiated emission spectrum is given:

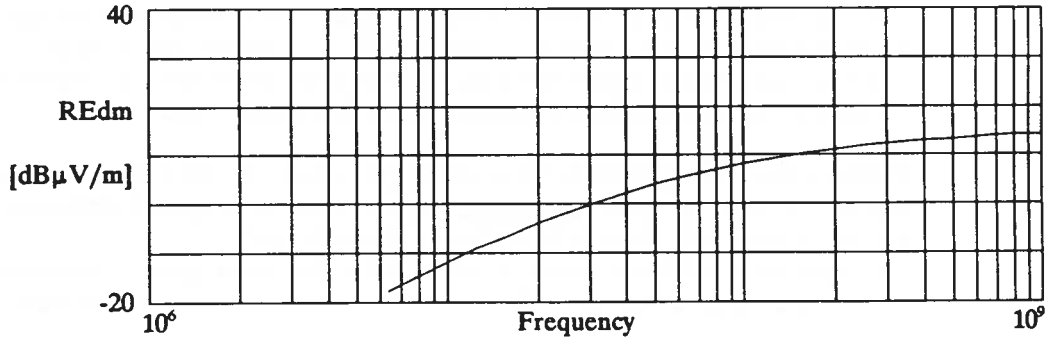

Figure 4.25: Radiated emission spectrum due to the DM current of Figure 4.24 for A = 1000 mm² and r = 3 m.

4.4.2.COMMON MODE.

We will use Formula 4.18 as a basis which is repeated here:

$$E_{cm} = \frac{1.15\ 10^{-6}\ f\ I_{cm}\ l}{r} \quad [V/m] \tag{4.65}$$

In Paragraph 4.3.1. and 4.3.5. it is found that, when maximal matching is achieved (when the impedance of the ground lift voltage is equal to the antenna impedance: $Z_{Ugl}=Z_{ant}$):

$$I_{cm} = \frac{U_{gl}}{2\ Z_{ant}} \quad [A] \tag{4.66}$$

as can be seen in Figure 4.26:

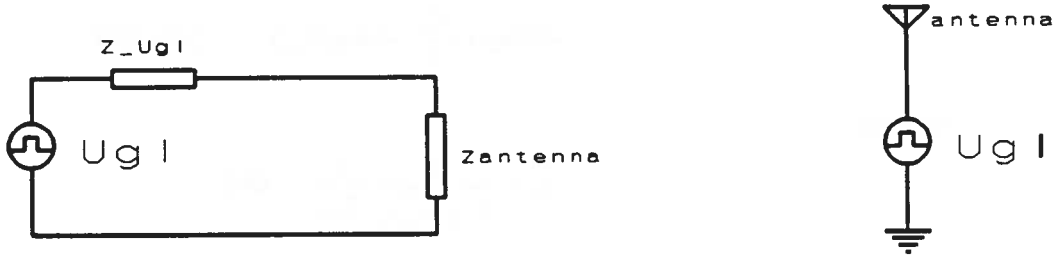

Figure 4.26: The ground lift voltage as a driving antenna source.

Combining Formula 4.65 and Formula 4.66:

$$E_{cm} = \frac{0.58\ 10^{-6}\ f\ U_{gl}\ l_{ant}}{r\ Z_{ant}} \quad [V/m] \tag{4.67}$$

Note: the length l_{ant} of the antenna must be used in the above mentioned formulas, hence in the formula for the cross-over frequency for the DM-CM transformation the length l_{pcb} applies to the length of the PCB track!!! When no interconnecting cables are attached then $l_{ant}=l_{PCB}$.

All legislative requirements and all measurements are carried out using logarithms (the electric fieldstrength unit is dBμV/m). Thus we can transform Formula 4.65 into:

$$E_{cm[dB]} = -5 + 20\ \log(\frac{f\ l_{ant}}{r}) + 20\ \log(U_{gl}) - 20\ \log(Z_{ant}) \quad [dB\mu V/m] \tag{4.68}$$

When the transmission line on the PCB is properly terminated then the ground lift voltage U_{gl} is simply determined only by the cross-over frequency f_c and the attenuation in the pass band, see Paragraph 4.3.5. When the termination is not 'neat' then aspects such as resonance and 40 dB/decade slopes must be considered, see Paragraph 4.3.5, which makes this compilation (of Formula 4.68) of the data more complicated.

Repeating Formula 4.52:

$$U_{g[dB]} = 20 \log U_{signal} + 20 \log(1-asym) - 6 - 20 \log(1+\frac{f_c}{f}) \quad [dBV] \tag{4.69}$$

and combining this with Formula 4.68 results in:

$$E_{cm[dB]} = -11 + 20\log(\frac{f\, l_{ant}}{r}) + 20\log(U_{signal}) + 20\log(1-asym) - 20\log(1+\frac{f_c}{f}) - 20\log(Z_{ant}) \quad [dB\mu V/m] \tag{4.70}$$

Rearranging it in frequency dependant and positive and negative parts:

$$E_{cm[dB]} = -11 + 20\log(1-asym) + 20\log(U_{signal}) + 20\log(\frac{f\, l_{ant}}{r}) - 20\log(1+\frac{f_c}{f}) - 20\log(Z_{ant}) \quad [dB\mu V/m] \tag{4.71}$$

Wherein:

$$f_c = \frac{c}{2\sqrt{\mu_r\, \epsilon_r}} \frac{1}{l_{PCB}} \quad [Hz] \tag{4.72}$$

as in Formula 4.47.

Instead of the asymmetry factor *asym* the ground inductance L_{ground} and the signal inductance L_{signal} can be used. Then Formula 4.69 becomes:

$$E_{cm[dB]} = -5 + 20\log(\frac{L_{ground}}{L_{ground}+L_{signal}}) + 20\log(U_{signal}) + 20\log(\frac{f\, l_{ant}}{r}) - 20\log(1+\frac{f_c}{f}) - 20\log(Z_{ant}) \quad [dB\mu V/m] \tag{4.73}$$

Note again: This formula is for manual calculations only. For computer simulations, use the basic formulas!!!

Now it is possible to graphically construct the radiated emission spectrum, as given in Figure 4.27. The x-scale is the logaritmic frequency scale. The y scale is linear. All graphs are drawn using the same scale.

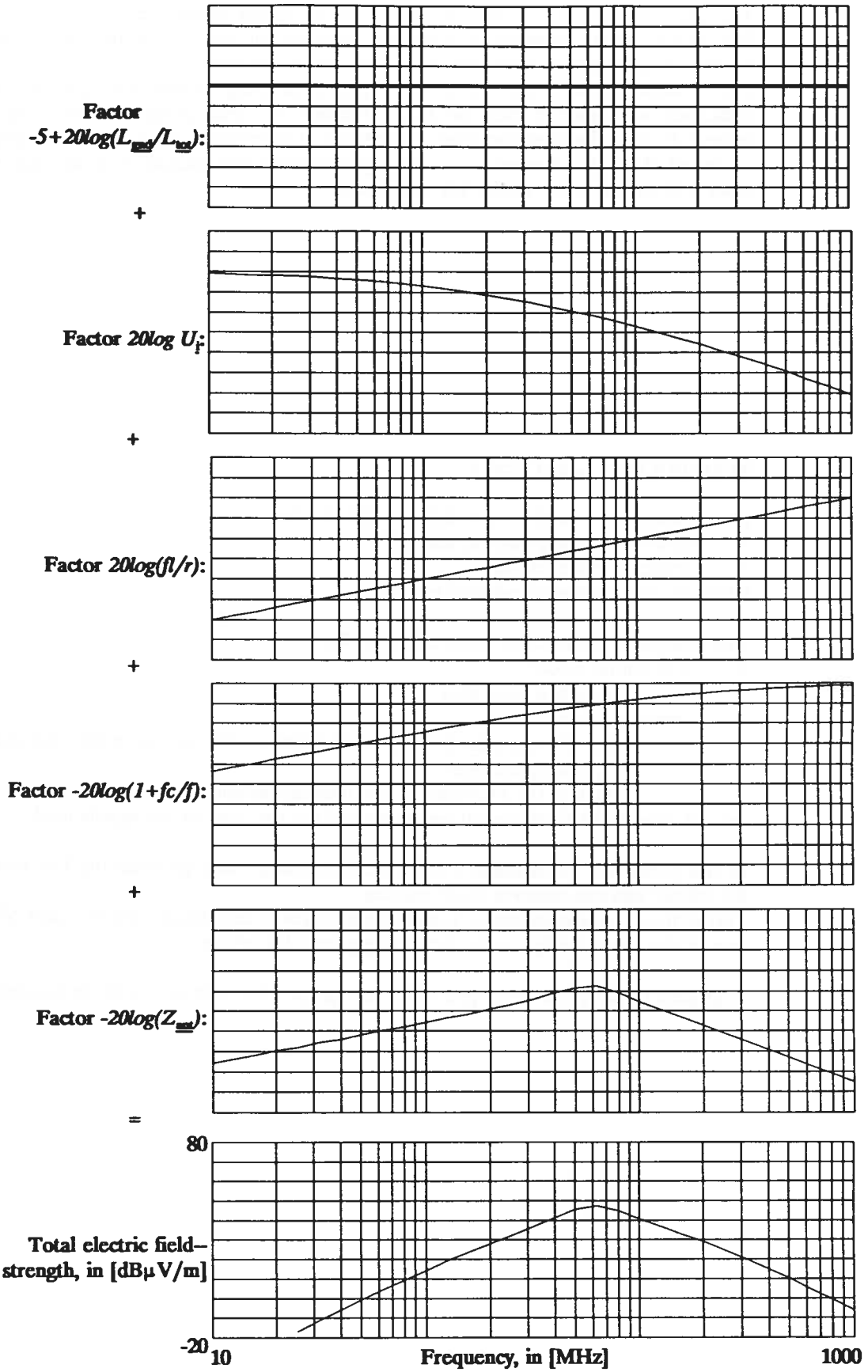

Figure 4.27: Graphic compilation of the data.

The same procedure for hand-calculations as explained above can be used for any transmission line, as long as the impedances (generator-characteristic-load) are in the same order of magnitude. So, basically, for power leads, the same formulas can be used.
For a construction where the power supply decoupling capacitor is placed nearby the power consumer, a correction must be made. Because the decoupling capacitance is very large with respect to the characteristic lead capacitance (transmission line), this line capacitance can be neglected. Then the current has more high-frequency components in it and the spectrum has an extra +20 dB slope due to this HF components.

SUMMARY OF CHAPTER 4.

In this chapter we developed models to calculate the:
+ differential mode current, and the
+ common mode current,
which are the sources of radiated emission.

The designable parameters appeared to be, for:
+ differential mode:
  - the current loop area.
+ common mode:
  - ratio of the ground (or return) inductance with respect to the total inductance (ground + signal inductance).
  - length of the PCB and, if any, interconnection cable.

and, of course, the fundamental frequency and the rise time of the signals used.

In this paragraph the antenna impedance is deduced, which provides the link between the ground lift voltage and the common mode current.
Furthermore the inductance of a large return track is calculated, which is part of the transformation of the signal voltage to the disturbing ground lift voltage.

A graphic technique is developed which can be used for 'rule of thumb' techniques.

5. VERIFICATION OF THE RADIATION MODELS.

In this chapter we will verify the developed models with two practical circuits. These circuits are respectively:

* Two symmetric transmission lines, driven by a clock generator IC, on a one-layer PCB.
* An asymmetric transmission line, i.e. a signal line above a ground plane, also driven by a clock generator IC, on a bi-layer PCB.

The verification is carried out using:

+ Manual calculations, using the models developed in Chapter 4.
+ Computer simulations, using the models developed in Chapter 4.
+ Radiated emission measurements.

In Chapter 6 a general method is given to analyse whether the EMI requirements can be met for an arbitrarily circuit. As an example, a multilayer (4 layers) PCB with a complex clock generator IC (CGIC) mounted on it is analysed.
A circuit simulator such as MINNIE is strongly recommended although in this chapter some manual calculations are carried out. The purpose of these manual calculations is to get more insight and so to deduce EMI design rules.

For the calculations and simulations we need to know the parameters for the differential mode and common mode radiation. Also we need to know the signal current I_{sig} or the signal voltage U_{sig} and the power supply decoupling current I_{dec}. Also the power supply current I_{pwr} must be known when the power supply decoupling capacitor is not mounted properly. For this test PCB this is not the case and we will neglect this part of the circuit. All these signals are frequency dependant, see for an explanation Appendix 3.
Furthermore the lay-out parameters, such as the loop area A and the track length l, must be calculated. Because we are always interested in the weakest link, we have to look only for the largest loop areas and track lengths. In Chapter 6 this is discussed in general.

In Paragraph 5.1 the test PCB's are described and the lay-out parameters are calculated. In Paragraph 5.2 some manual calculations are performed. In Paragraph 5.3 the simulation results are discussed while in Paragraph 5.4 the measurement results are discussed.
In Paragraph 5.5 the simulation and measurement results are compared with each other.

5.1. DESCRIPTION OF THE TEST-PCB's.

5.1.1. SYMMETRIC TRANSMISSION LINES.

Two symmetric transmission line are designed for a PCB. In Figure 5.1. the lay-out of one transmission line is depicted.

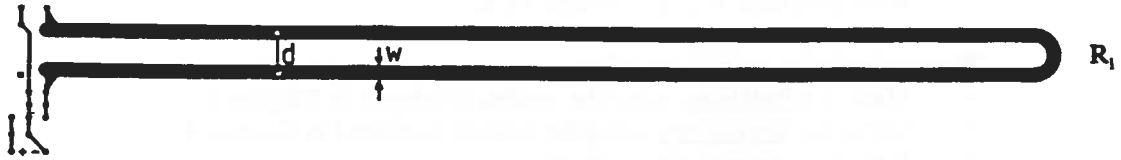

Figure 5.1: Print layout for symmetric test PCB.

The driving circuit consist of a clock generator IC, operating at 10 MHz, with a risetime τ_r≈2.2 ns and a fall time τ_f≈1.5 ns and an internal impedance Z_i= *220 Ω*. These times are very sensitive to the capacitive load. When the transmission line was attached then the risetime was τ_r≈4.0 ns and the fall time was τ_f≈3.6 ns The clock generator is supplied by a battery via a voltage stabiliser.
The output amplitude of the IC is 5V.
The circuit is drawn in Figure 5.2.

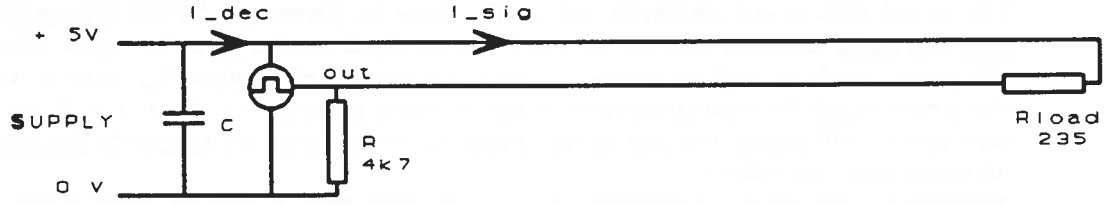

Figure 5.2: Circuit for test PCB.

(Note: for AC the + supply and 0 supply are both ground.)
Both transmission lines have a length *l* of 300 mm. The only difference between the two transmissionlines is the width *w* of the signal and return trace and the separation distance *d* (heart to heart) between them.
In the table below the differences between the transmission lines are given (note: the C and L_{self} are for the whole length *l* of the line and the inductance $L_{eff}/2$ is per lead):

	width w [mm]	separation d [mm]	C [F]	Lself [H]	Leff/2 [H]
PCB 1	1.0	3.06	4.2p	412n	155n
PCB 2	4.0	12.0	4.2p	330n	155n

Table 5.1.: Characteristics of symmetric test PCBs.

Because the ratio L_{eff}/C is constant, the characteristic impedance *Z* for all transmission lines is constant and equal to 270 Ω.

For differential mode radiation we are interested in the two loop areas:
I the loop area of the transmission line with the signal current I_{sig}, and
II the loop area of the power supply with decoupling current I_{dec}.

I The first loop area is calculated by $A_{sig}=(d-w)l$, which is:
$A_{sig}=$ $618\ mm^2$ for PCB1, and
$2400\ mm^2$ for PCB2.

II The power supply decoupling loop area is determined by the placing of the decoupling capacitor. Because the clock IC has a metallic housing, the boundary for us is the housing of the IC. Then, for both PCB's the largest current loop is the loop normal to the PCB. This area is:
$A_{dec}=$ $5.04 \times 7.6 = 38\ mm^2$.

For common mode radiation we are interested in the lengths of the PCB and the length of the antenna. For these examples this length is equal, and $l_{pcb}= l_{ant}= 300\ mm$.

The symmetric construction will cause a positive groundlift voltage U_{gl+} over the signal track and a negative groundlift voltage U_{gl-} over the return track, which are causing common mode radiation. At large observation or measuring distance these two groundlift voltage are thought to cancel the radiated emission so effectively the PCB is thought not to radiate common mode fields (see [Hardin 1991]). In Paragraph 5.4. we will prove that these symmetric PCBs will, contriraly to this assumption, also radiate a large amount of electromagnetic energy.

The test PCBs are antennas for electromagnetic energy itself. We are neglecting the cancelling effect of the two driving ground lift voltages and assume that only one is active (the other has the same strength but is 180 degrees phase shifted). The antenna impedance can be calculated using Formula 4.23.
The values are given in the table below:

	radius a≈w/2 [mm]	Cant [F]	Lant1 [H]	Lant2 [H]	Rant [Ω]
PCB 1	1.53	3.9p	104 n	26 n	k.f.f
PCB 2	2.0	4.2p	96.5 n	24 n	k.f.f

Table 5.2.: Characteristics of antenna of symmetric test PCBs.

Wherein: k = $3.95\ 10^{-16}$.

Lant1 is for creating the first resonance frequency (for $\lambda/4$) and Lant2 is for the second resonance frequency ($\lambda/2$).

5.1.2. ASYMMETRIC TRANSMISSION LINE.

The asymmetric transmission line consists of a 100 x 160 mm² bi-layer PCB. One layer is used as a ground plane. At the other side a 1 mm wide track is etched which is driven by a similair circuit as was used for the symmetric test PCBs

An interconnection cable is simulated by a 1.85 m long thin copper strip (so the total antenna length is 2 m) which is attached as an extra test to the ground plane.

In Figure 5.3. this test PCB is drawn in perspective.

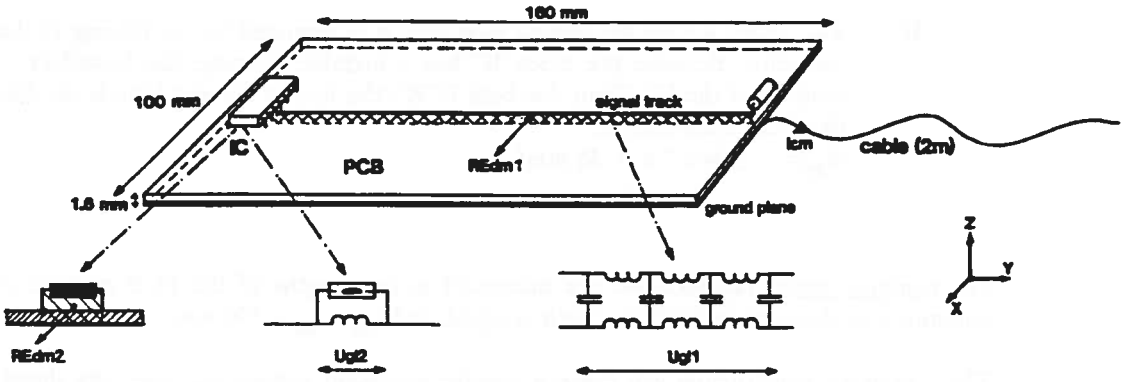

Figure 5.3: Asymmetric test PCB.

The driving circuit consist of a clock generator IC, operating at 1 MHz or at 10 MHz, with a risetime $\tau_r \approx 2$ ns and a fall time $\tau_f \approx 3$ ns and an internal impedance $Z_i = 220\ \Omega$. When the transmission line was attached the risetime was $\tau_r \approx 3{,}5$ ns and the fall time $\tau_f \approx 4$ ns. The output amplitude of the IC is 5V. The clock generator is supplied by a battery via a voltage stabiliser, see Figure 5.2 and Paragraph 5.1.

The thickness of the PCB, which results in the distance d for the formulas, is 1.6 mm. The length l of the transmission line is approximately 150 mm.

For differential mode radiation we are interested in the two loop areas

I the loop area of the transmission line (REdm1 in Figure 5.2.) with the signal current I_{sig}, and

II the loop area of the power supply (REdm2 in Figure 5.2.) with decoupling current I_{dec}.

(the loop area parallel to the ground plane can be neglected with respect to REdm2 because both areas are of similair dimension and the same current is flowing through them, but the loop parallel to the ground plane is much less effective due to the Quasi Active Shielding, see Paragraph 4.2).

I The first loop area is calculated by $A = d.l$, which is:

$$A_{sig} = 240\ mm^2.$$

II The power supply decoupling loop area is determined by the heigth of the clock IC, which is approximately 2.5 mm, and the width of the IC, which is approximately 7.5 mm, which results in a loop area:

$$A_{dec} = 19\ mm^2.$$

For common mode radiation we are interested in the ground lift voltage U_{gl}.
This ground lift voltage is determined by the inductances of the transmission line. Using Formula 4.57 results in ($l = 150mm$, $d = 1.6$ mm, $w_{ground} = 100$ mm and $w_{signal} = 1$ mm) gives:

L_{ground} = 1.47 nH,
L_{signal} = 53.9 nH,
$L_{effective}$ = 55.4 nH.

The capacitance C of the transmission line can be calculated from the formulas given in Appendix 4.
This results in $C = 9.3$ pF.
From L_{eff} and C we can obtain the characteristic impedance Z of this test PCB, which results in $Z = 77\ \Omega$.

The antenna impedance can be calculated using Formula 4.23. Two measurement sessions are performed. The first without the 'interconnecting cable' and the second with the interconnecting cable attached. These setups are only influencing the characteristics of the antenna. Because the ground plane is not a round conductor as was assumed in Formula 4.23, we will take for the radius a of the groundplane $a = w/2$.
The values are given in the table below:
(PCB- stands for: 'without interconnecting cable',
PCB+ stands for: 'interconnecting cable attached'.)

	radius, a≈w/2 [mm]	Cant [F]	Lant1 [H]	Lant2 [H]	Rant [Ω]
PCB -	50	55p	2.1 n	0.52 n	k1.f.f
PCB +	2	19p	948 n	237 n	k2.f.f

Table 5.3.: Characteristics of antenna of asymmetric test PCB.

Wherein: k1 = $1.12\ 10^{-16}$.
k2 = $1.75\ 10^{-14}$.
Lant1 is for creating the first resonance frequency (for $\lambda/4$) and Lant2 is for the second resonance frequency ($\lambda/2$).

5.2. MANUAL CALCULATIONS.

For manual calculations the formulas expressed in dB's are useful. Then we need the following two formulas, Formula 4.10 and Formula 4.73, which are repeated here:

$$E_{dm[dB]} = -152 + 20\log(A) - 20\log(r) + 20\log(I_{dm}) + 20\log(f^2) \quad [dB\mu V/m] \tag{5.1}$$

$$E_{cm[dB]} = -5 + 20\log\left(\frac{L_{ground}}{L_{ground}+L_{signal}}\right) + 20\log(U_{signal}) + 20\log\left(\frac{f\, l_{ant}}{r}\right) - 20\log\left(1+\frac{f_c}{f}\right) - 20\log(Z_{ant}) \quad [dB\mu V/m] \tag{5.2}$$

Wherein:

E_{dm}	=	electric fieldstrength due to differential mode current, in [dBμV/m],
E_{cm}	=	electric fieldstrength due to common mode current, in [dBμV/m],
A	=	current loop area, in [m^2].
r	=	measuring distance, in [m],
f	=	frequency, in [Hz],
I_{dm}	=	differential mode current, in [A],
U_{signal}	=	generator signal, in [V],
l_{ant}	=	length of the radiating antenna, in [m],
L_{gnd}	=	ground inductance, in [H],
L_{sig}	=	signal track inductance, in [H],
Z_{ant}	=	antenna impedance (|absolute value|), in [Ω],
f_c	=	cross-over frequency, in [Hz],

and Formula 4.47:

$$f_c = \frac{c}{2\, l_{PCB}\sqrt{\mu_r\, e_r}} \quad [Hz] \tag{5.3}$$

Wherein:

c	=	speed of light, 3.10^8 m/s,
l_{PCB}	=	length of PCB signal track,
e_r	=	relative permitivitty of PCB,
μ_r	=	relative permeability of PCB, usually equal to 1.

In this paragraph only examples are given for test PCB's which are terminated.
Formula 5.2 and 5.3 can be used because these are developed with the assumption that the transmission lines have a characteristic impedance which is the same order of magnitude than the generator impedance.

5.2.1. SYMMETRIC TRANSMISSION LINES.

As an example we will show only the PCB with 1 mm trackwidth (PCB 1).

DM Differential mode.

Using Formula 5.1 and knowing the areas *A*, using the legislative requirement E_{dm} < 100 dBμV/m @ 3 m distance (*r=3 m*) (see Chapter 4), all we need to know is the differential mode current I_{dm} as a function of frequency.

I_{sig} The signal current is equal to about the signal voltage level divided by the load impedance plus the internal generator impedance:

$$I_{[dm]} \approx \frac{U_{sig}}{Z_i + Z_l} \quad [A] \tag{5.4}$$

Wherein: I_{dm} = signal current, frequency dependant, in [A],
U_{sig} = signal voltage, U_{sig} = 5 V,
Z_i = generator impedance, Z_i = 200 + 0j Ω,
Z_l = load resistance, 235 Ω.

Then I_{dm} = *7.4 mA*.

Because the current is frequency dependant, see Appendix 3, the current amplitude must be corrected. The fundamental frequency *f0* is equal to 10 MHz, and the risetime is measured, and appeared to be τ_r = *4 ns*, so *f1* equals 80 MHz.

Now the differential mode signal current spectrum $I_{sig}(f)$ can be such as drawn in Figure 5.4:

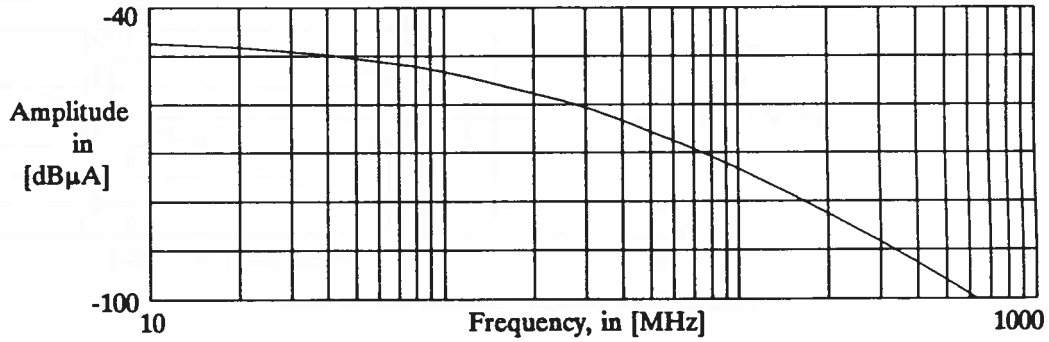

Figure 5.4: Frequency spectrum of Isig.

The complete radiated emission spectrum for the differential mode signal loop (A_{sig} = *618 mm²*) can now be drawn:

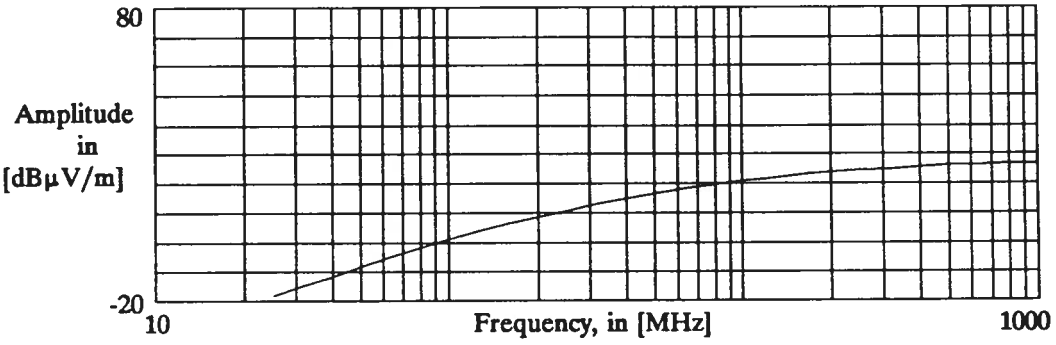

Figure 5.5: Radiated emission due to Isig.

I_{dec} Without any theory I state that the power supply decoupling current is:

$$I_{dec} \approx 2\ n\ I_{sig} \quad [A] \tag{5.5}$$

Wherein: n = number of outputs.
AND: the frequency spectrum is flat between I_{dm0} and I_{dm1} and falling off with a slope of 20 dB/dec for higher frequencies. This is drawn in Figure 5.6 (the upper line is I_{dec} and the lower line is I_{sig}):

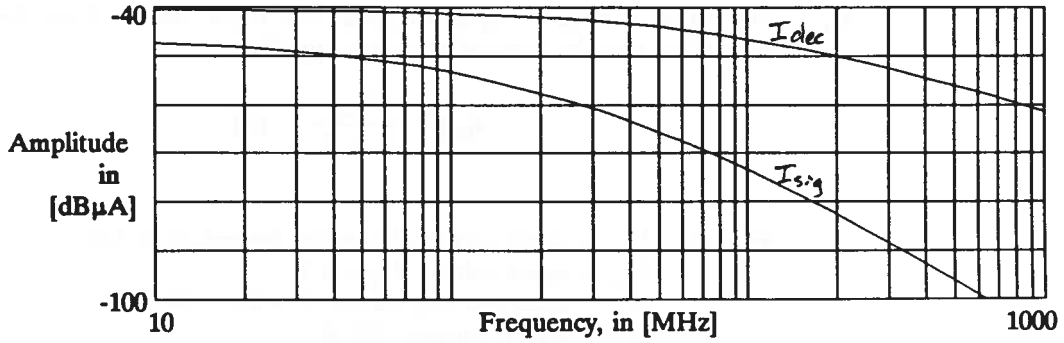

Figure 5.6: Frequency spectrum of Isig and Idec.

Then the complete radiated emission spectrum for the differential mode power supply decoupling loop (A_{dec} = *38 mm²*) can be drawn:

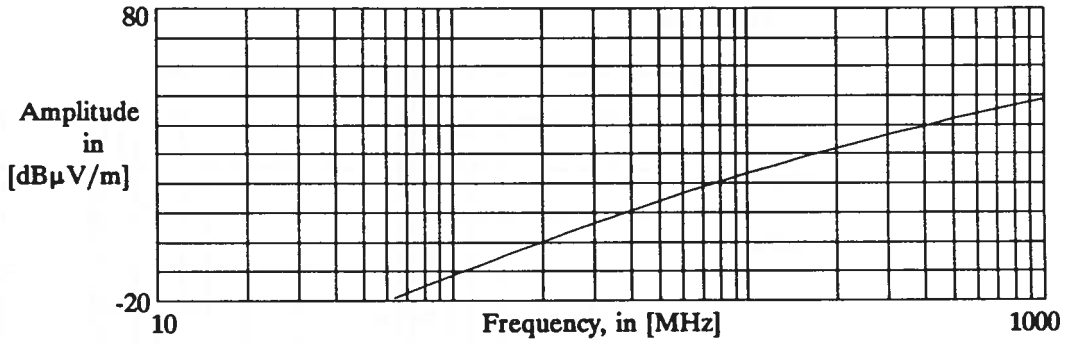

Figure 5.7: Radiated emission due to Idec.

CM Common mode.

Using Formula 5.2 and using the legislative requirement E_{cm} < 100 dBμV/m @ 3 m distance ($r=3\ m$) (see Chapter 4), and:

L_{gnd} = 77.5 nH,
L_{sig} = 77.5 nH,
U_{sig} = 5 V @ f0=10 MHz, falling with 20 dB/dec to f1=80 MHz, then 40 dB/dec,
l_{ant} = 0.3 m,
f_c = 250 MHz (l_{PCB}= 0.3 m and $\epsilon_r \approx 4$),

all we have to do is draw all data in a diagram, using the compilation method as described and drawn in Figure 4.23. This is done for PCB1 (with 1mm track width):

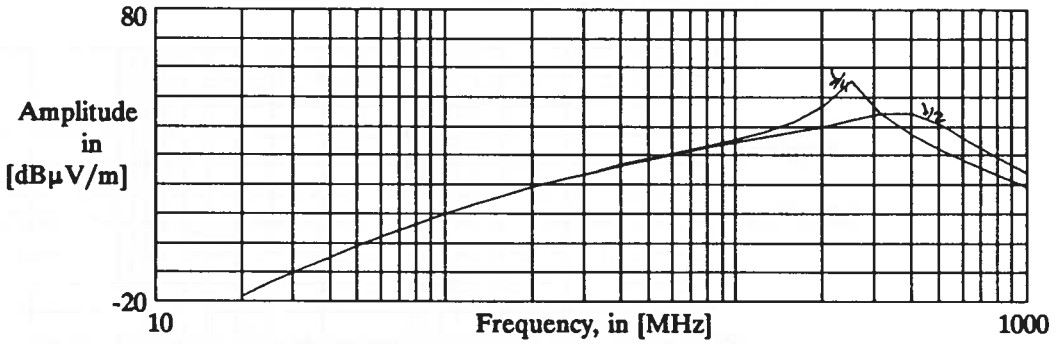

Figure 5.8: Radiated emission due to common mode current.

5.2.2. ASYMMETRIC TRANSMISSION LINE.

DM Differential mode.

Using Formula 5.1 and knowing the areas A, using the legislative requirement E_{dm} < 100 dBμV/m @ 3 m distance ($r=3\ m$) (see Chapter 4), all we need to know is the differential mode current I_{dm} as a function of frequency.

I_{sig} The signal current is $I_{dm} = 7.4\ 10^{-3}\ A$, see Paragraph 5.2.1.
The differential mode current spectrum is the same as that in Figure 5.4 in Paragraph 5.2.1.
The complete radiated emission spectrum for the differential mode signal loop ($A_{sig} = 240\ mm^2$) can now be drawn:

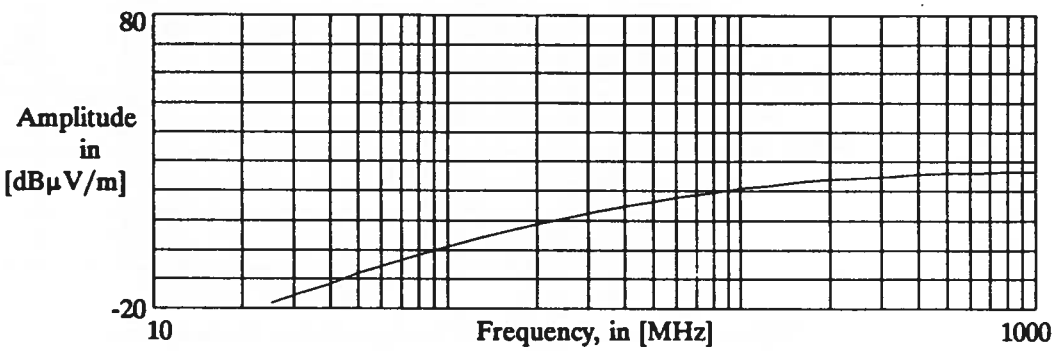

Figure 5.9: Radiated emission due to Isig.

I_{dec} The power supply decoupling current is also the same as found in Paragraph 5.2.1.
Then the complete radiated emission spectrum for the differential mode power supply decoupling loop ($A_{dec} = 15\ mm^2$) can be drawn:

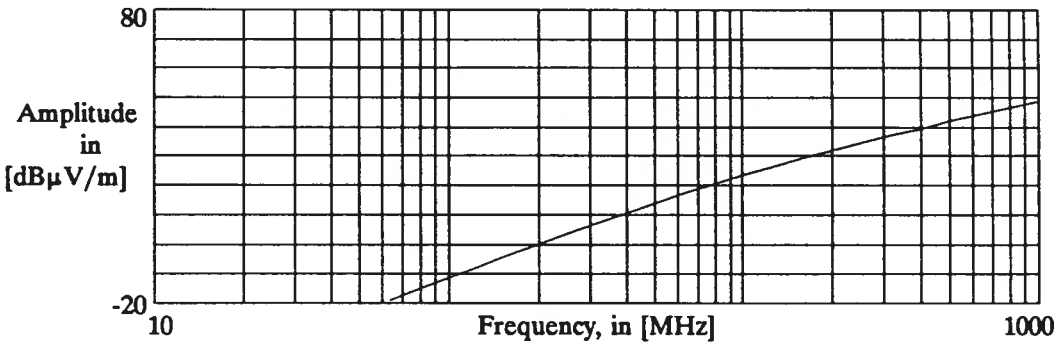

Figure 5.10: Radiated emission due to Idec.

CM Common mode.

Using Formula 5.2 and using the legislative requirement E_{cm} < 100 dBμV/m @ 3 m distance (*r=3 m*) (see Chapter 4), and:

L_{gnd} = 1.47 nH,
L_{sig} = 53.9 nH,
U_{sig} = 5 V @ f0=10 MHz, falling with 20 dB/dec to f1=80 MHz, then 40 dB/dec,
l_{PCB} = 0.16 m,
l_{ant1} = l_{PCB},
l_{ant2} = l_{PCB} + 1.85 m ≈ 2 m.
f_c ≈ 500 MHz (l_{PCB}= 0.15 m and e_r≈ 4),
all we have to do is draw all data in a diagram:

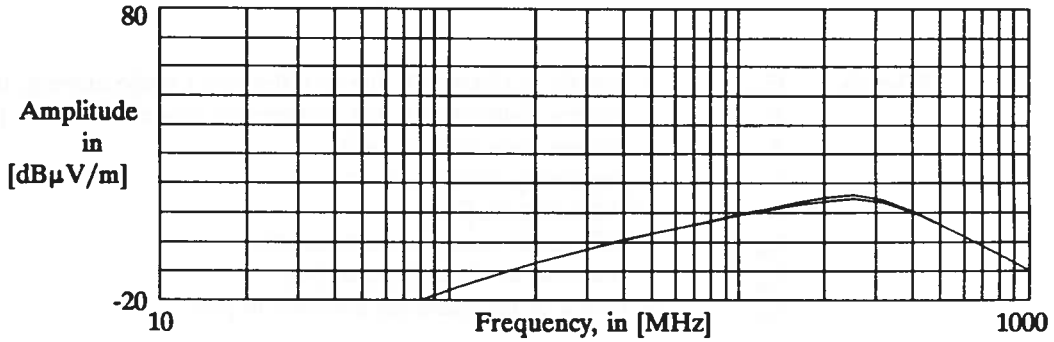

Figure 5.11: Radiated emission due to common mode current, without I/O cable attached.

This is done for a signal frequency *f= 10 MHz*. When using a clock generator IC with *f= 1 MHz*, then the whole spectrum is 20 dB lower.

When a interconnecting cable of length l_{ant}= *1.85 m* is attached then only a constant factor (due to the 20log(f.l_{ant}/r) must be added and the antenna impedance is changed. This antenna impedance is changed not in amplitude, but in frequency (but here we use another clockfrequency). The results for this change is drawn in Figure 5.13, using a 1 MHz clock generator:

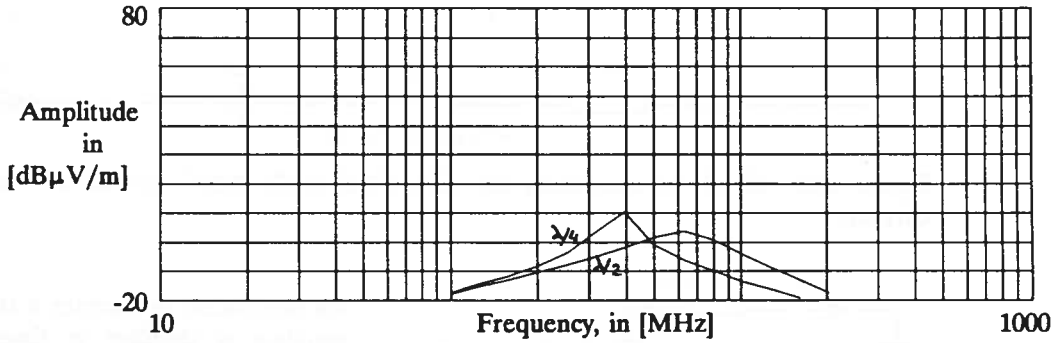

Figure 5.12: Radiated emission due to common mode current, with I/O cable attached, and using a 1 MHz clock generator instead of a 10 MHz type.

5.3. COMPUTER SIMULATIONS.

For computer simulations the basic formulas must be used. Then we need the following two formulas, Formula 4.8 and Formula 4.18, which are repeated here:

$$E_{dm} = \frac{24.16\ 10^{-15}\ f^2\ A\ I_{dm}}{r} \quad [V/m] \tag{5.6}$$

$$E_{cm} = \frac{1.15\ 10^{-6}\ f\ I_{cm}\ l_{ant}}{r} \quad [V/m] \tag{5.7}$$

Wherein:
- E_{dm} = electric fieldstrength due to differential mode current, in [V/m],
- E_{cm} = electric fieldstrength due to common mode current, in [V/m],
- A = current loop area, in [m^2].
- r = measuring distance, in [m],
- f = frequency, in [Hz],
- I_{dm} = differential mode current, in [A],
- I_{cm} = common mode current, in [A],
- l_{ant} = length of the radiating antenna, in [m],

The models used for the simulations are drawn in Figure 5.13 for the REdm and REcm due to the signal current, and in Figure 5.14 for the REdm due to power supply decoupling current. For these testboards the common mode current due to the groundlift voltage generated by the power supply decoupling current can be neglected.
In the first model only the value for the antenna inductance L_{ant} to create the different resonance frequencies must be changed. In the simulations only the $\lambda/4$ and $\lambda/2$ resonances are calculated.

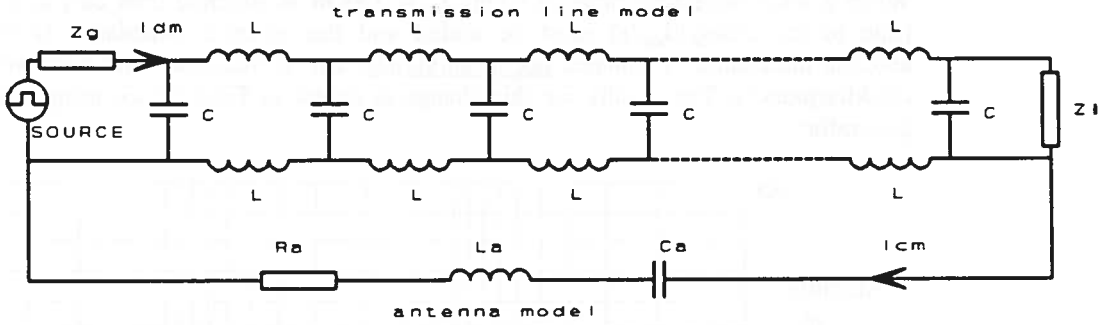

Figure 5.13: Model for simulating the differential mode signal current and the common mode current.

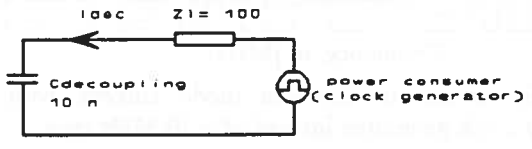

Figure 5.14: Model for differential mode power supply decoupling current.

As mentioned in Chapter 4 the best method to simulate is simulate in time domain for the differential mode currents and simulate in frequency domain for the common mode currents. Several simulations are carried out using MINNIE (and Pstar). The time domain data can be transformed to the frequency domain via the FFT algorithm in MATLAB and corrected with the layout parameters. However, because in this specific example the signal current spectrum is well known, the simulations are carried out in the frequency domain. The advantage is that now the results of the DM and CM simulation can be given in one graph.

The frequency domain data is corrected with the layout parameters in the *'results'* block of MINNIE.

When simulating in the frequency domain MINNIE is setup in the *'analysis'* block to give the voltage and current levels in dB and the phases in degrees.

In Appendix 5 the simulation results are given. The input data is already obtained in Paragraph 5.1. In the tables below the several different simulation results, together with the pagenumber in Appendix 5, are collected.

SIMULATION RESULTS DM & CM CAN BE FOUND IN AP.5 PAGE:		symmetric circuit PCB 1	PCB 2	asymmetric circuit
without I/O 'cable'	terminated with Z	2	4	6
	not terminated	3	5	7
with I/O 'cable'	terminated with Z	-	-	8
	not terminated	-	-	-

Table 5.3: Simulation results referring to pages in Appendix 5.

Note: the - sign stands for that no simulation has been carried out for this modus.

The PCB's are considered in three different setups:
1. Transmission line terminated with 2 resistors of 470 Ω in parallel (235 Ω).
2. Transmission line not terminated, so open ended.
3. Transmission line cut loose from the driving circuitry.

The aim of these tests were to measure the radiated emission due to common mode *REcm* and differential mode *REdm*, to measure only the *REcm* (the REdm from the power supply decoupling loop is herein neglected) and to measure the REdm of the power supply decoupling loop respectively.
Only for 1 and 2 simulations are carried out, because 3 is more or less a verification of the measurements.

5.4. RADIATED EMISSION MEASUREMENTS.

In Appendix 5 the measurement results are given. The measurements are carried out in a shielded anechoïc room with dimensions 12 x 7 x 6 m^3 (length x width x heigth m^3) according the legislative requirements, with a turntable and an antenna mast.

When measuring at a distance $r = 3\ m$ (as in our case) the results for frequencies lower than 80 MHz are not accurate. Furthermore, when measuring in a shielded enclosure the measured fieldstrength can be higher than when measuring on an open test-site, especcially in the low frequency range, but never will be lower!!
Another practical aspect is the so-called site-attenuation (SA). This SA is a correction factor for the site. Therefore below 80 MHz the measured values are always higher than theoretically expected.

In the tables below the several different measurement results, together with the pagenumber in Appendix 5 are collected.

MEAUSREMENT RESULTS DM & CM CAN BE FOUND IN AP.5 PAGE:		symmetric circuit PCB 1	circuit PCB 2	asymmetric circuit
without I/O 'cable'	terminated with Z	2	4	6
	not terminated	3	5	7
	transm. line disconn.	10	-	-
with I/O 'cable'	terminated with Z	-	-	8
	not terminated	-	-	9

Table 5.4 Electric field measurement results referring to pages in Appendix 5.

Note: the - sign stands for that no measurement has been carried out for this modus.

5.5. DISCUSSION OF THE VERIFICATION.

In this paragraph we will discuss the results of the manual calculations, the simulations and the measurements.
Only the first two resonance frequencies are simulated and calculated manual since these are the most interesting frequencies because of their highest amplitude.

Considering Page 2 of Appendix 5, where the simulation and measurement results are given, the first remarkable result is that the peak in the radiated emission spectrum in the simulation is not the same as in the measurements. When we calculate the relative permittivity, using the equation $L.C=\epsilon\mu$, then this results in $\epsilon_r=8.4$, and we know from experience that ϵ_r is equal to approximately 4 for this PCB!! When the relative permittivity is a factor 2 lower, then the cross-over frequency is a factor 1.4 higher (square root).
Furthermore, the amplitude differs. With respect to the measurement results:

* the simulation results are approximately 20 dB too high,
+ the manual calcultions are within 10 dB with the measurement results.

Also the common mode radiation is in the simulations higher than the differential mode radiation. Because we are using worst-case models, the emission level cannot be higher than is simulated, so we must conclude that a symmetric transmission line still radiates far more than generally assumed, due to the common mode current.

The results given on Page 3 of Appendix 5 prove that without any load connected to the circuit (and no differential mode current available at the end of the line), the test PCB still radiates as much as it does with a load attached.

On Page 6 the asymmetric PCB results are given. Again the amplitude levels differ. With respect to the measurement results:

* the simulation results are approximately 20 dB too high,
+ the manual calculations are within 10 dB with the measurement results.

When we consider the results on Page 8, we see that the simulation results results are within a few dB with the measurement results, while the manual calculations give a 20 dB underestimated value. Another remarkable result can be seen in the measurement graph. The exact resonance frequencies are a little lower than theoretically deduced. This is caused by the 'hat-capacitance' of the ground plane of the PCB with respect to the wire. In communication antennes such a 'hat' is used to lower the resonant frequency of the antenna, which is also the case here.

When a thicker I/O cable is used, then the capacitance is larger. The result in the frequency spectrum is that the radiated emission is more broadband with a thicker cable than using a thin cable. This is in agreement with antenna theory.

The assumption that the power supply decoupling current has an extra factor f in it, as is made in the deduction of the formulas for manual-calculations, is propably overkill since this leads to very high differential mode radiation for frequencies where the parasitics of the bonding leads (>500 MHz) are more dominant.

A peculiar phenemenon is that there is a large difference (approximately 20 dB) between the simulation results and the manual-calculations, while the input parameters are similar. The only difference between these two methods is that for manual-calculations more simplifications are used.

GENERALLY

* The simulation results are very accurate when the 'antenna' is a thin wire. When the PCB forms the antenna by itself, then the measured fieldstrength is 10 to 20 dB lower than the simulated fieldstrength.
  Therefore the antenna impedance of a PCB should be further investigated.

* The common mode emission dominated the radiated emission behaviour of the test PCB's. Therefore, all radiated emission programs which are using only differential mode models are virtually worthless.

* The common mode emission dominates also the EMI performance of symmetric PCB's.

* The effective relative permittivity can influence the radiated emission behaviour in such a manner that the largest emission peaks are at other frequencies than expected.

* The simulations always yield the worst case situation. The practical EMI performance will always be better (=lower radiated emission level) than is simulated, when the proper models are applied.

* Whether a load is attached at the transmission line or not, the EMI performance is hardly influenced (within a few dB).

SUMMARISING CHAPTER 5.

In this chapter we have discussed some practical test circuits. The expected radiated emission is calculated using manual-methods, with the purpose to get a better feeling for the several parameters.
Furthermore the test circuits are simulated and the radiated emission is measured in a shielded anechoïc room.

In the next chapter we will discuss general rules to analyse practical circuits in the design phase of the product. A specific integrated circuit is used as an example to show these general rules.

6. HOW TO TACKLE PRACTICLE CIRCUITS.

In this chapter we will discuss how to treat a practical circuit. This is one of the most difficult problems in EMI engineering. Using design rules, such as described in Appendix 7 give much insight and can be used in a step-by-step process with several proto-type PCB's.
The best method is to work in a structured way, to start in the definition phase of a product.
When the EMI measures are considered early then solutions are plentiful, see Figure 6.1.

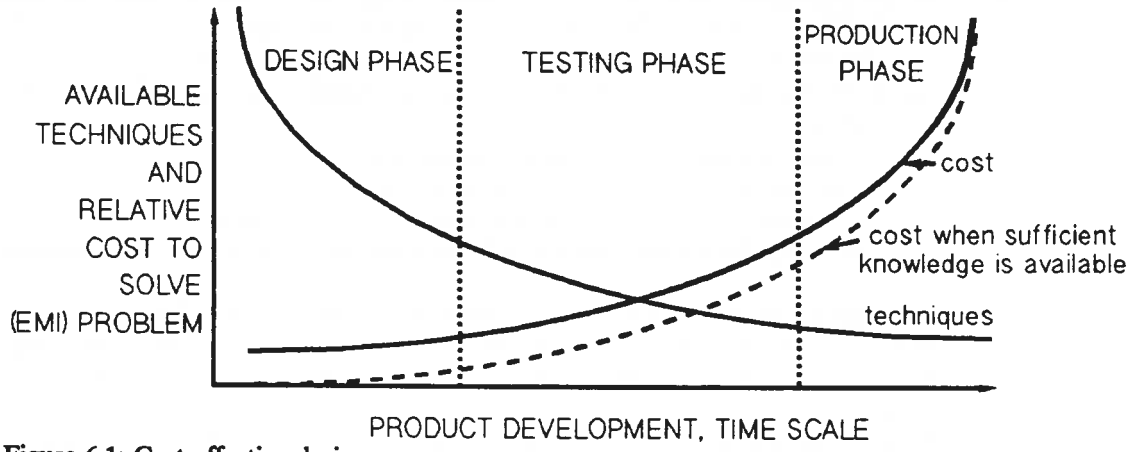

Figure 6.1: Cost effective design.

As can be seen in Figure 6.1, the more knowledge is available, the cheaper EMI precautions can be applied.

In Paragraph 6.1 we will discuss the several project phases in the development of a product. In Paragraph 6.2 the technique to calculate the EMI performance of a product in the design phase is discussed. In Paragraph 6.3 these techniques are applied on a practical circuit. In Paragraph 6.4 we will discuss some measures to improve the performance of that practical circuit.

6.1. PROJECT PHASES AND EMI MEASURES.

We can split the development of a new product in several stages:

- definition phase,
- development phase,
- proto-type phase,
- production phase.

\+ In the definition phase one has to decide what signals will be used, prescribed by the functional requirements. Because the requirements are not very specific, the clockfrequencies, rise times etcetera are often much higher than really needed.
For EMI the parameters which influence functionality are given below, with the EMI-preference:

- clockfrequency f as low as possible,
- rise time τ_r as long as acceptable,
- IC family as low power $P=U.I$ as possible,
- grouping clock areas: clock(s) must be used locally to prevent large antenna lengths.

\+ In the development phase one has to decide what type of PCB technology will be used. Until now this choice is based on rules of thumb and the experience of the (EMI) engineer, if any EMI engineer is involved. In the next paragraph quantitative methods using models developed in Chapter 4 are given.
Because the cross-over frequency (see Chapter 4) is very high for IC's these appear to be of less interest with respect to PCB when considering the inter-EMI effects.
The parameters which can be influenced in this stage of the project are:

- PCB technology, mono-, bi- or multilayer PCB,
- print layout the current loop areas must be as small as possible,
- power supply decoupling proper decoupling creating a loop as small as possible,
- interconnection cables cables must be connected to the reference of the PCB.

\+ In the proto-type phase it is possible to perform some measurements. This must be treated very carefully because another cable routing can result in a factor 10 more or less radiation! Therefore only some insight in the EMI performance can be obtained. It is possible to perform measurements according the prescribed test methods, such as on a open test site. In the proto-type stage it is often easier to use simpler methods, such as measuring the common mode current in interconnection cables.
The measurement results can necessite a re-design.

\+ In the production phase only the so-called crash methods can be used. Also when re-design in the proto-type phase is not cost-effective then the following methods can be used.

- ferrite beads over interconnection cables,
- 'destroying' of the antenna (the radiating parts) by shielding the product,
- shorting the ground lift voltage U_{gl} via a reference plane,
- creating a better coax construction to force the electromagnetic field between the signal- and return conductor.

Summarising, the part where the designer has most influence is during the design phase of the product. Quantitative methods must be available to base choices for specific technologies and reduce the costs.

6.2. QUANTITATIVE METHODS.

All the measures described in Paragraph 6.1 and Appendix 7 are qualitative. For really cost-effective design we need the quantitative methods described hereafter.
As described in Chapter 4 two different types of radiation are causing electromagnetic emission: the differential- and common mode current. The formulas developed there are repeated here:

$$E_{dm} = \frac{24.16\ 10^{-15}\ (f^2\ A\ I_{dm})}{r} \quad [V/m] \tag{6.1}$$

$$E_{cm} = \frac{1.15\ 10^{-6}\ f\ I_{cm}\ l_{ant}}{r} \quad [V/m] \tag{6.2}$$

$$I_{cm} = \frac{U_{gl}}{2\ Z_{ant}} \quad [A] \tag{6.3}$$

Wherein:
- E_{dm} = electric fieldstrength due to differential mode current, in [V/m],
- E_{cm} = electric fieldstrength due to common mode current, in [V/m],
- A = current loop area, in [m^2].
- r = measuring distance, in [m],
- f = frequency, in [Hz],
- I_{dm} = differential mode current, in [A],
- I_{cm} = common mode current, in [A],
- U_{gl} = ground lift voltage, in [V],
- l_{ant} = length of the radiating antenna, in [m],
- Z_{ant} = antenna impedance (|absolute value|), in [Ω],

For the circuit designer without EMI experience it is very difficult to determine the designable parameters and how these can be adjusted.
Fortunately in EMI technology the weakest link defines the EMI performance. The reasons for this are:

- Only signals with the same order of amplitude (and correlated) will result in a higher total signal. Signals which are an order of magnitude lower in amplitude than other signals (= -20 dB) can be neglected.
- Several signals can only add when they are completely correlated. For instance, clocksignals are correlated signals but data- and address signals are weakly correlated. Correlated signals have all their energy concentrated in narrow frequency bands consisting of the fundamental plus the harmonics.

Therefore we are only interested in the largest current loop areas, the largest common mode current etcetera.

Differential mode:
For differential mode radiation we are interested in the current loops. Trying to control each loop area formed by signal and power supply decoupling currents is a formidable job. However, it is not necessary to handle all loops individually. The most critical loops are those carrying the system clock(s) and those decoupling the clock circuit(s) because they are the primary sources of radiation. The power supply decoupling loop can be controlled by decoupling capacitors placed next to each IC.
Line and bus drivers may also be offenders since they carry high currents but there energy is more broadband with less energy per unit bandwidth.
Address and data buses and other miscellaneous signal leads are secondary sources of radiation. Not as important as the clock leads their loop areas should be kept to a minimum, by providing at least one signal return lead adjacent to the least significant address lead.

In general:
- each loop must be made as small as possible by providing a return lead adjacent to a signal lead. A simple way to achieve this is using power planes or power grids, when the return is led via the ground.
- each logic IC must be decoupled by a decoupling capacitor.

In Figure 6.2 the loop currents which can cause differential mode radiation are drawn schematically:

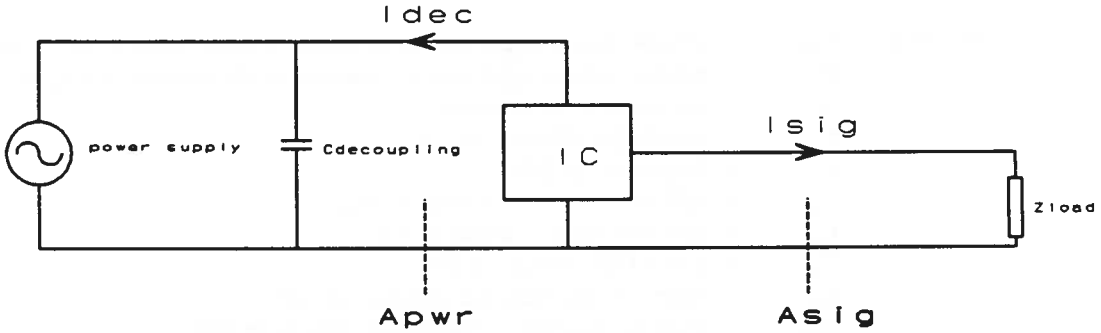

Figure 6.2: Loop currents with their loop areas causing differential mode radiation.

To determine the largest loop area(s) which defines the radiation behaviour:

I. I_{sig} For clock signals:
   1. Determine the area A_{11} of the largest clock signal loop.
   2. Determine if any loops with exact the same clock signal have the same order of dimension. Then these areas can be added: $A_{tot} = A_{11}+A_{12}+A_{13}$....
      Loop areas with area smaller than $0.1*A_{11}$ can be neglected.
   3. Determine the frequency spectrum (I=f(frequency)), see Appendix 3, of the clocksignal.
   4. Determine the differential mode fieldstrength by means of Formula 6.1.
   5. When the loop is nearby a conductive plane then the fieldstrength level must be corrected by the quasi active shielding (QAS), see Paragraph 4.2.

II. I_{sig} For other signals, such as address and data signals, the same procedure can be carried out but this is only of interest when the loop area A is more than a factor 3 greater than the total clock loop area A_{tot}.

III. I_{dec} For the power supply decoupling loop of those parts which are using the system clock(s) the steps I1-6 must be followed, with an exception for step 3. Since the power supply decoupling current frequency spectrum is not known, the frequency spectrum must be estimated, maybe by simulations,. This is explained in Appendix 3.

IV. I_{dec} For other signals, such as address and data signals, the same procedure III can be carried out but this is only of interest when the loop area A is more than a factor 3 greater than the total clock loop area A_{tot}.

The total differential mode radiation is the maximum of I+II(correlated) or III or IV!!

Common mode:
A similar procedure as described for differential mode radiation must be used for the common mode radiation.
Now we are interested in:

* the current path lengths:
  + the clock signal lead length l_{sig},
  + the power supply decoupling current path length l_{dec} and
  + the power supply current path length l_{pwr}.

The second important parameter is:

* the inductances:
  + the inductance L_{sig} of the signal lead,
  + the inductance L_{gnd} of the ground or return lead,
  + the inductance L_{dec} of the power supply decoupling path, and
  + the inductance L_{pwr} of the power supply leads for each power consuming component.

Furthermore:

* the length l_{ant} of any interconnection leads which can be driven by any ground lift voltage U_{gl} must be determined.

All these parameters are drawn in Figures 6.3 and 6.4 below:

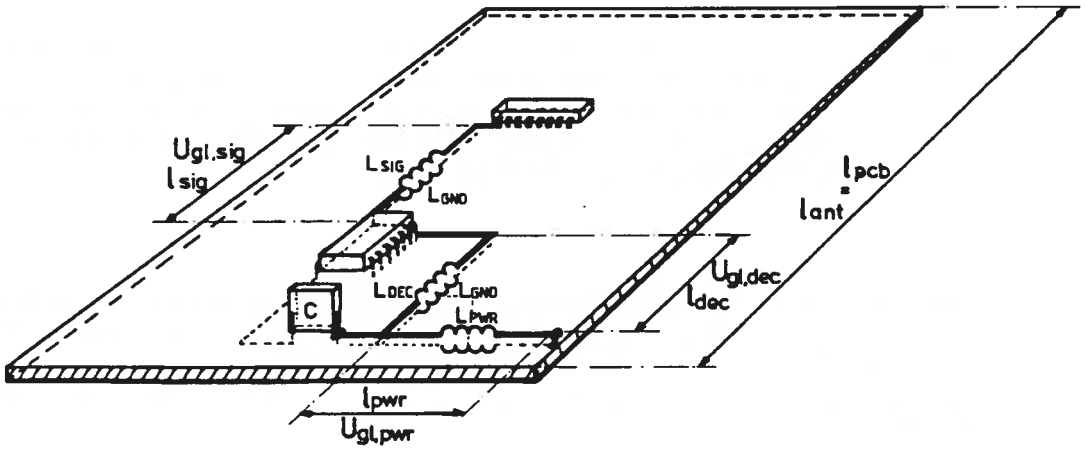

Figure 6.1: The common mode radiation sources.

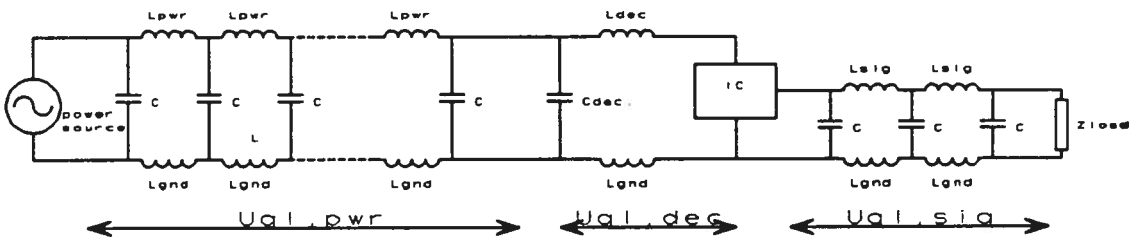

Figure 6.4: The common mode radiation sources.

The following procedure must be carried out (in order of importance) for the clock signals, the line and bus drivers, the address and data signals and other miscellaneous signals.

$U_{gl,sig}$

1. Determine the length of the clock signal track(s). When not known, use the length l_{PCB} of the PCB.
2. Only when several clock signals from the same source are laid parallel then correct the fieldstrength level later, after step 6, by multiplying the fieldstrength with the number of the parallel leads.
3. Determine the length l_{ant} of any antenna (interconnection cables).
4. Determine the inductances L_{gnd} and L_{sig}.
5. If possible, determine the antenna impedance Z_{ant}. When this is not known, use $Z_{ant} = 50\ \Omega$.
6. Determine the common mode fieldstrength by using Formula 6.2.

$U_{gl,dec}$ A similar procedure must be followed for the power supply decoupling signal I_{dec}. The main problem is however that the driving voltage U_{sig} is unknown because now the driving voltage is a function of the power supply decoupling current. Therefore it is strongly recommended to simulate these parts of the circuit.

When the decoupling capacitor is well mounted and the capacitor is well choosen (for instance a ceramic surface mounted type) and all power consuming circuits are decoupled locally (nearby the device) then we can neglect the power supply path. Otherwise we must consider this path as well.

$U_{gl,pwr}$ When the supply lead is long with respect to the wavelength (see Formula 4.36) then the supply current flows through a transmission line, see Figure 6.3 and 6.4.
Also when an active output buffer is not connected, then still supply current will flow to operate the buffer. Therefore, the same procedure as mentioned for $U_{gl,sig}$ must be used to calculate the radiated emission.

I state that not only for the signal leads but also for the supply leads a large asymmetry must be used!! So, when applying multilayer PCB's it is better to use ground planes and for all other signals, including the supply, using thin, i.e. high-inductive leads.
Basically, any power consuming part (and also not-connected but active buffers) must always be decoupled locally.

6.3. APPLYING THEORIES ON A PRACTICAL CIRCUIT.

A multilayer PCB is used as the carrier for a complex clock generator IC (CGIC) mounted in a PLCC 44 (leadless chip carrier) housing. The IC is mounted in the centre of the PCB, which has dimension of 200 x 250 mm^2.
In Figure 6.5 the thickness of the different layers in the multilayer is drawn.

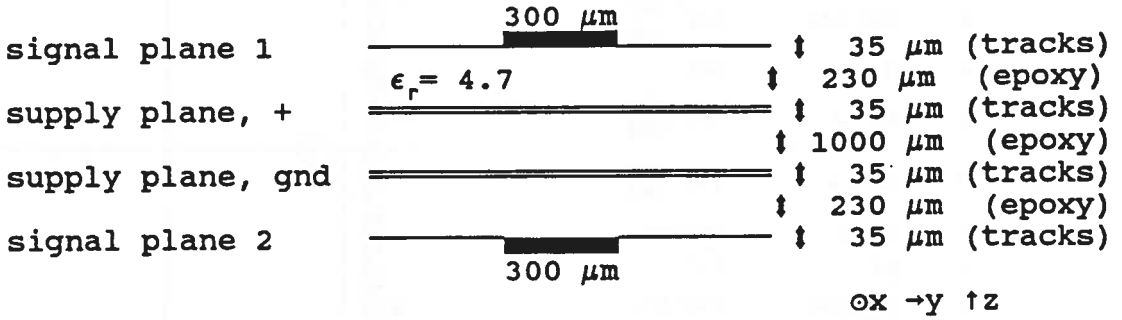

Figure 6.5: Cross section of multilayer PCB.

The CGIC has 10 outputs operating at 27 MHz, 3 outputs operating at 20 MHz and 1 output operating at 40 MHz. The output impedance of all outputs is about 60 Ω in low state and about 70 Ω in high state. The transmission lines on the PCB have a characteristic impedance Z equal to 60 Ω.

For differential mode we are interested in the largest loop areas for the signal loop and for the power supply decoupling loop:
A_{sig} the loop area of the transmission line,
A_{dec} the power supply decoupling loop area.

Because the power supply is also decoupled via a small on-chip decoupling capacitor this decoupling loop will not conduct all power supply decoupling current.
Furthermore the choice of the pins has a large influence on the loop area. For this CGIC all pins are selected so that the current loops will be as small as possible.

In Figure 6.6 the housing (PLCC) of the chip is drawn. The dimension of the chip is 3.8 x 3.8 mm^2. From this figure the dimensions of the loops can be determined.

Now, on the PCB the following current loops can be deduced:
1. loop formed by transmission line above the ground plane, *A1 = 100x.23 mm²*.
   (IC in centre of board with dimension ~ 200x250, so length *l* transmission line is ≈100 mm, and heigth above return (see Figure 6.5) is 230 µm.)

On the IC the following loops can be deduced:
2. loop formed by transmission line between chip and points where the IC pins are making contact with the PCB, in x/y- and z- direction.
3. loop formed by the power supply decoupling loop, between the chip and points where the IC pins are making contact with the PCB.

The heigth of the IC above the ground plane is approximately 5 mm.
Summarizing:

$A_{sig,pcb,x}$		= 23 mm^2,
$A_{sig,ic,x}$	= 1.27x5	= 6.4 mm^2 (separation between two pins x heigth IC)
$A_{sig,ic,z}$	= 1.27x1.9	= 2.4 mm^2 (separation pins x distance IC-pin to chip)
$A_{dec,ic,x}$	= 1.27x5	= 6.4 mm^2,

Item	Millimeters	Inches
A	17.5 +.2	.689 ±.008
B	16.58	.653
C	16.58	.653
D	17.5 ±.2	.689 ±.008
E	1.94 ±.15	.076 $^{+.007}_{-.006}$
F	.8	.024
G	4.4 ±.2	.173 $^{+.009}_{-.008}$
H	2.8 ± .2	.110 $^{+.008}_{-.008}$
I	.7 min	.028 min
J	3.6	.142
K	1.27 [TP] Note 1	.050 [TP]
L	.7	.028
M	.40 ± .10	.016 $^{+.004}_{-.005}$
N	15.50 ± .20	.610 $^{+.009}_{-.008}$
O	.15 Note 2	.006
P	1.0	.040
Q	R .8	R .031
R	.20 $^{+.10}_{-.05}$	.008 $^{+.004}_{-.002}$

te:

Each lead centerline is located within .12 mm [.005 inch] of its true position [TP] at maximum material condition.

Flat within .15 mm [.006 inch] total.

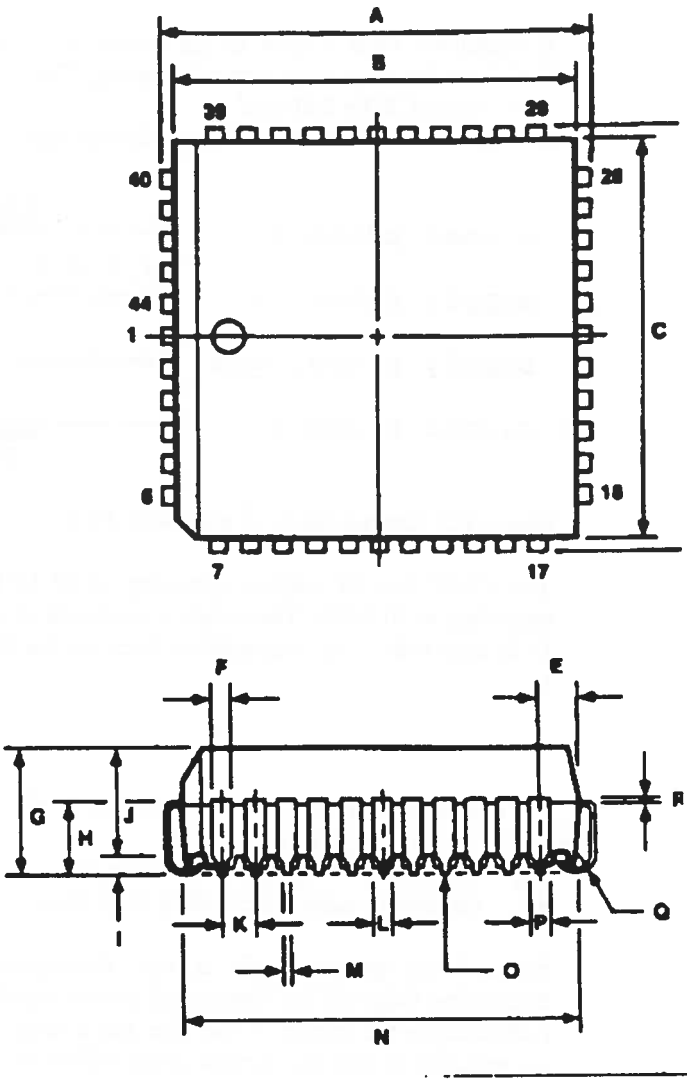

Figure 6.6: 44-pen plastic leaded chip carrier (44-PLCC).

$A_{dec,ic,z}$ = 1.27x1.9 = 2.4 mm^2.

In EMI we are only interested in the weakest link, so the largest area. This results in :

A_{sig} = 23 mm^2,
A_{dec} = 6.4 mm^2,

and we can neglect the other areas.

For common mode radiation the parts where a groundlift voltage can be created are:

$U_{gl,sig}$ over the whole area of the PCB, where the return current flows through the groundplane,

$U_{gl,dec}$ the area below the IC where only a part (on-chip power supply decoupling capacitor takes the largest portion of the HF decoupling current) of the power supply current decoupling current flows,

$U_{gl,pwr}$ a ground lift voltage can be developed by the power supply current flowing through those parts that are not separately decoupled. Especialy in multilayer technology one assumes that the voltage drop over the power planes is negligible. However, these can also be a source of radiation.

The ground inductances can be determined from Formula 4.57.

Then, for the ground plane with
width $w = 200\ mm$ and
distance $d = 0.23\ mm$
the ground inductance $L_{gnd} = 0.72\ pH/mm$.

Also for the transmission line with
width $w = 0.3\ mm$ and
distance $d = 0.23\ mm$
the signal inductance $L_{sig} = 0.245\ nH/mm$,

and for the power supply line in the IC with
width $w = 0.1\ mm$ and
distance $d = 5\ mm$
the inductance $L_{dec} = 1.0\ nH/mm$.

Because for the positive power supply a 'ground plane' is used, the same inductance can be used for this supply plane:
width $w = 200\ mm$ and
distance $d = 0.23\ mm$
the positive supply inductance $L_{pwr} = 0.72\ pH/mm$.

For the ground lift voltages $U_{gl,sig}$, $U_{gl,dec}$ and $U_{gl,pwr}$ (see Figure 6.4 and the circuit drawing in Appendix 6):

$U_{gl,sig}$: $L_{gnd,sig}$ = 0.072 nH (l = 100mm), L_{sig} = 24.5 nH (l = 100mm),

$U_{gl,dec}$: $L_{gnd,IC}$ = 0.018 nH (l = 25mm), L_{dec} = 25 nH (l = 25mm),

$U_{gl,pwr}$: L_{gnd} = 0.072 nH (l = 100mm), L_{pwr} = 0.072 nH (l = 100mm).

These parameters are used in the simulations of the circuit. The circuit drawing is given in Appendix 6. The following simulations were planned:

+ simulation with a local decoupling capacitor and an on-chip decoupling capacitor,
+ simulation without decoupling capacitors,
+ simulation without the signal transmission line connected and without decoupling capacitors,

Unfortunately the circuit could not be simulated by MINNIE due to convergence problems. The moment these convergence problems were solved a new version of MINNIE was installed. This new version does not function properly up to now....

6.4. HOW TO IMPROVE THE EMI PERFORMANCE OF THE CGIC.

As a result of this research we can state that, when the asymmetry (between signal-return) is not very large, any return current or power supply decoupling current should not flow through the 'reference plane'. Only when large asymmetry can be achieved the reference plane (in most cases equal to ground) can be used as the return lead.

Considering this rule the EMI performance can be approved when:

- The power supply decoupling current should be kept local, on the IC or just below. This can be achieved via (for <u>each</u> supply pin):
  - + On-chip capacitors.
  - + Applying decoupling capacitors just below the IC without feeding the current through the ground plane, for instance Q-packs.
  - + Ferrite beads in the supply leads beyond the decoupling capacitor. This is a well known method, but never proven theoretically.

  Considering these methods there is no need to mount the IC in a smaller housing than this PLCC housing, because the on-chip decoupling capacitor is already effective and the parasitic lead inductance amplifies the low-pass effect of this L-C circuit.
- The ground planes must only be used for all return currents. The other supplies should be fed through small, relatively high inductivance tracks to achieve a large asymmetry.

The power supply L-C combination must be designed in such a manner that the capacitor can supply sufficient energy during switching and the $L_{pwr,track}+L_{pwr,parasitic}+L_{choke}$ is not too large to prevent recharging of the capacitor during the steady-state.

We can make a comparison between a two-wire cable and a coax cable. The coax cable is the most asymmetric cable one can imagine. Therefore, when applying multi-layer PCB's, the ground plane should be the outer planes, see Figure 6.7.

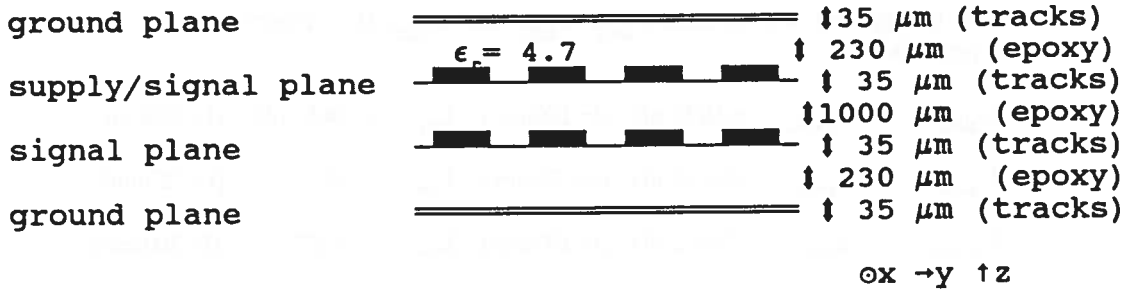

Figure 6.7: Cross section of improved multilayer PCB.

7. CONCLUSIONS AND RECOMMENDATIONS FOR FURTHER RESEARCH.

The greatest EMI problems in modern (digital) electronics are caused by electromagnetic radiation (radiated emission, RE). The sources of the radiation appeared to be the interconnection leads between devices. These interconnection leads can be modelled by transmission lines conducting the signal- and return current, the power supply decoupling current and the power supply current.

Models were available to calculate the radiated emission from current loops which results in differential mode radiation (REdm).
However, no models were available for calculating the displacement current which results in common mode radiation (REcm)
In practical situations the common mode radiated emission is often much larger than the differential mode emission.
In this report a simple and accurate model is developed for determining the REcm via a ground lift voltage and an antenna impedance.

The common mode current can be determined via the groundlift voltage U_{gl} and the antenna impedance Z_{ant}.

The antenna impedance can be modelled for the lowest resonant frequencies in a simple manner using a R-L-C circuit.

Using the developed antenna model, several effects can be explained. For instance a thicker antenna results in a larger antenna capacitance and a broader frequency spectrum.

The well known effect of Quasi Active Shielding is treated for near fields to gather some numerical insight in this, up to know, known, applied, but never quantitative treated effect. As a result, and also keeping in mind that the greatest EMI radiated emission constraint is caused by common mode radiation, we can neglect the radiation due to differential mode current loops can be neglected when a large conductive ground plane is applied.

Contrarily to popular belief, the inductance of a (finite) groundplane is not negligible.

The concept of self-inductance is often unknown. Self-inductance is only a theoretical inductance because any return lead will cancel some of the generated flux and the net inductance is always smaller than the self-inductance. Generally the term self-inductance should not be used but the term inductance should be used instead.
The formulas developed by Grover ([Grover, 1945]) are used very often in EMI applications. These are, however, not suitable because Grover assumes symmetric circuits. In practice, nearly all circuits are asymmetric.

In this report we are using the term asymmetry.
The definition for the asymmetry is: the difference in inductance between signal lead and the return lead.
A symmetric circuit is, according to this definition, a circuit which has for the signal and the return lead a similar conductor with the same inductance.

Contrarily to what is assumed by some authors, symmetry in an electronic circuit does not cancel the radiated electromagnetic field. As mentioned before, one should strive for a large asymmetry, not only in the signal with respect to its return inductance, but also in the positive supply with respect to the negative supply inductance, when the return c.q. the negative inductance is connected to the 'reference' of the circuit.

The designable, or controllable by the circuit designer, parameters are the loop current area A and the asymmetry, determined by $L_{gnd}/(L_{gnd}+L_{sig})$.

The power supply circuit must be treated as carefully, or even more, than the signal circuit because all signal frequency components are also part of the power supply spectrum.
Because the power supply decoupling current has, due to the relatively large decoupling capacitor, large high-frequency components. Therefore any decoupling current should be routed in such a manner that the 'reference' is by-passed. For integrated circuits (IC's) an on-chip capacitor is advisable. Furthermore, each power supply should be decoupled in this way, so, when applying IC's with several power supply pins, each pin must be decoupled separately to prevent the excitation of the reference.
When not every power supply pin is decoupled, the power supply circuit must be treated as carefully as the signal circuit, i.e. providing a large asymmetry between the positive (and/or negative) supply track/lead with respect to the return or reference track/lead.
Until now, an ideal power supply seamed to be a very low-inductive supply. This must be changed into asymmetric, locally decoupled, supply schemes.

A way of thinking in preventing common mode radiation is to compare symmetric cables with coax cables, with respect to the confination of magnetic flux lines. The only possible construction which can confine all magnetic flux lines is a coax construction and a coax construction is the most asymmetric circuit one can imagine. Therefore, when applying multi-layer PCB's, the outer planes must be the ground planes.

Until now, the PCB's are still the EMI constraint, and not the IC's since their dimension is too smaal to play a role.

With the developed models, the derived manual methods and design rules, it is possible to predict whether the product can fulfil the requirements in the design phase of a project. Also a founded choice for specific precautions, such as multi-layer printed circuit boards, can be made.

RECOMMENDATIONS FOR FURTHER RESEARCH.

The antenna impedance is very sensitive to other than round geometries. Research must be carried out for the antenna impedance (as a function of the frequency) for several constructions, such as the ground plane of a PCB acting as an antenna, the effectiveness of the antenna when large conducting planes are nearby etc.
Maybe the antenna capacitance for 'PCB' antennas is influenced by a capacitive voltage division with respect to the 'other' conductors.

Models should be developed for the 'coaxial' constructions. This can be a sort of parallel switching of ground inductances.

In this research the complex amplitude of the currents is used. Maybe only these real part should be used because these real parts contribute to the (far field) radiation. However, not everyone has the same opinion with respect to this subject.

Because the formulas we are using are based on uniform current distribution, but in the most interesting parts of the frequency spectrum these currents are not uniform, some research should be done for the transition quasi-stationary <-> resonance approach.

Especially for multilayer PCB's research must be carried out for the inductances of the ground planes. A comparison with cables (two-wire <-> coax) could clarify several effects.

More general design rules (such as: 'if τ_r>...ns, than l<... m and/or asymm>...')must be developed.

APPENDIX 1: USED SYMBOLS.

β	$2\pi/\lambda$, in [1/m]
δ	skindepth, in [m]
ϵ	permittivity, equal to $\epsilon_r.\epsilon_0$, in [F/m]
ϵ_r	relative permittivity, dimensionless
ϵ_0	absolute permittivity, eual to $8.84\ 10^{-12}$, in [F/m]
λ	wavelength, in [m]
λ_c	cross-over wavelength, in [m]
μ	permeability, equal to $\mu_r.\mu_0$, in [H/m]
μ_r	relative permeability, dimensionless
μ_0	absolute permeability, equal to $4\pi 10^{-7}$, in [H/m]
ρ	reflection coëfficient, dimensionless
σ	conductivity, in [S/m]
σ_r	relative conductivity, equal to 1 for copper, in [S/m]
τ_r	rise time signal, in [s]
υ	wave velocity, in [m/s]
ω	$2\pi f$, in [rad/s]
Φ_k	coupled magnetic flux, in [Am]
Φ_{return}	magnetic flux due to return conductor, in [Am]
Φ_{signal}	magnetic flux due to signal conductor, in [Am]
Φ_{tot}	total magnetic flux, in [Am]

a	radius of current carrying loop, in [m]
a	radius of antenna, in [m]
as	asymmetry factor, dimensionless
asym	asymmetry factor, dimensionless
c	speed of light, in vacuum 3.10^8, in [m/s]
d	distance, in [m]
f	frequency, in [Hz]
f_c	cross-over frequency, in [Hz]
f_{dip}	dip frequency, in [Hz]
f_{res}	resonance frequency, in [Hz]
$f_{[MHz]}$	frequency, in [MHz]
k	constant factor, dimensionless
k1	constant factor, dimensionless
k2	constant factor, dimensionless
l	length, in [m]
l_{ant}	length antenna, in [m]
l_{PCB}	length PCB, in [m]
$l_{section}$	length of section of transmission line, in [m]
n	integer, 1..∞
r	distance radiator - receiver, in [m]
w	width of conducting track, in [m]
w_r	width of return track, in [m]
w_s	width of signal track, in [m]

A	area of current carrying loop, in [m^2]
A	area of conductor, in [m^2]
A_{dec}	area of power supply decoupling current loop, in [m^2]
A_{pwr}	area of power supply current loop, in [m^2]
A_{sig}	area of signal current loop, in [m^2]
C	capacitance, in [F]
C_a	capacitance of antenna, in [F]
D	displacement current, in [C/m^2]
E_{cm}	electric fieldstrength due to common mode current, in [V/m]
E_{dm}	electric fieldstrength due to differential mode current, in [V/m]
E_r	electric fieldstrength in r direction, in [V/m]
E_θ	electric fieldstrength in θ direction, in [V/m]
E_ϕ	electric fieldstrength in ϕ direction, in [V/m]
G	conductance, in [S]
H	magnetic fieldstrength, in [A/m]
H_r	magnetic fieldstrength in r direction, in [A/m]
H_θ	magnetic fieldstrength in θ direction, in [A/m]
H_ϕ	magnetic fieldstrength in ϕ direction, in [A/m]
I	current, in [A]
I_{cm}	common mode current, in [A]
I_{dm}	differential mode current, in [A]
I_{short}	short ciruit current, in [A]
L	inductance, in [H]
L_a	inductance of antenna, in [H]
L_{dec}	inductance of power supply conductor beteen decoupling C and consumer, in [H]
L_e	external inductance, in [H]
L_{eff}	effective inductance, as seen by the 'world', in [H]
L_g	inductance of ground lead/plane, in [H]
L_{gnd}	inductance of ground lead/plane, in [H]
L_{ground}	inductance of ground lead/plane, in [H]
L_i	internal inductance, in [H]
L_{mutual}	mutual inductance, in [H]
L_{return}	inductance of return conductor, in [H]
L_{pwr}	inductance of power supply conductor beteen supplier and decoupling C, in [H]
L_{self}	self inductance, in [H]
L_s	inductance of signal conductor, in [H]
L_{signal}	inductance of signal conductor, in [H]
M	mutual inductance, in [H]
R_a	resistance of antenna, in [Ω]
R_{loss}	loss resistance of antenna, in [Ω]
R_{DC}	DC resistance, in [Ω]
R_{AC}	AC resistance, in [Ω]
U	voltage, in [V]
U_{gl}	ground lift voltage, in [V]
U_{sig}	generator signal voltage, in [V]
Z	characteristic transmission line impedance, in [Ω]
Z_0	wave impedance, $\sqrt{(\mu/\epsilon)}$, in far field equal to 377 Ω, in [Ω]
Z_{ant}	antenna impedance, in [Ω]
Z_{gen}	generator internal impedance, in [Ω]
Z_{load}	load impedance, in [Ω]
Z_{Ugl}	internal impedance of ground lift voltage 'source', in [Ω]

APPENDIX 2: MAXWELL'S LAWS, DISPLACEMENT AND COMMON MODE CURRENT.

In my opinion the common mode current, causing common mode radiation, is in the low frequency range a displacement current. All other currents are basically differential mode currents from the local circuit or descended from another circuit.

To enable the continuity of electric current to be retained across a capacitor Maxwell proposed a displacement current, which is a mathematical manipulation of the electric field:

$$\oint_l H.dl = I + \frac{\partial \Phi_D}{\partial t}$$

Drawn in a figure:

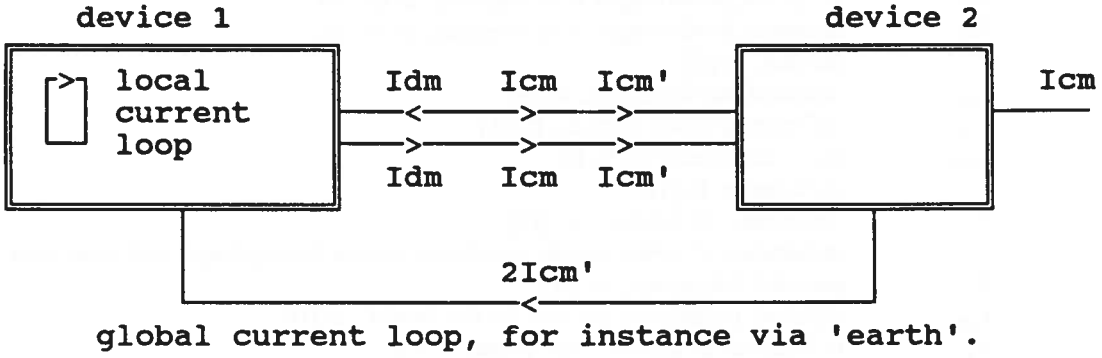

The Icm' is just another differential mode current, belonging to a larger circuit. The common mode current is the displacement current Icm.

The differential mode current is often translated in symmetric current, while the common mode current is translated in asymmetric current.

In a circuit wherein we consider only the conducted current, we can never deduce the common mode current which is responsible for the electromagnetic radiation.
In a simple circuit which does not contain the environment, the common mode current seams to be caused by asymmetry. The simple conclusion made by several people is: common mode is caused by asymmetry, common mode radiation is caused by asymmetry. This last conclusion is not true.

Our definition of common mode current is similar to the definition everyone uses for the common mode radiation: 'common mode current is equal to (electric dipole) antenna current'. Therefore we can only determine the common mode current when the environment ('antenna impedances') is included!

In other words: Two definitions for the common mode current exist. Asymmetry in a circuit is not directly the source of common mode radiation....

APPENDIX 3: TIME AND FREQUENCY DOMAIN; FFT.

This appendix will concentrate on presenting the basic mathematical tools needed to deal with EMI problems. The cornerstone of this appendix is Fourier analysis which explains how periodic non-sinusoidal waveforms actually contain a whole spectrum of sinusoidal components with frequencies which are multiples of the fundamental frequency. This feature is vitally important, for it has been stressed repeatedly that there are many frequency dependant aspects to consider when tackling an EMI problem, so that before any effective action can be taken it is necessary to be able to identify and measure the spectrum of frequencies involved.
Spectral analysis is based on the Fourier theorem which states that periodic waveforms *f(t)* can be expressed as the sum of a series of sinusoidal signals. There is an extensive literature on this theorem but we will only summarise some results of intermediate interest.
A train of rectangular pulses of amplitude A, duty cycle d and period T the Fourier coëfficients are found as [Reference Data for Engineers, 1988]:

$$C_n = \frac{2Ad}{T}\left|\frac{\sin(n\pi\frac{d}{T})}{n\pi\frac{d}{T}}\right| \qquad (1)$$

Wherein: A = amplitude,
d = duty cycle, in [s]
T = period, in [s].

and:

$$f_0 = \frac{1}{T} \qquad (2)$$

Wherein: f_0 = fundamental frequency, in [Hz].

Because we are interested in the magnitude, and not in the phase, of the signal the modulus of the function is taken.

Real pulses in circuits will have finite rise times τ_r. Waveforms like this are called trapezoidal waveforms. The Fourier coëfficients are found as [Reference Data for Engineers, 1988]:

$$C_n = 2A(d+\tau_r)f_0\left|\frac{\sin(n\pi f_0\tau_r)}{n\pi f_0\tau_r}\ \frac{\sin(n\pi f_0(d+\tau_r))}{n\pi f_0(d+\tau_r)}\right| \qquad (3)$$

Wherein: τ_r = rise time, in [s].
d = time wherein signal is high, in [s]

Equation 3 assumes that the rise time equals the fall time. If it does not, the smaller of the two should be used for worst-case result.

An approximation of these coëfficients can be made.
Due to the sin(x)/x terms the value this term cannot exceed 1, so at large x the coëfficients are dominated by the 1/x term, which is small as x becomes large. The maxima of the function sin(x)/x lie on the curve 1/x so that the amplitude of any Fourier component will be bound by this curve.
Thus this much simpler equation can be used to calculate the maximum possible amplitude of each Fourier component (see for instance [Chatterton 1992]).

Then the spectrum is flat between the fundamental frequency f_0, falling off with 20 dB/dec between $f = 1/(\pi d)$ and $f_1 = 1/(\pi \tau_r)$. For higher frequencies the slope is 40 dB/dec.
The amplitude at the fundamental frequency f_0 is equal to $A_0 = 2A(d + \tau_r)f_0$. For 50 % duty cycle: $A_0 = A$.
One remark must be made: it is mentioned that 'falling off with 20 dB/dec between $f = 1/(\pi d)$ and $f_1 = 1/(\pi \tau_r)$...'. However, the fundamental frequency f_0 is always higher than $f = 1/(\pi d)$!!
Therefore it is better to start this asymptotic graph at the fundamental frequency f_0, where the slope is 20 dB/dec and the amplitude is 4 dB below (or a factor 0.64 times[Ott,1988]) the amplitude A_0. This correction is within 1 dB with respect to the former method.

A simple formula can be constructed to include the graph in any formula, and so to correct for the frequency dependancy of signals:

$$I(f) = I_0 \frac{1}{1+\frac{f}{f0}} \frac{1}{1+\frac{f}{f1}} \qquad (4)$$

Wherein:
- I(f) = frequency dependant signal,
- f0 = fundamental frequency, in [Hz],
- f1 = $1/(\pi \tau_r)$, in [Hz]
- τ_r = rise time of signal, in [s],
- I_0 = amplitude at fundamental frequency - 4 dB.

This is also possible for 'high-pass' asymptotic graphs:

$$I(f) = I_0 \frac{1}{1+\frac{f0}{f1}} \frac{1}{1+\frac{f1}{f0}} \qquad (5)$$

In the following figure both 'low-pass' and 'high-pass' graphs are drawn for
- f0 = 10 MHz, and
- f1 = 100 MHz.

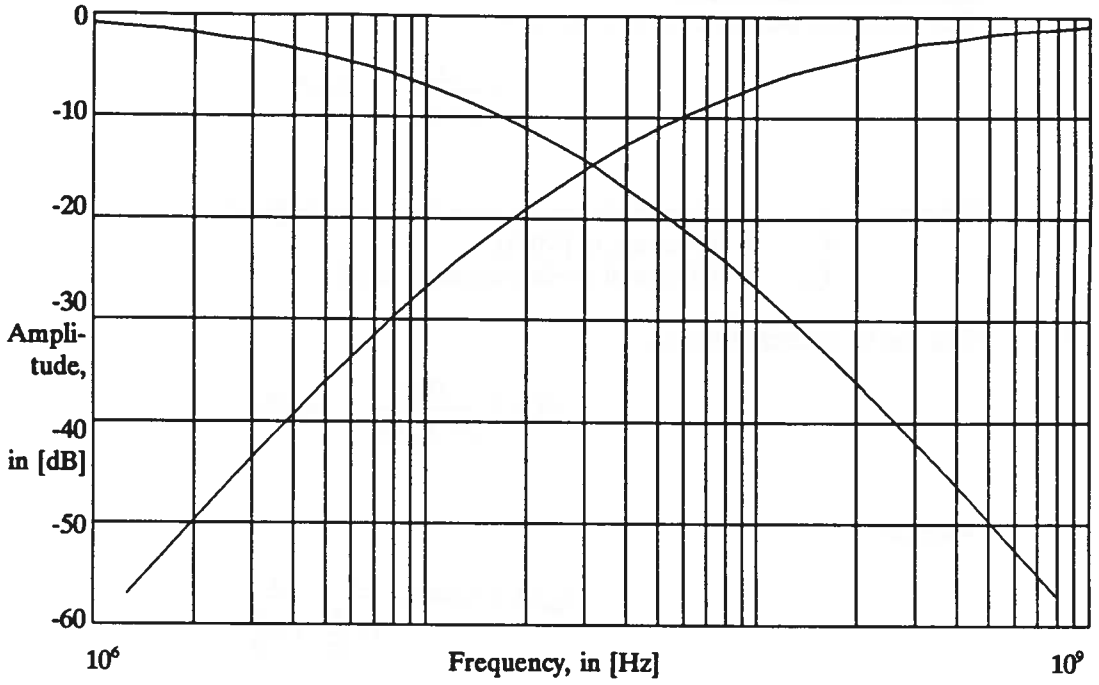

Figure 1: Frequency response of 'low-pass' and 'high-pass' circuit.

Remember always: with 50% duty cycly only odd harmonics are present!

In the report two formulas are mentioned wherein one parameter is defined as a designable parameter. For differential mode radiation it is the loop area A, and for the common mode radiation it is the quotient L_{gnd}/L_{eff}.
These designable parameters are however frequency dependant, not only by the factor f (frequency) in the formula, but also because the current and voltage are frequency dependant.
We will deduce the frequency dependant designable parameters hereafter.
Note: all signals are frequency dependant.....

DIFFERENTIAL MODE:

The designable parameter A is found to be:

$$A < \frac{12.4}{f^2 I_{dm}} \quad [mm^2] \tag{6}$$

Wherein: A = maximal allowed current loop area, in [mm²],
f = frequency, in [MHz],
I_{dm} = differential mode current, in [mA].

This can be written better as:

$$A(f) < \frac{12.4}{f^2 I_{dm}(f)} \quad [mm^2] \tag{7}$$

Wherein:

$$I_{dm}(f) = 0.64\, I_0 \frac{1}{1+\frac{f}{f0}} \frac{1}{1+\frac{f}{f1}} \tag{8}$$

or:

$$I_{dm}(f) = 0.64\, I_0 \frac{f0}{f0+f} \frac{f1}{f1+f} \tag{9}$$

Combining this with Formula 7, and split it into two regions:

f< <f0:

$$A < \frac{19.4}{f^2 I_0} \quad [mm^2] \tag{10}$$

f>f0, and f>f1:

$$A < \frac{19.4}{f0\, f1\, I_0} \quad [mm^2] \tag{11}$$

The loop area A calculated by Formula 11 is always the greatest, so:

$$A_{max} < \frac{19.4}{f0\, f1\, I_0} \quad [mm^2] \tag{12}$$

Wherein the loop area A is directly related to the spectrum, via $f0$ and $f1$, of the loop current.

COMMON MODE:
Using the formula for hand calculations the designable parameter(s) is found to be:

$$\frac{L_{gnd}}{L_{gnd} + L_{sig}} < \frac{533\ 10^3\ Z_a\ (1+\frac{f_c}{f})}{U_{signal}\ f\ l_{ant}} \qquad (13)$$

and:

$$f_c = \frac{c}{2\ l_{PCB}\ \sqrt{e_r}} \quad [Hz] \qquad (14)$$

Wherein:
- L_{gnd} = ground or return inductance, in [H],
- L_{sig} = signal line inductance, in [H],
- Z_a = impedance antenna, in [Ω],
- f = frequency, in [Hz],
- f_c = cross-over frequency, in [Hz],
- U_{sig} = signal amplitude, in [V],
- l_{ant} = length antenna, in [m].
- l_{PCB} = length PCB, in [m].
- c = speed of light, in [m/s],
- e_r = permittivity of medium, in [F/m].

Formula 13 can be written better as:

$$\frac{L_{gnd}}{L_{gnd} + L_{sig}} < \frac{533\ 10^3\ Z_a(f)\ (1+\frac{f_c}{f})}{U(f)_{signal}\ f\ l_{ant}} \qquad (15)$$

Combining this with Formula 4, and concluding that the maximum value is for frequencies $f>f0,f1$:

$$\frac{L_{gnd}}{L_{gnd} + L_{sig}} < \frac{833\ 10^3\ Z_a(f)\ (f+\frac{c}{2\ l_{PCB}\sqrt{e_r}})}{U_0\ l_{ant}\ f0\ f1} \qquad (16)$$

The maximum possible radiation of the PCB itself(without any interconnection cables) is for $l_{PCB} = l_{ant}$ and then $f = f_c$. Then the antenna impedance is (worst case) $Z_a = 25\ \Omega$. Furthermore, $e_r \approx 5$, then the following designable parameters prescription can be deduced:

$$\frac{L_{gnd}}{L_{gnd} + L_{sig}} < \frac{2793}{U_0\ l^2\ f0\ f1}$$

APPENDIX 4: CAPACITANCE AND INDUCTANCE.

1. INTRODUCTION.

The concept of inductance is explained only in a few text books. A very well known book is written by Grover(1945). Nearly all inductance formulas found in EMI books and papers are based on the formulas of this book. Grover calculates the effective inductance by calculating the self inductance and correcting this with the mutual inductance.
Another method of calculating the inductance is by determining the coupled flux as Kaden does ([Kaden 1959]).
A third method of calculating inductance is based on capacitance calculations. The inductance L can then be found using

$$L = \frac{\epsilon.\mu}{C} \quad [H] \tag{1}$$

This is valid as long as the TEM approximation holds. Even for Quasi-TEM waves this equation is valid according to several papers. However, when a configuration with ϵ_r and μ_r equals 1 then in the first order a TEM wave can be chosen.
In general the formulas are derived for DC/static conditions. These formulas are then valid when the wave is propagating as a TEM wave.

In this appendix some background of the formulas of Grover, which are appropriate for the EMI calculations, is given.

Furthermore several inductance, capacitance and characteristic impedance formulas are given which are based on the above mentioned methods.

2. INDUCTANCE CALCULATIONS BY GROVER.

2.1. GENERAL.

Grover assumes the current density to be uniform in the whole conductive area. This will lead to large errors when signal and return leads are nearby because the currents attrack eachother. This effect is called the proximity effect. Also Grover does not take into account the skin effect.

For several configurations Grover uses the concept of Geometric Mean Distance. In calculating the mutual inductance of two conductors whose cross sectional dimensions are small compared with their distance apart, it suffices to assume that the mutual inductance is the same as the mutual inductance of the filaments along their axes.
For conductors whose cross section is too large it is necessary to average the mutual inductance of all the the filaments of which the conductors may be supposed to consist. That is, the basic formula for the mutual conductance is to be integrated over the cross section of the conductors.

Assuming any number of figures having area A, B, C, etc. whose geommetric distances from another area S are Ra, Rb, Rc etc., the GMD R of their sum from the area S is given by:

$$\ln R = \frac{A.\ln Ra + B.\ln Rb + C.\ln Rc + ...}{A + B + C + ...}$$

The GMD R can be used instead of the distance d in the formulas hereafter.

Grover gives several tables and approximations using series expansions. We will use as long as possible the appropriate formulas.

The concept of self-inductance appeared to be not well known. In real world, self-inductance does not exist! We should use the word inductance instead.
A change of current in a conductor will induce a voltage due to the changing flux linkage of its self-produced magnetic field. The conductor is said to have self-inductance. A field produced by another conductor (with another current or the return current) will also produce a voltage in the first conductor. This coupling is called mutual-inductance.
When two wires are conducting the same current but with opposite direction then the effective inductance can be calculated using:

$$L_{eff} = L1_{self} + L2_{self} - M_{12} - M_{21}$$

Because $M_{12} = M_{21}$:

$$L_{eff} = L1_{self} + L2_{self} - 2M$$

The ground inductance is:

$$L_g = L2_{self} - M$$

Wherein:
- Li = internal inductance due to the internal magnetic field.
- Le = external inductance due to the external magnetic field.
- Lself = Li+Le
- Leff = effective inductance as seen by the 'world'.
- Lg = ground lead inductance.

2.2. INDUCTANCE OF PARALLEL ELEMENTS OF EQUAL LENGTH.

The internal self-inductance of a round conductor, according Grover, is:

$$L = \frac{\mu l}{8\pi} \quad [H]$$

Wherein: l = length conductor [m]
μ = permeability = $4\mu 10^{-7}$ [H/m]

The length l must satisfy the condition $l_{segment} < 5\ \tau_r$ otherwise the transmission line must be divided in several segments Δl with $\Sigma\ \Delta l = l$.

This inductance formula applies for DC. For higher frequencies the skin effect will cause a lower internal inductance. In the frequency range of interest (1 MHz - 1 GHz) this internal inductance can be neglected.

The mutual inductance of two equal parallel straigth filaments, according Grover, is exactly:

$$M = \frac{\mu l}{2\pi}\left[\ln\left(\frac{l}{d}+\sqrt{1+\frac{l^2}{d^2}}\right)-\sqrt{1+\frac{d^2}{l^2}}+\frac{d}{l}\right] \quad [H]$$

Wherein: d = distance between conductors [m]

For filaments very close to eachother, i.e. d/l is very small, then the following expansion (Grover) can be used:

$$M = \frac{\mu l}{2\pi}\left[\ln\frac{2l}{d}-1+\frac{d}{l}-\frac{d^2}{4l^2}+ \ldots.\right] \quad [H]$$

In the rare cases where the distance between the filaments is large compared to their lengths, the following series development (Grover) is simple and accurate:

$$M = \frac{\mu l}{2\pi}\left(\frac{1}{2}\frac{l}{d}\right)\left[1-\frac{1}{12}\frac{l^2}{d^2}+\frac{1}{40}\frac{l^4}{d^4}-\ldots.\right] \quad [H]$$

The self-inductance of a straigth conductor is the mutual inductance wherein the distance d is replaced by the radius r (Grover):

$$L_{self} = \frac{\mu l}{2\pi}\left[\ln\frac{2l}{r}-1\right] \quad [H]$$

Wherein: r = radius conductor [m]
This is the external self-inductance without the internal self-inductance! The formula for the total self-inductance (Grover), Lself=Li+Le:

$$L_{self} = \frac{\mu l}{2\pi}[\ln\frac{2l}{r} - \frac{3}{4}] \quad [H]$$

For a wire of rectangular cross section of side w and thickness t (Grover):

$$L_{self} = \frac{\mu l}{2\pi}[\ln\frac{2l}{w+t} + \frac{1}{2}] \quad [H]$$

Wherein: w = width [m]
t = thickness [m]

This formula is inclusive the internal self-inductance. An approximation made by Kalantarov gives for the external self-inductance for higher frequencies, so that the current flows through an infinite thin slab due to the skineffect:

$$L_{self} = \frac{\mu l}{2\pi}[\ln\frac{2l}{w} + 1] \quad [H]$$

One problem of the above mentioned two formulas is that these formulas assume an uniform current distribution. In real circuits this is not true! Kaden has shown that the proximity effect causes the current density to be very high at the edges!!

The inductance of multiple conductors, that is, of groups of several members joined in parallel, may be found by circuit theory using the formulas for the self-inductance and mutual inductance of parallel conductors. This technique, although very complex, can be used for conductors with a current density which is not uniform.

An important case in practice is a loop formed of two parallel conductors whose length l is great compared with their distance d apart. The conductors carry equal, oppositely directed currents. Such a case is an ordinary transmission line. In the simplest case of equal round wires of radius r, the effective inductance is given by (Grover):

$$L_{eff} = \frac{\mu l}{\pi}[\ln\frac{d}{r} + \frac{1}{4}] \quad [H]$$

For equal parallel rectangular cross sections spaced at distance d between centers (Grover):

$$L_{eff} = \frac{\mu l}{\pi}[\ln\frac{d}{w+t} + 1.5 + \zeta] \quad [H]$$

Wherein: ζ = correction factor, from a table, negligable.

2.4. INDUCTANCE OF PARALLEL ELEMENTS OF UNEQUAL LENGTH.

The formula to be used is, according Grover:

$$2M = (M_{m+p}+M_{m+q})-(M_p+M_q)$$

Wherein:

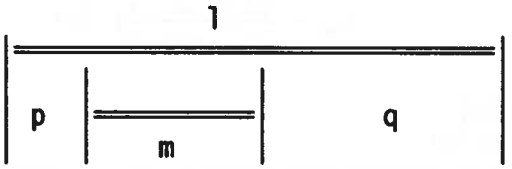

The individual terms are to be calculated by the formulas for the mutual inductance using for l in these formulas the length given by the subscripts.

The mutual inductance of parallel conductors of unequal length but however placed is found using the above formule. For round wires this formula applies without change. For other cross sectional shapes the same formula has to be used with the difference that for the distance d there is to be placed the geometrical mean distance of the cross section of the conductors.

2.5. CORRECTION FOR NON-UNIFORM CURRENT DISTRIBUTION:

Grover has determined the formulas assuming an uniform current distribution. In chapter 2 the concept of geometric mean distance (GMD) is explained. It is possible to calculate the inductance of a construction with a non-uniform current distribution when the current distribution is used is stead of the areas A, B, C etc. in the formula for the GMD.
The current distribution in a construction is proportional to the magnetic field at the surface. A wire produces a magnetic field:

$$H = \frac{I}{2\pi r} \quad [A/m]$$

Wherein: I = current in the wire [A]
r = distance between wire and point of obeservation [m]

When a conducting plane is nearby and parallel with the wire the magnetic field parallel to the plane can be calculated:

$$H_{\parallel} = \cos^2\alpha \frac{I}{2\pi d} \quad [A/m]$$

Wherein: α = corner between H and H//
d = distance ⊾ between wire and plane [m]

Or:

$$H_{\parallel} = \{\frac{d^2}{d^2+x^2}\}\frac{I}{2\pi d} \quad [A/m]$$

Wherein: x = distance.

The current density for several distances d is calculated as an example. The results are given below:

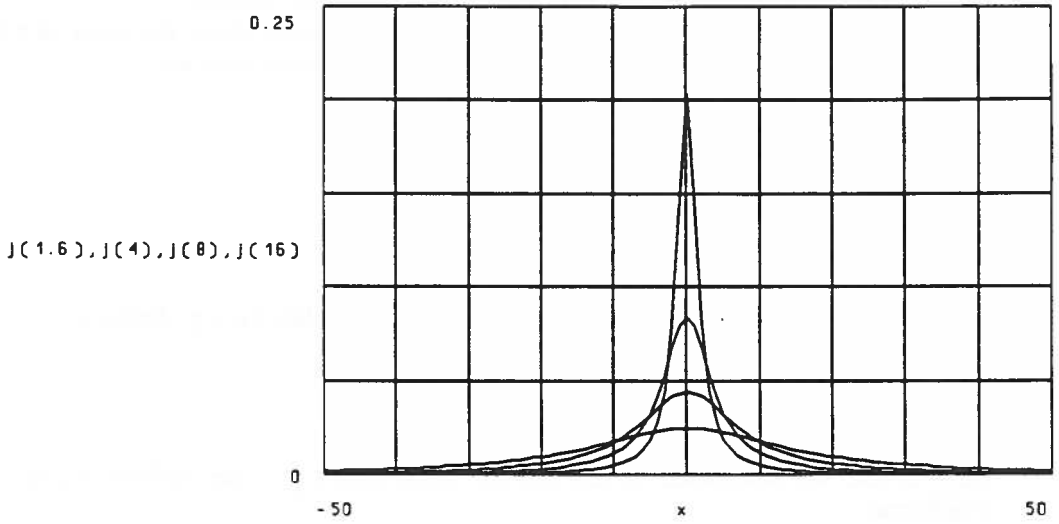

Now the formula for the GMD with the non-uniform current, due to the proximity effect, taken into account, wherein the integral has boundaries: -w/2 to w/2:

$$\ln R = \frac{1}{2}\frac{\int \frac{\ln(d^2+x^2)}{d^2+x^2}\,dx}{\int \frac{1}{d^2+x^2}\,dx}$$

2.6. INDUCTANCE OF SEVERAL PARALLEL ELEMENTS.

When a stripline with two groundplanes with the signal tracks in between is used the formulas are valid. However, the mutual inductances will cause very difficult circuit manipulations. The formula for the ground lift voltage will be given hereafter. The condition for this formula is that the construction is symmetric with respect to the signal track. This means that the ground planes have equal dimensions and are mounted at the same distance to the signal track:

$$U_{gl} = U_i \frac{j\omega(L_3 - 2M_{13} + M_{23})}{j\omega((L_3 - 2M_{13} + M_{23}) + (2L_1 - 2M_{13})) + 2Z}$$

Wherein: L_1 = self-inductance of the signal conductor,
L_3 = self-inductance of one ground plane,
M_{13} = mutual inductance between the signal conductor and the ground plane,
M_{23} = mutual inductance between the two ground planes
Z = impedance of generator + line capacitance in parallel with load impedance.

The factor composed of the inductances can be seen as the amplification of Ui. This factor must be made as small as possible. The corner frequency Ugl is determined by Z and the total inductance in the denominator.

In general, using matrix manipulations (for i=1 to n):

$$U_{gl} = -\sum (L_s - M_i) I_i$$

2.8. APPLICATION OF THE FORMULAS.

We will using a practical example to show that the formulas developed by Grover cannot be used for asymmetric circuits, which are the most applied circuits in practice.
A two-sided printed circuit board (bilayer), one side as ground plane, the other carrying an 1 mm wide signal conductor over the whole length, is used. The dimensions are:

PCB: $l = 160$ mm
$w_r = 100$ mm
$d = 1.6$ mm
conductor on PCB: $t = 0.035$ mm
$l = 160$ mm,
$w_s = 1$ mm.

The GMD for the non-uniform current distribution is calculated using Mathcad:
$R = 8.762.10^{-6}$ m
Then $M = 304.2$ nH,
and $L_{12} = 69.2$ nH,
$L_{11} = 216.5$ nH.
(L_{12} is the self-inductance of the ground plane and L_{11} is the self-inductance of the signal conductor).
Then $Lg = -235$ nH !!!

2.9. CONCLUSION.

The formulas developed by Grover cannot be used for asymmetric circuits. The method of calculating inductance via self-inductance and mutual-inductance can be made applicable when a sort of correction for the mutual inductance is found.

The concept of inductance is not well known. Most EMI text books and papers use the methods developed by Grover and are still using the word self-inductance. Self inductance is only possible in theory....

Remark: The formulas developed by Grover can be recognised by the length l in the natural logarithm ln, so ln(..l). However, when these formulas are simplified and only used for the effectiev inductance of the transmission line, then the factor l in the ln(..l) disappears.

3. OTHER INDUCTANCE CALCULATIONS.

Another method of calculating the inductance is by determining the coupled flux as Kaden does ([Kaden 1959]). Kaden includes the skin effect and the proximity effect but always considers infinite large areas. Therefore the edge effects are not taken into account. This can be recognised by the length *l* not behind the *ln* (natural log).
Despitely Kaden calculates only for some specific (transmission line) constructions the inductances.

The third method is applied extensively in the microwave area and based on capacitance formulas. Especcially in the last decade several computer programs are developed to calculate the capacitance (and from this we can deduce the inductance) using BEM, FEM (Boundary-, Finite-Element Method) etcetera. The best methods are based on conformal mapping, because this results in analytical solutions, and edge effects can be taken into account.
These edge effects are very important because these are the contributors to radiated emission!!
According to Grivet([Grivet,1970]), using conformal mapping, the capacitance of two parallel plates is:

$$C = \epsilon[\frac{w}{d}+\frac{1}{\pi}\{1+\ln(\frac{\pi w}{d}+1)\}] \quad [F/m]$$

The first term is the well known formula without considering any edge effect. The second term describes the edge effect.
Now:

$$L_{eff} = \frac{\mu\epsilon}{C} \quad [H/m]$$

For a stripline (signal conductor between two ground planes):

$$C = \epsilon[\frac{2w}{d}+\frac{8}{\pi}\ln 2] \quad [F/m]$$

Conditions: $w << t$
$w > d$
Also in this formula the second term is the edge effect of the inner signal conductor.

4. TABLES.

Walker ([Walker 1990]) has given several formulas for capacitance and inductance calculations. We will follow a similar approach by discussing the capacitance C, the inductance $L_{\underline{eff}}$(!) and the characteristic impedance Z for each construction.
The formulas described here are similar to those found in:
[Walker 1990], [Chatterton 1992], [Reference Data 1988], [Meinke &Gundlach 1987], [Durcansky 1991], [Kaden 1959]. Only the way the simplifications are made can be different.

The dimensions are given using the following terms:

l	= length transmission line,
d	= distance between lines,
r	= radius conductor,
ϵ_r	= relative permittivity,
ϵ_0	= permittivity,
h	= heigth of conductor above a plane,
w	= width of flat conductor,
t	= thickness of flat conductor,

Remark: when the electromagnetic field <u>partially</u> flows through a medium wherein $\epsilon_r \# 1$ then for this ϵ_r the <u>effective</u> relative permittivity must be used, which is in first order equal to $\sqrt{\epsilon_r}$.

4.1. LCZ BETWEEN TWO CIRCULAR CONDUCTORS.

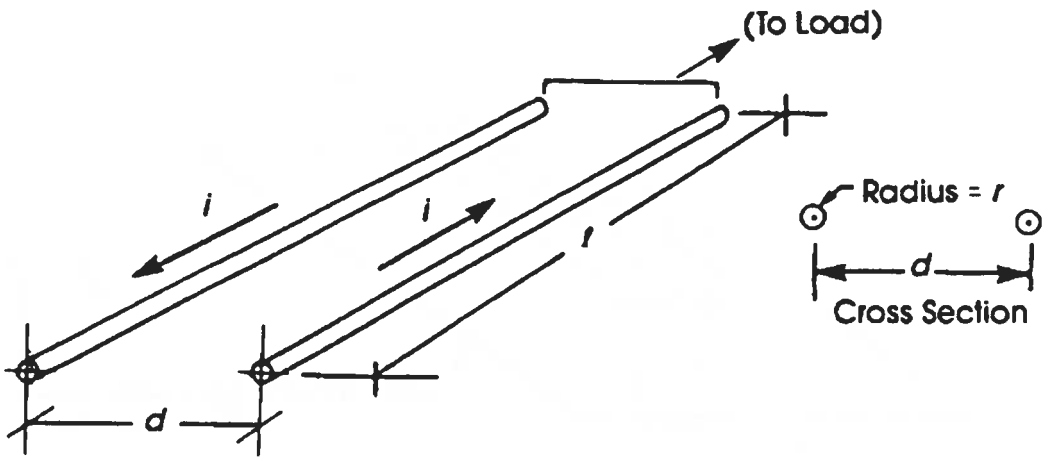

Figure A4.2: Two long circular conductors each have radius r and are separated by distance d.

$$C = \frac{\pi \epsilon_r \epsilon_0 \, l}{\ln(\frac{d}{2r}) + \sqrt{(\frac{d}{2r})^2 - 1}} \quad [F] \qquad \text{(A4.1.1)}$$

or, for $2r/d << 1$:

$$C = \frac{\pi \epsilon_r \epsilon_0 \, l}{\ln(\frac{d}{r})} \quad [F] \qquad \text{(A4.1.2)}$$

$$L = \frac{\mu_r \mu_0 \, l}{\pi} \ln(\frac{d}{r}) \quad [H] \qquad \text{(A4.1.3)}$$

$$Z = \frac{120}{\sqrt{\epsilon_r}} \ln[\frac{d}{2r}(1 + \sqrt{1 - (\frac{2r}{d})^2})] \quad [\Omega] \qquad \text{(A4.1.4)}$$

or, for $2r/d << 1$:

$$Z = \frac{120}{\sqrt{\epsilon_r}} \ln(\frac{d}{r}) \quad [\Omega] \qquad \text{(A4.1.5)}$$

4.2. LCZ FOR A CIRCULAR CONDUCTOR ABOVE A GROUND PLANE.

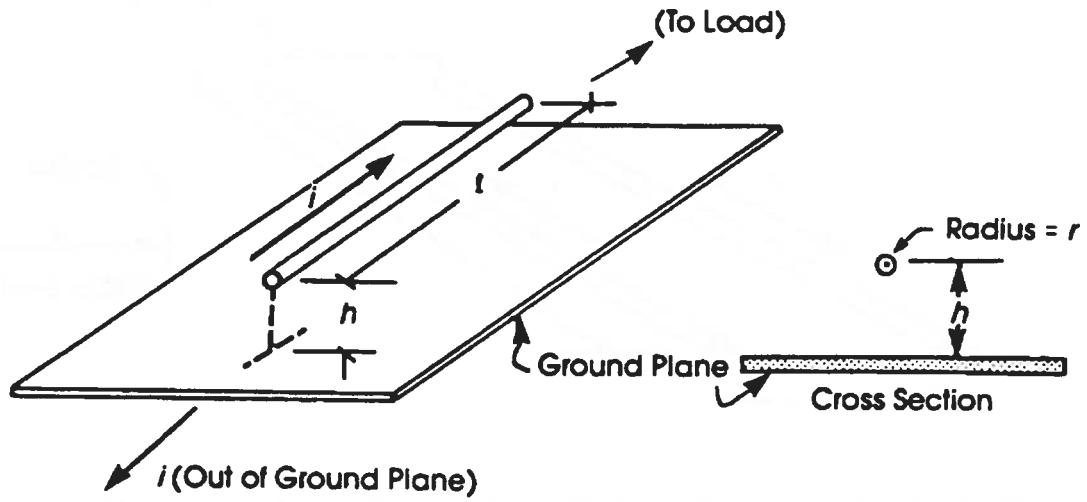

Figure A4.3: A long circular conductor spaced heigth h over a ground plane.

for h>>r:

$$C \approx \frac{2\pi e_r e_0 \, l}{\ln(\frac{2h}{r})} \quad [F] \qquad \text{(A4.2.1)}$$

$$L \approx \frac{\mu_r \mu_0 \, l}{2\pi} \ln(\frac{2h}{r}) \quad [H] \qquad \text{(A4.2.2)}$$

Comparing this formula with Formula 4.1.3 it will be clear that all inductance is thought to be in the conductor, and not in the ground plane!

$$Z = \frac{60}{\sqrt{e_r}} \ln[\frac{h}{r}(1+\sqrt{1-(\frac{r}{h})^2})] \quad [\Omega] \qquad \text{(A4.2.3)}$$

or, for 2/h<<1:

$$Z \approx \frac{60}{\sqrt{e_r}} \ln(2\frac{h}{r}) \quad [\Omega] \qquad \text{(A4.2.4)}$$

4.3. LCZ FOR PARALLEL, VERTICAL, FLAT CONDUCTORS.

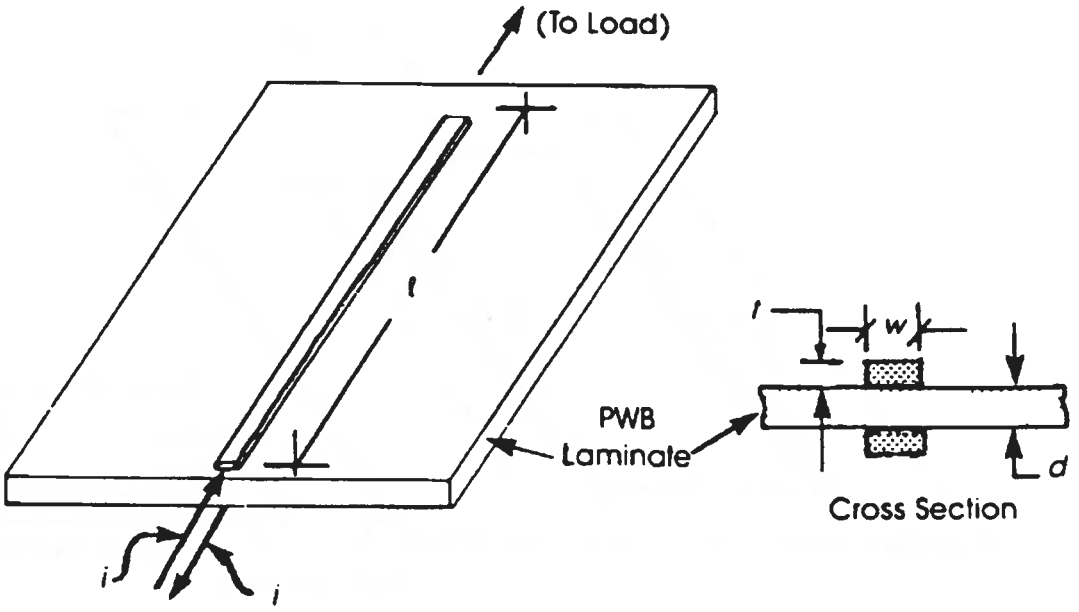

Figure A4.3: Two conductors representing lands on a printed circuit board.

$$C = e_r e_0 K1 \; l(\frac{w}{d}) \quad [F] \tag{A4.3.1}$$

Wherein the fringing factor K1:

$$K1 = 1.5 + (0.4\frac{d}{w}) \tag{A4.3.2}$$

for d/w >1, and k1=1 for d/w<1.

$$L \approx \frac{\mu_r \mu_0 \; l}{K3}(\frac{d}{w}) \quad [H] \tag{A4.3.3}$$

and K3:

$$K3 \approx 2+0.65\frac{d}{w} \tag{A4.3.4}$$

$$Z = \frac{120\pi}{\sqrt{K1K3}\sqrt{e_r}}(\frac{d}{w}) \quad [\Omega] \tag{A4.3.5}$$

4.4. LCZ FOR HORIZONTAL FLAT CONDUCTORS.

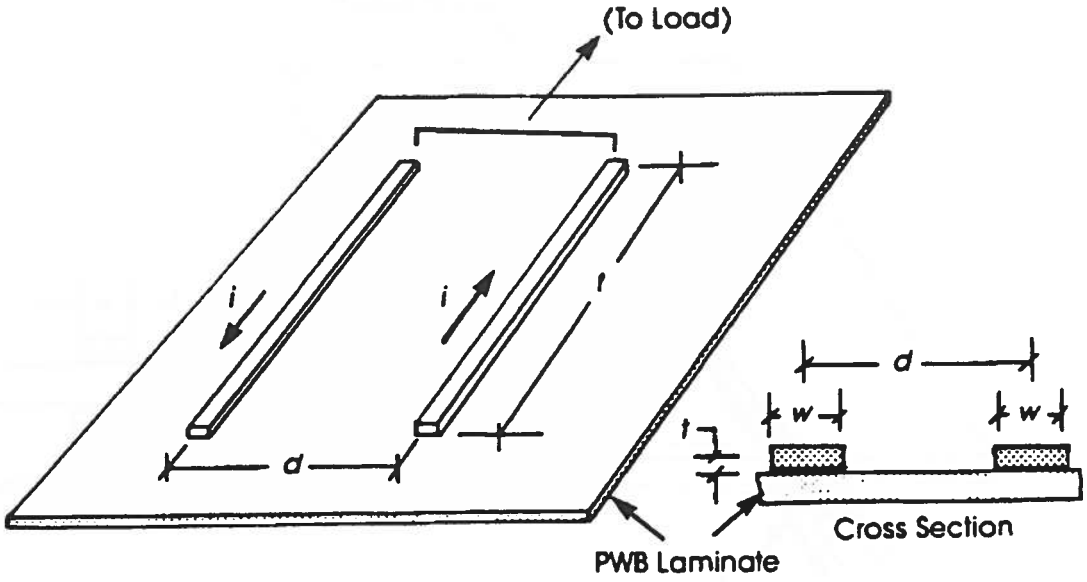

Figure A4.4: Two parallel, flat conductors represent lands on a printed circuit board.

$$C \approx \frac{\pi e_r e_0 \, l}{\ln\left(\frac{\pi(d-w)}{w+t}+1\right)} \quad [F] \tag{A4.3.1}$$

$$L \approx \frac{\mu_r \mu_0 \, l}{\pi} \ln\left(\frac{\pi(d-w)}{w+t}+1\right) \quad [H] \tag{A4.4.2}$$

$$Z \approx \frac{120}{\sqrt{e_r}} \ln\left(\frac{\pi d}{w+t}\right) \quad [\Omega] \tag{A4.4.3}$$

4.5. LCZ FOR FLAT CONDUCTOR ABOVE A GROUND PLANE.

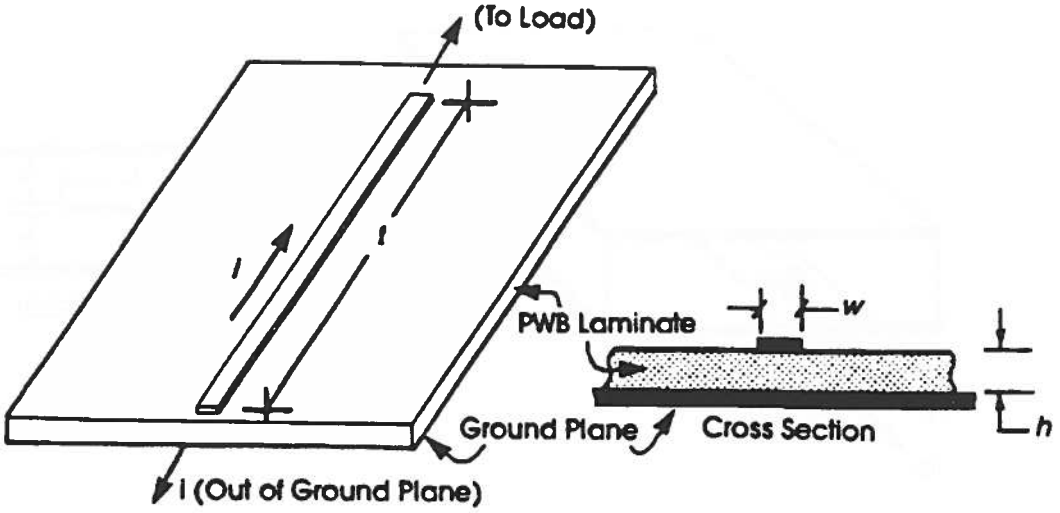

Figure A4.5: A flat conductor above a ground plane.

$$C = e_r e_0 K1 (\frac{w}{d}) \quad [F] \tag{A4.5.1}$$

Wherein K1 is as in paragraph 4.3.

$$L \approx \frac{\mu_r \mu_0 \, l}{K3} (\frac{h}{w}) \quad [H] \tag{A4.5.2}$$

and K3:

$$K3 \approx 2 + 0.65 \frac{2h}{w} \tag{A4.5.3}$$

$$Z \approx \frac{120\pi}{\sqrt{K1K3}\sqrt{e_r}} (\frac{h}{w}) \quad [\Omega] \tag{A4.5.4}$$

4.6. LCZ FOR A FLAT CONDUCTOR BETWEEN TWO GROUND PLANES.

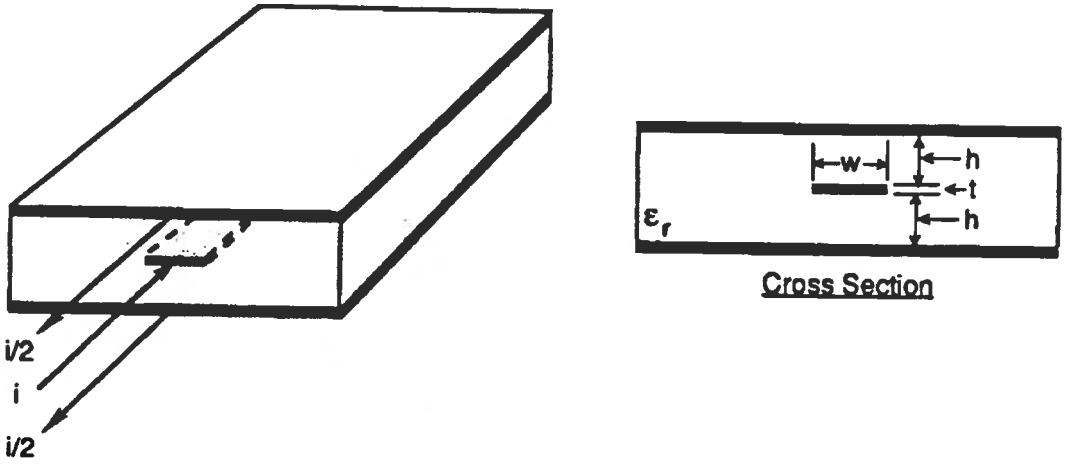

Figure A4.6: A flat conductor between two ground planes.

$$C = 2\varepsilon_r\varepsilon_0 K2\ l(\frac{w}{h}) \quad [F] \tag{A4.6.1}$$

Wherein the fringing factor K2:

$$K2 = 1 + (0.5\frac{2h}{w}) \tag{A4.6.2}$$

$$L = \frac{\mu_r\mu_0\ l}{2K2}(\frac{h}{w}) \quad [H] \tag{A4.6.3}$$

Wherein the factor K4:

$$K4 = 1 + (0.5\frac{2h}{w}) \tag{A4.6.4}$$

$$Z = \frac{60\pi}{K2\sqrt{\varepsilon_r}}\frac{h}{w}) \quad [\Omega] \tag{A4.6.5}$$

4.7. LCZ FOR A COAXIAL CABLE.

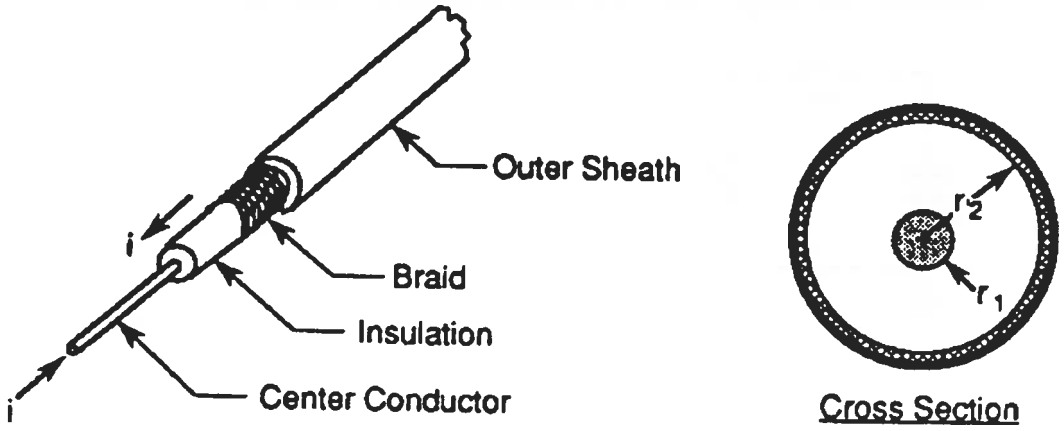

Figure A4.7: Coaxial cable.

$$C = \frac{2\pi e_r e_0 \, l}{\ln}\left(\frac{r2}{r1}\right) \quad [F] \tag{A4.7.1}$$

$$L = \frac{\mu_r \mu_0 \, l}{2\pi}\ln\left(\frac{r2}{r1}\right) \quad [H] \tag{A4.7.2}$$

Wherein r1 and r2 are the radius of the outer and inner conductor respectively.

$$Z = \frac{60}{\sqrt{e_r}}\ln\left(\frac{r2}{r1}\right) \quad [\Omega] \tag{A4.7.3}$$

APPENDIX 5: SIMULATION RESULTS AND MEASUREMENT RESULTS.

In this appendix the measurement and simulation results of the test PCB's are collected. For the symmetric and the asymmetric test PCB the same circuit is used for the simualtions. Only the parameters are changed. This basic circuit is drawn in Figure A5.1:

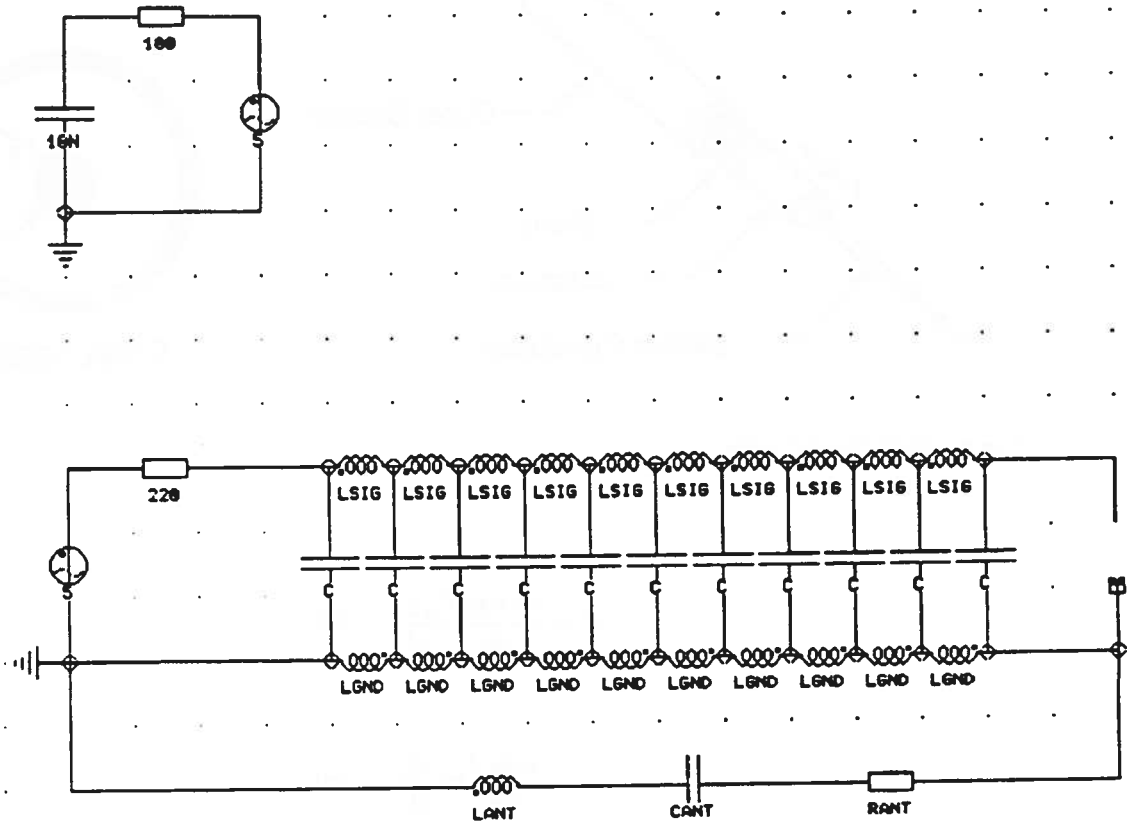

Figure A5.1: Simulated circuit for test boards.

In the pages hereafter the simulation results are given in the upper half and the measurements are given in the lower half of the page. The simulation results are from top to bottom:

+ Electric fieldstrength due to differential mode signal current.
+ Electric fieldstrength due to common mode current.
+ Electric fieldstrength due to differential mode power supply decoupling current.

For some setups no simulation or measurements are carried out. Then only one of the two is given.

The frequency scale is for all graphs between 10 MHz and 1 GHz. The amplitude scale is for all simulation results similar (0-100 dBμV/m), but for the measurement results two different scales are used.

SIMULATED ELECTRIC FIELD STRENGTH [dBμV/m]

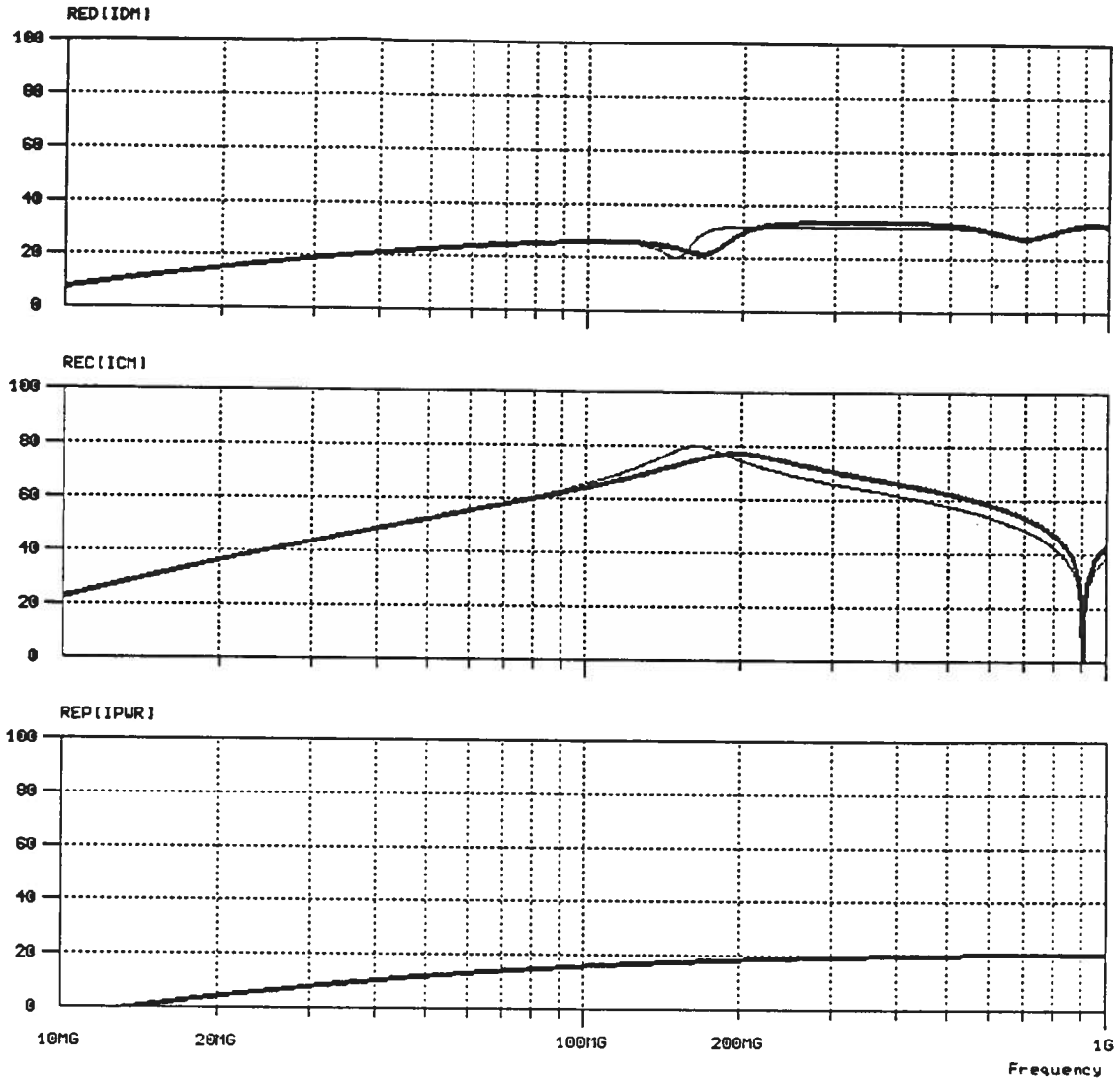

MEASURED FIELD STRENGTH [dBμV/m]

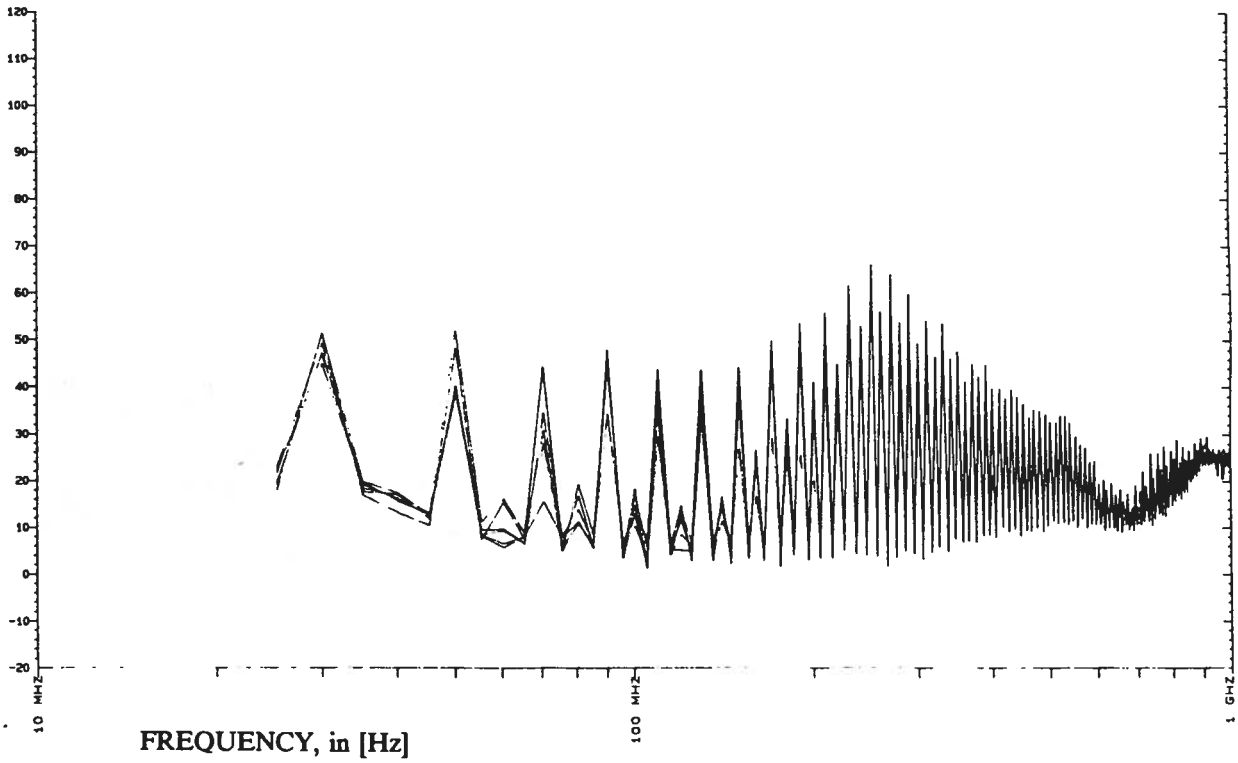

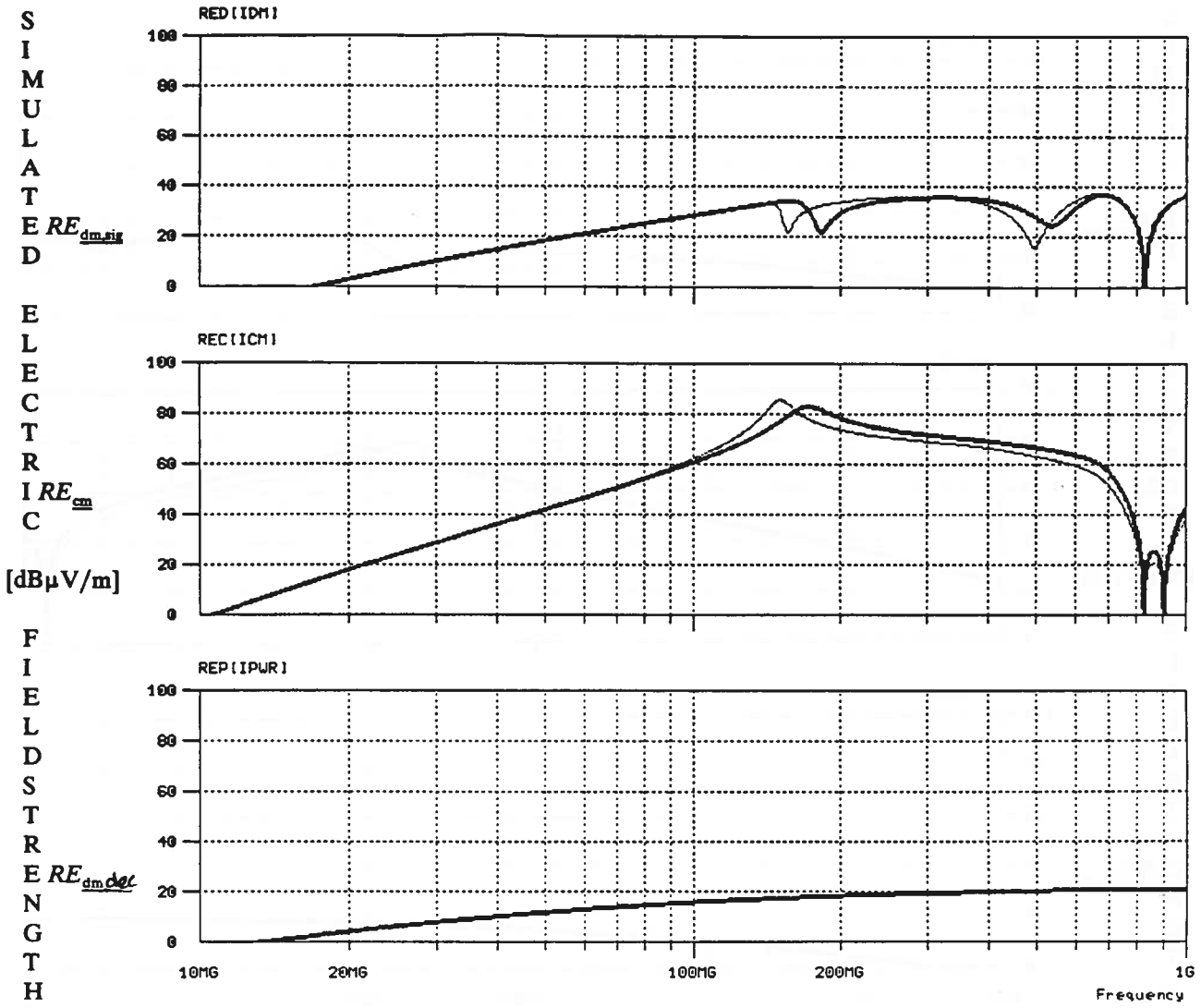
SIMULATED ELECTRIC FIELD STRENGTH
[dBμV/m]
RE_dm,sig
RE_cm
RE_dm,del
RED[IDM]
REC[ICM]
REP[IPWR]
100
80
60
40
20
0
10MG
20MG
100MG
200MG
1G
Frequency

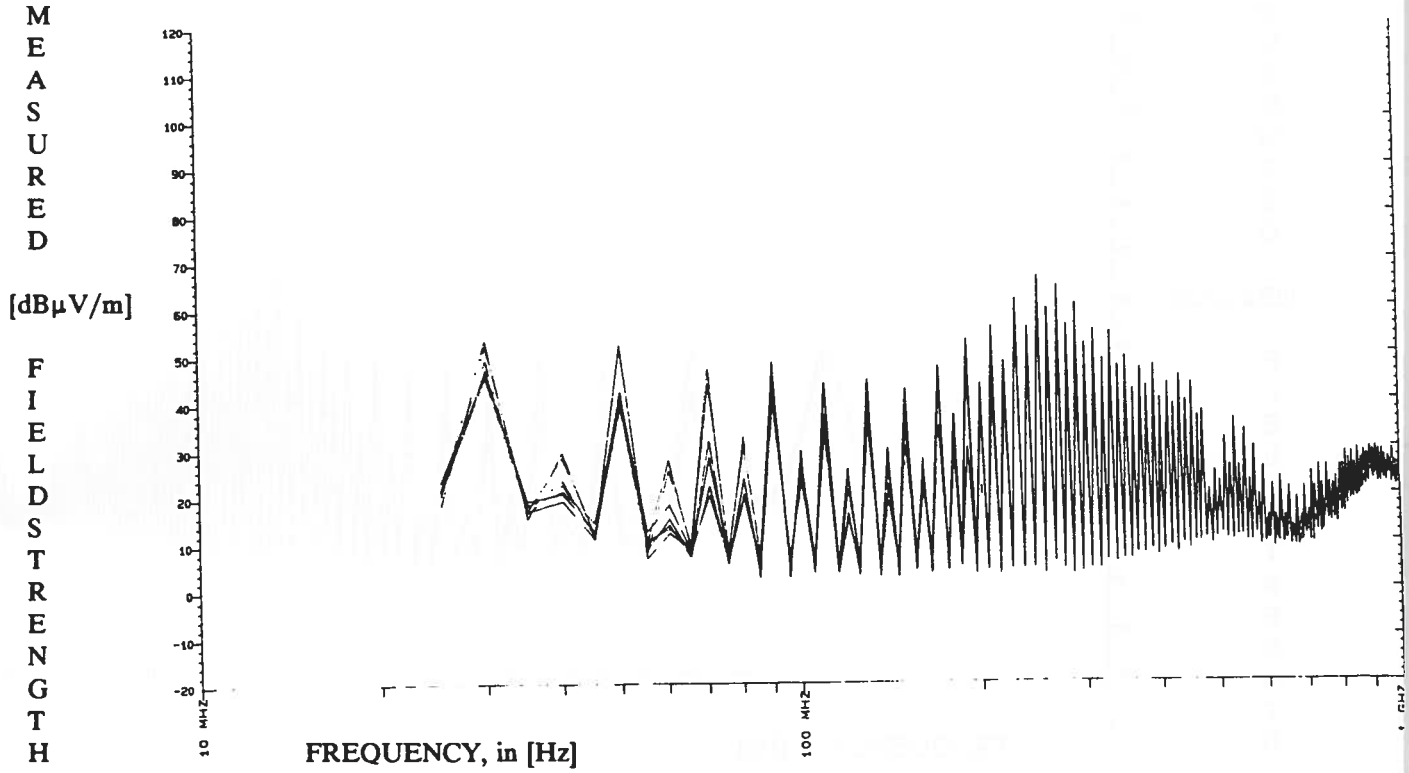
MEASURED FIELD STRENGTH
[dBμV/m]
120
110
100
90
80
70
60
50
40
30
20
10
0
-10
-20
10 MHz
100 MHz
FREQUENCY, in [Hz]

SIMULATED ELECTRIC FIELD STRENGTH [dBµV/m]

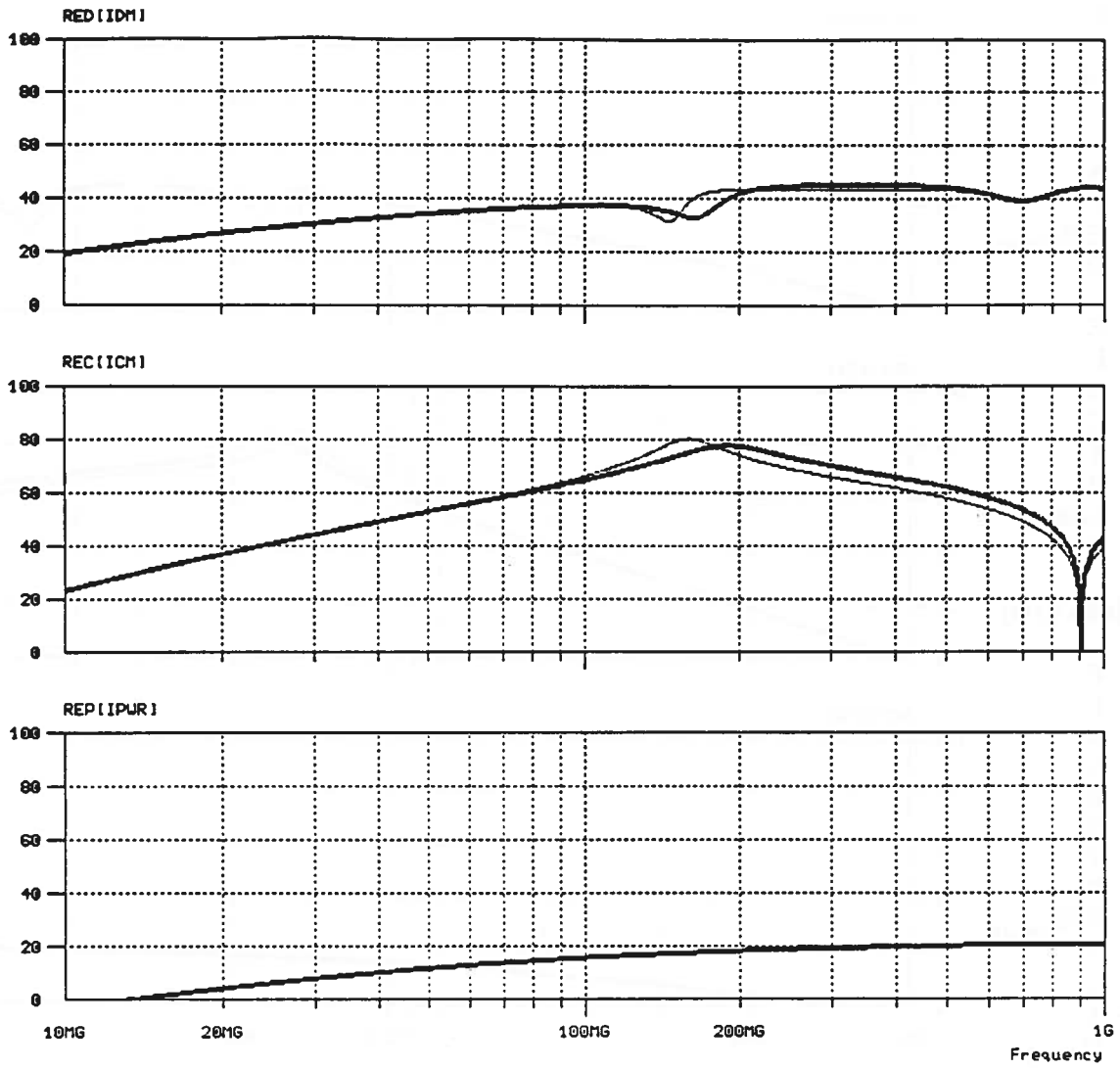

$RE_{dm,sig}$

RE_{cm}

$RE_{dm,det}$

MEASURED FIELD STRENGTH [dBµV/m]

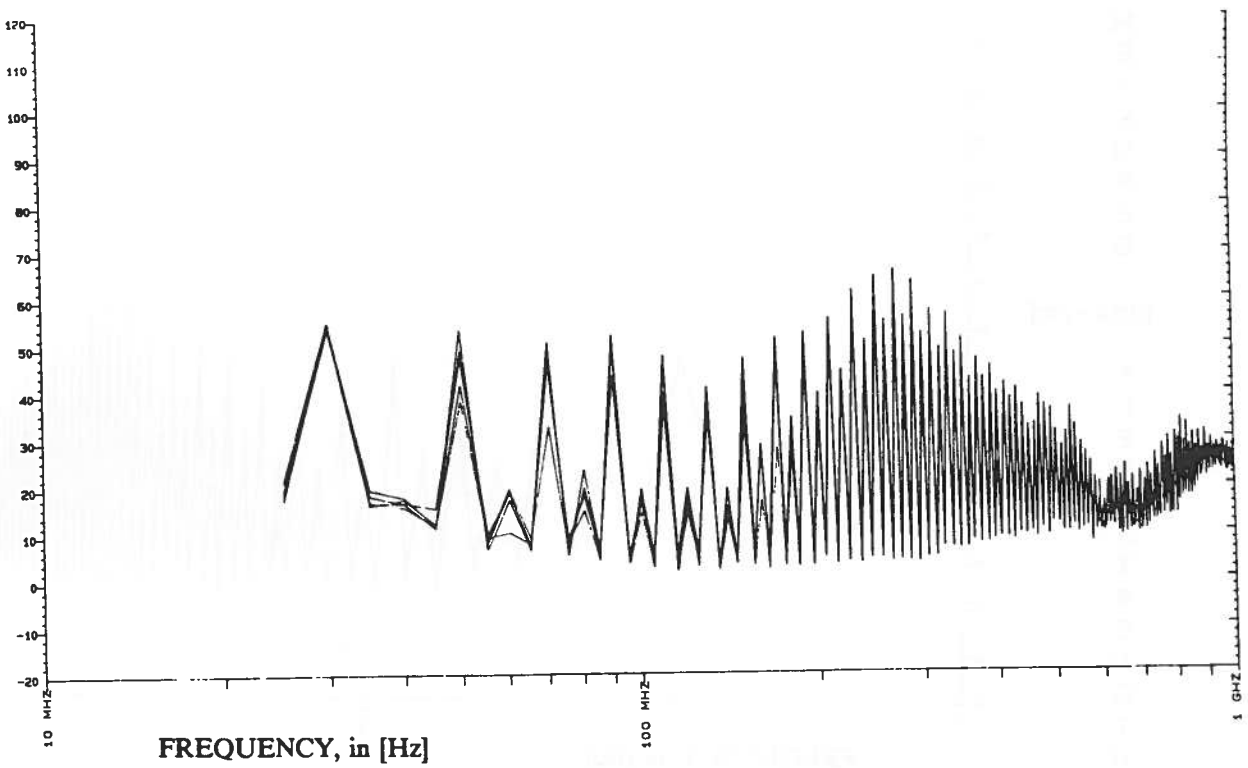

SIMULATED ELECTRIC FIELD STRENGTH [dBμV/m]

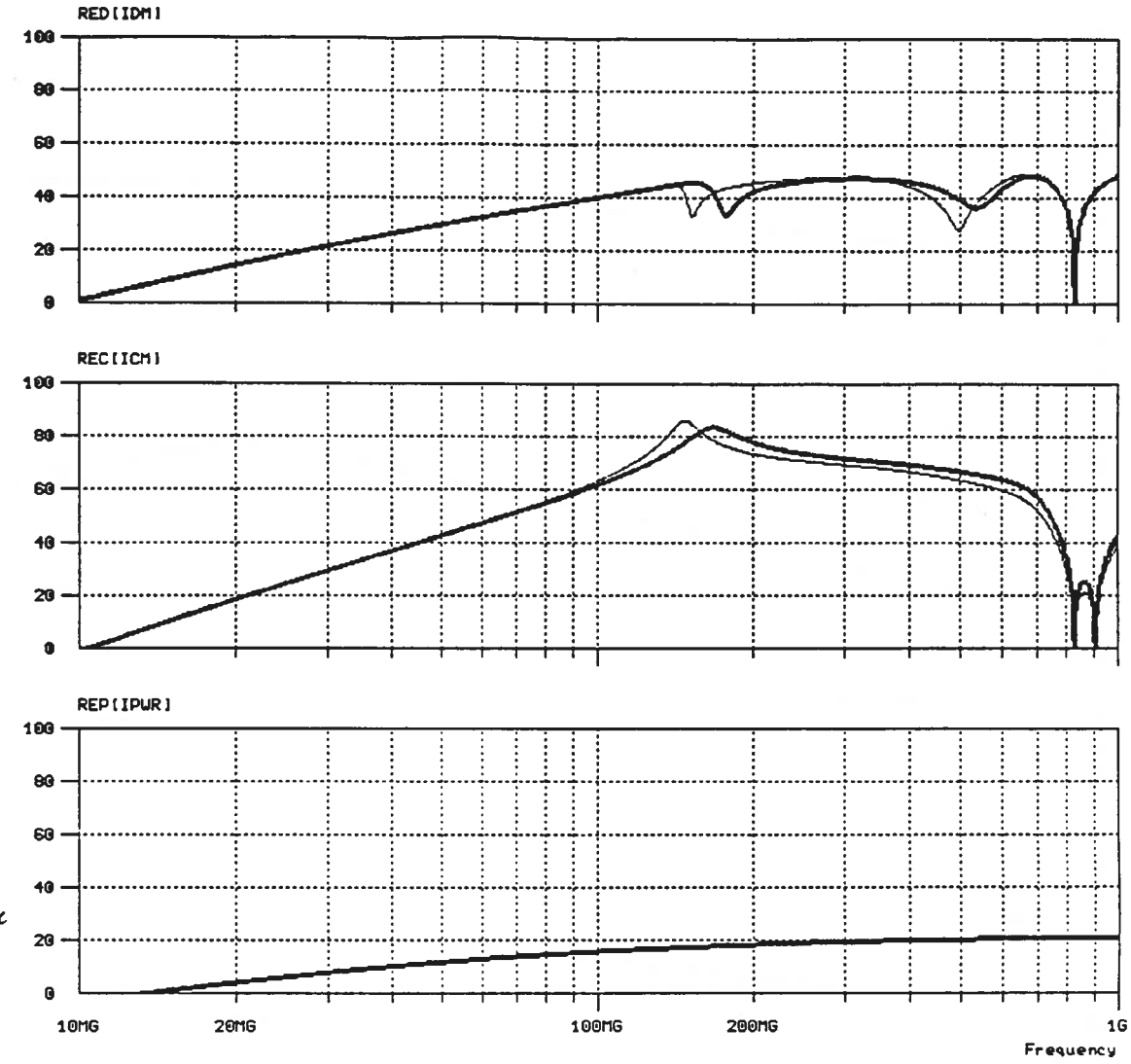

$RE_{dm,sig}$

RE_{cm}

$RE_{dm,dec}$

MEASURED FIELD STRENGTH [dBμV/m]

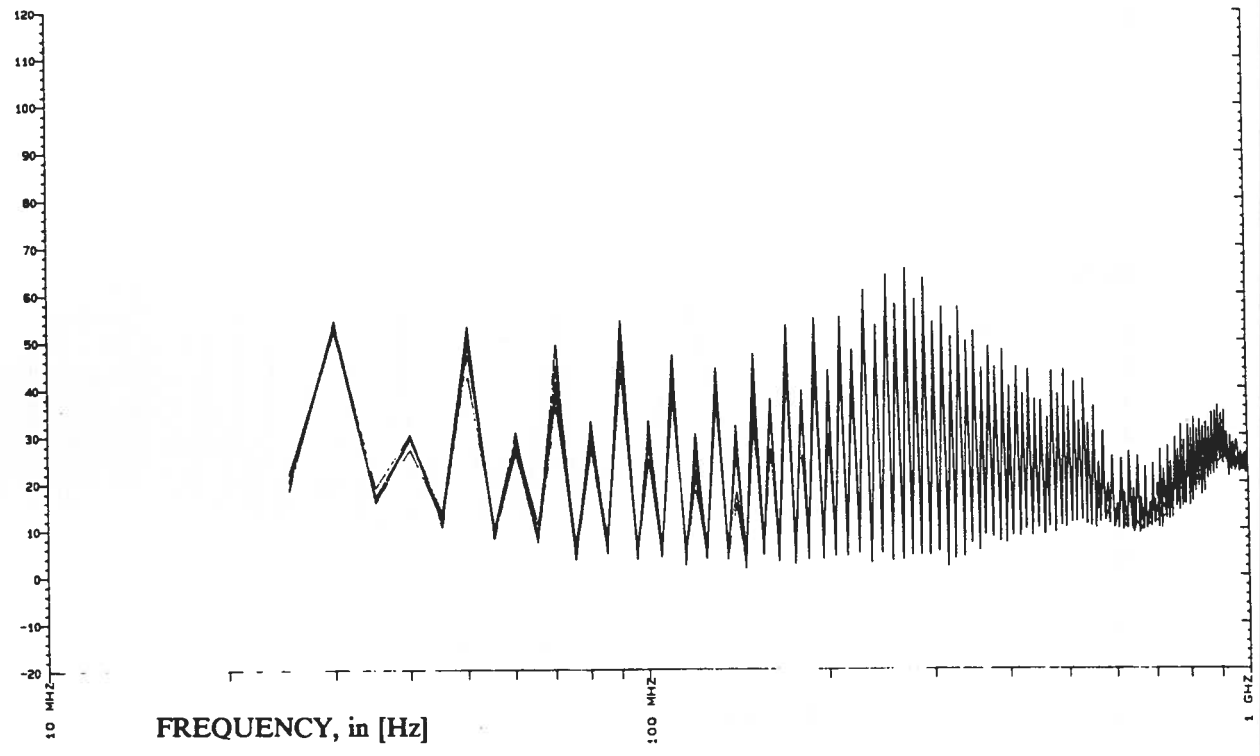

SIMULATED ELECTRIC FIELD STRENGTH [dBμV/m]

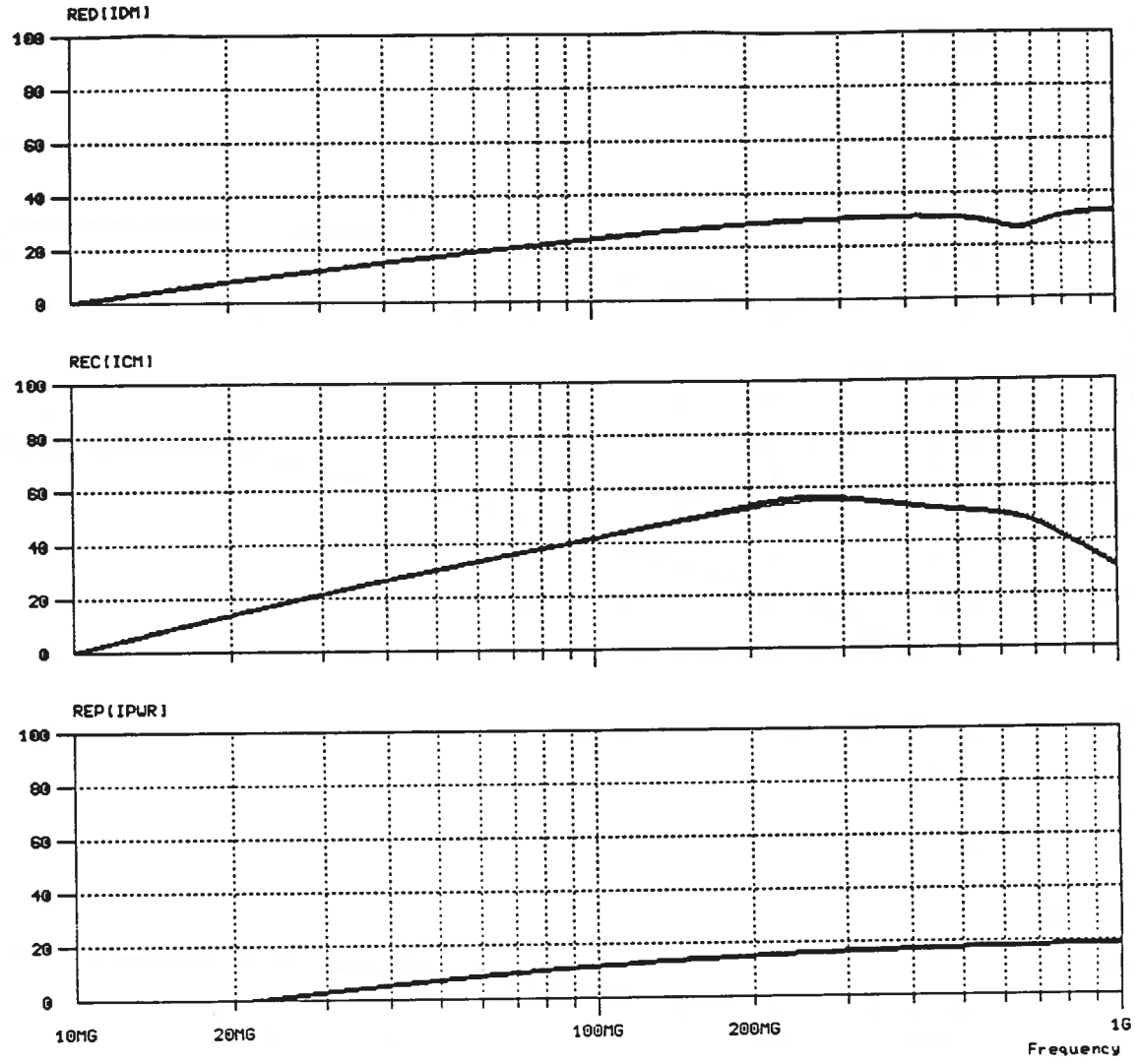

MEASURED FIELD STRENGTH [dBμV/m]

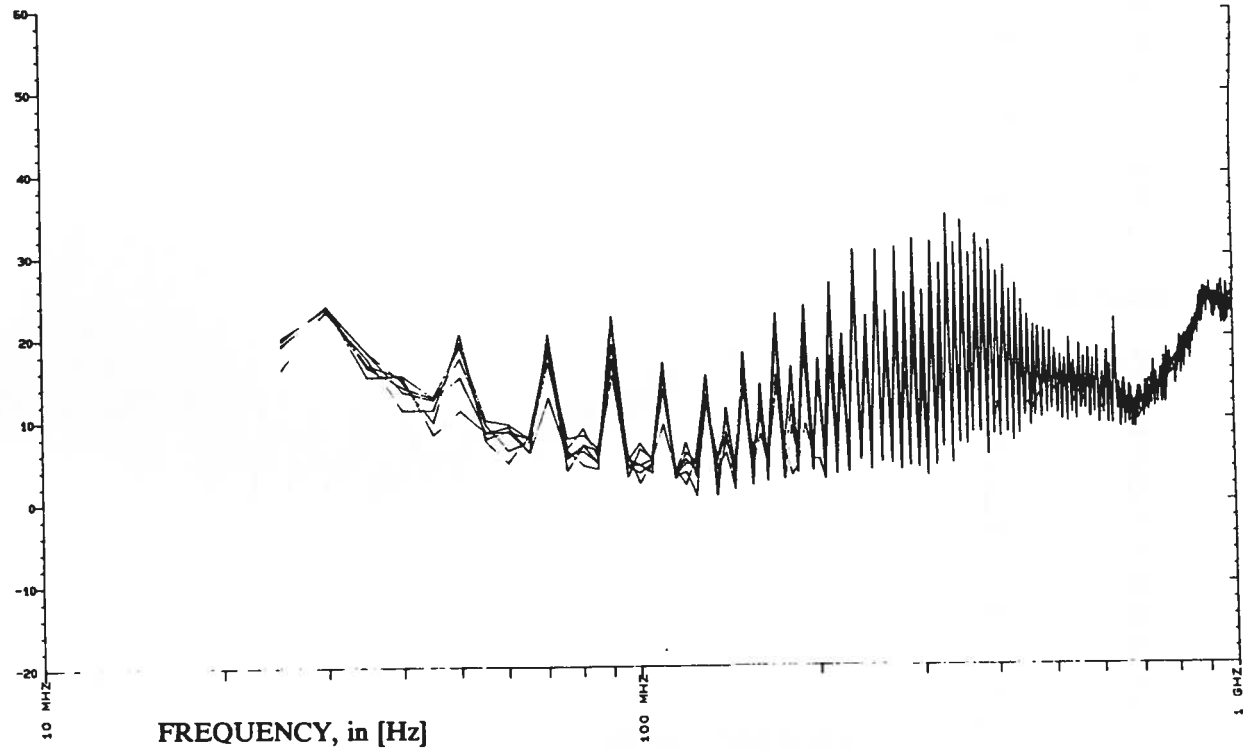

SIMULATED ELECTRIC FIELD STRENGTH [dBμV/m]

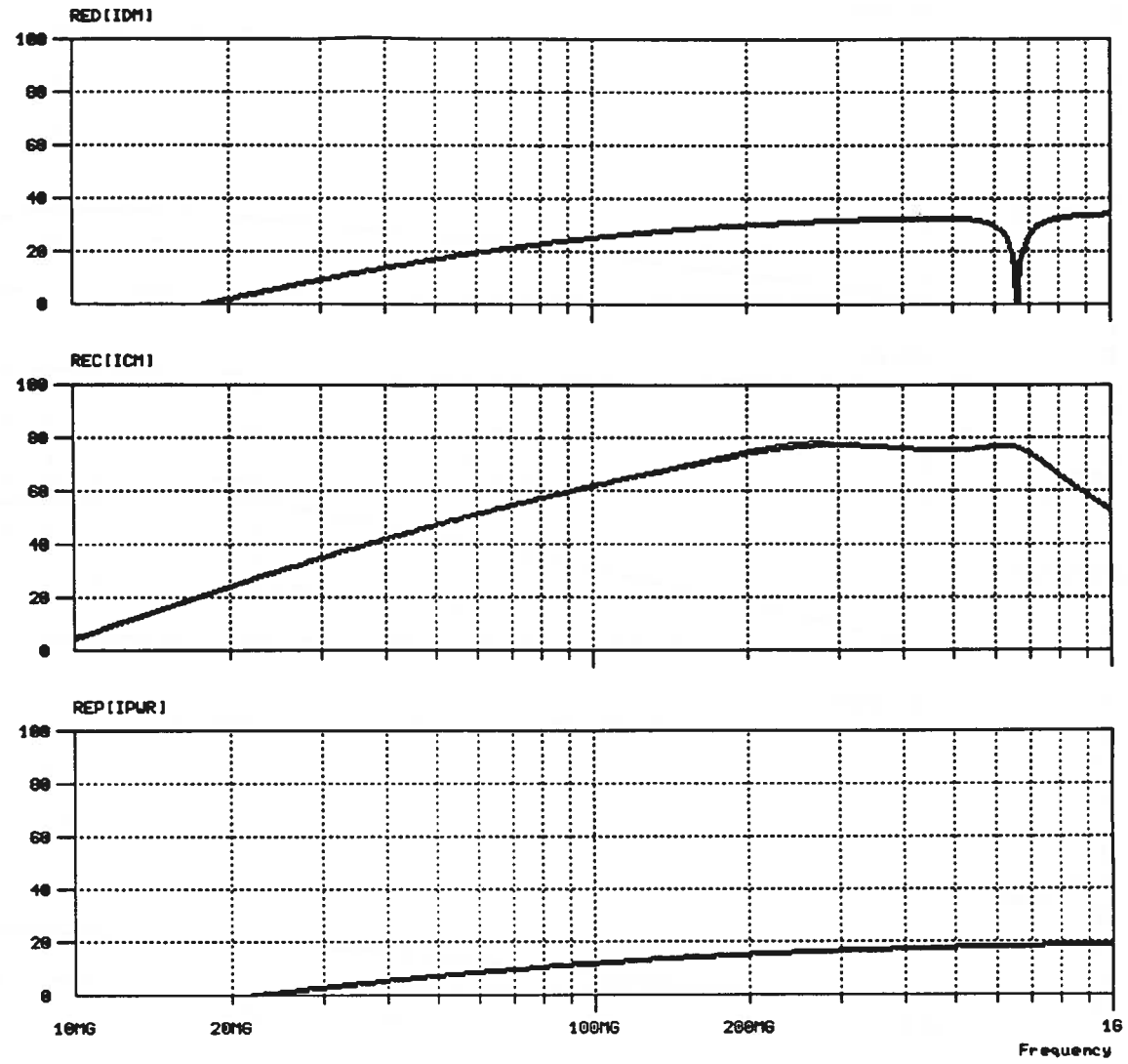

$RE_{dm,sig}$

RE_{cm}

$RE_{dm,dec}$

MEASURED FIELD STRENGTH [dBμV/m

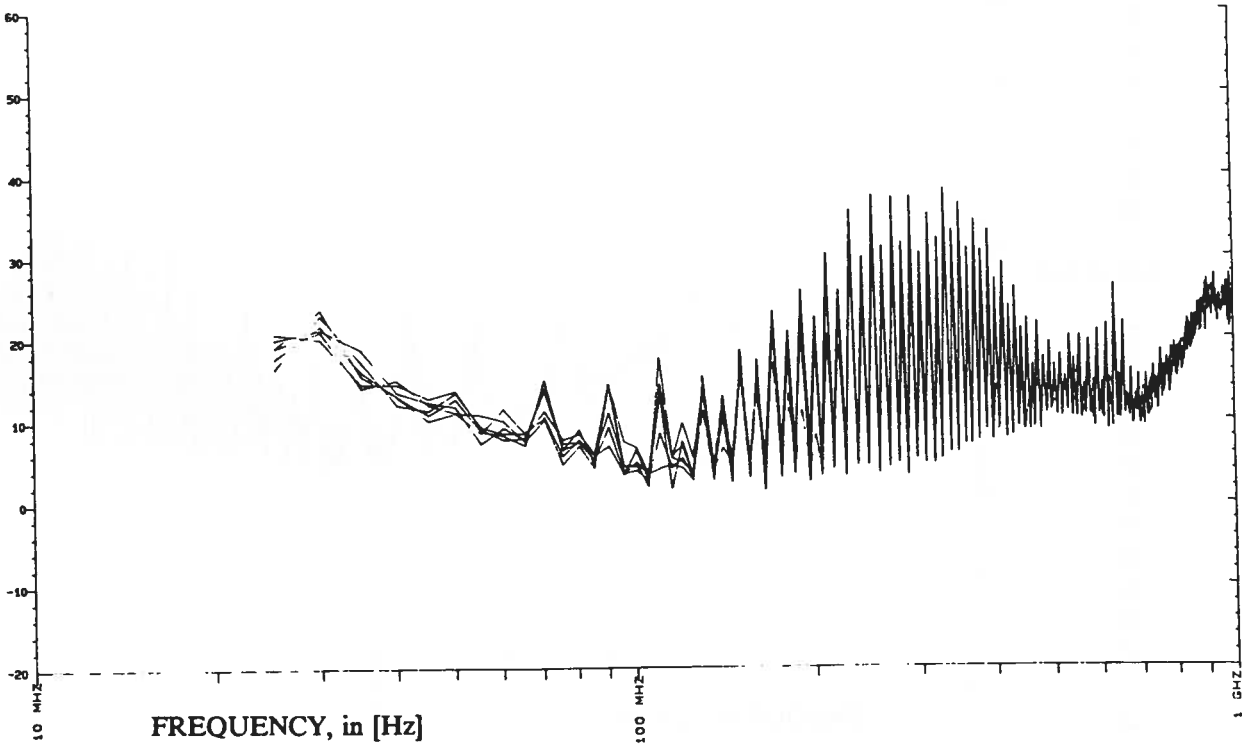

SIMULATED ELECTRIC FIELD STRENGTH [dBμV/m]

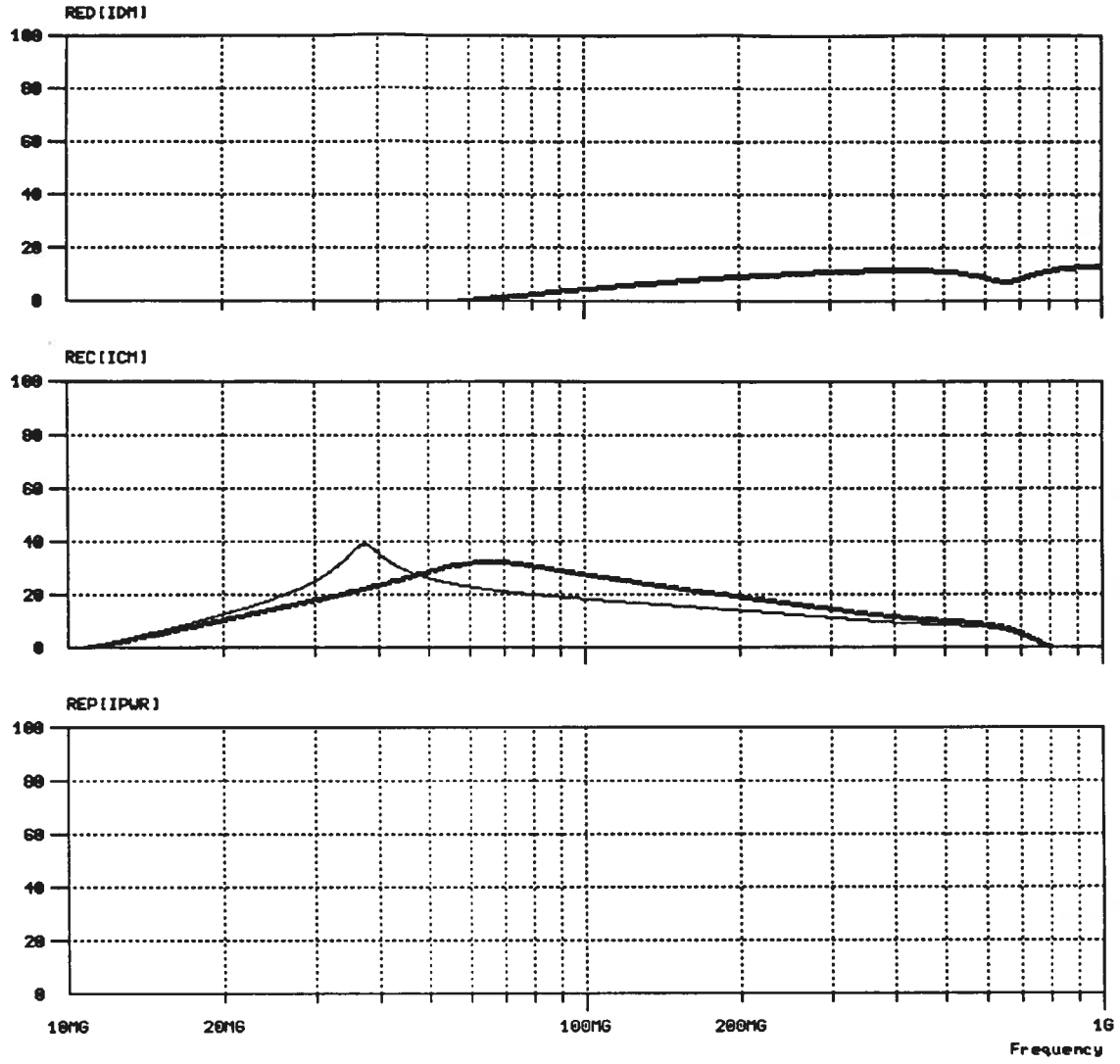

$RE_{dm,sig}$

RE_{cm}

$RE_{dm,dec}$

MEASURED FIELD STRENGTH [dBμV/m]

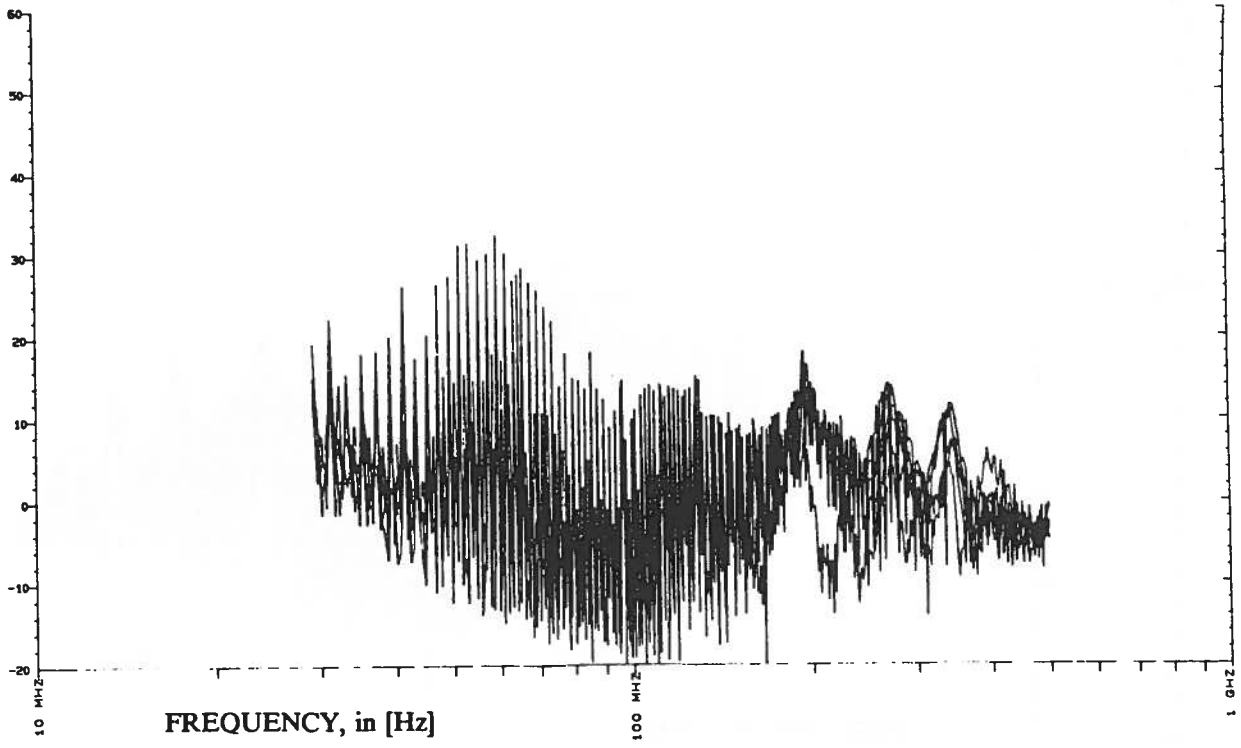

SIMULATED ELECTRIC FIELD STRENGTH $RE_{dm,sig}$ RE_{cm} $RE_{dm,clk}$

[dBμV/m]

MEASURED FIELD STRENGTH

[dBμV/m]

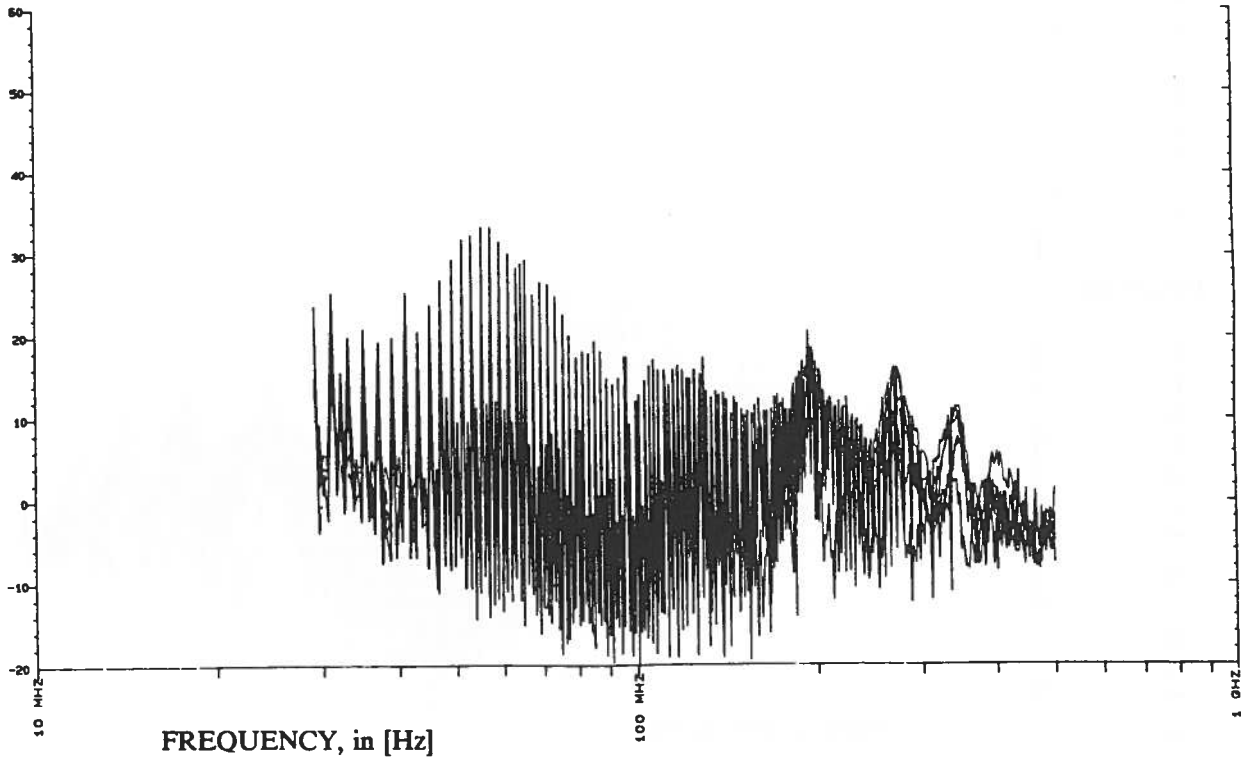

SIMULATED ELECTRIC FIELD STRENGTH $RE_{dm,sig}$

RE_{cm}

[dBμV/m]

$RE_{dm,elec}$

MEASURED ELECTRIC FIELD STRENGTH

[dBμV/m]

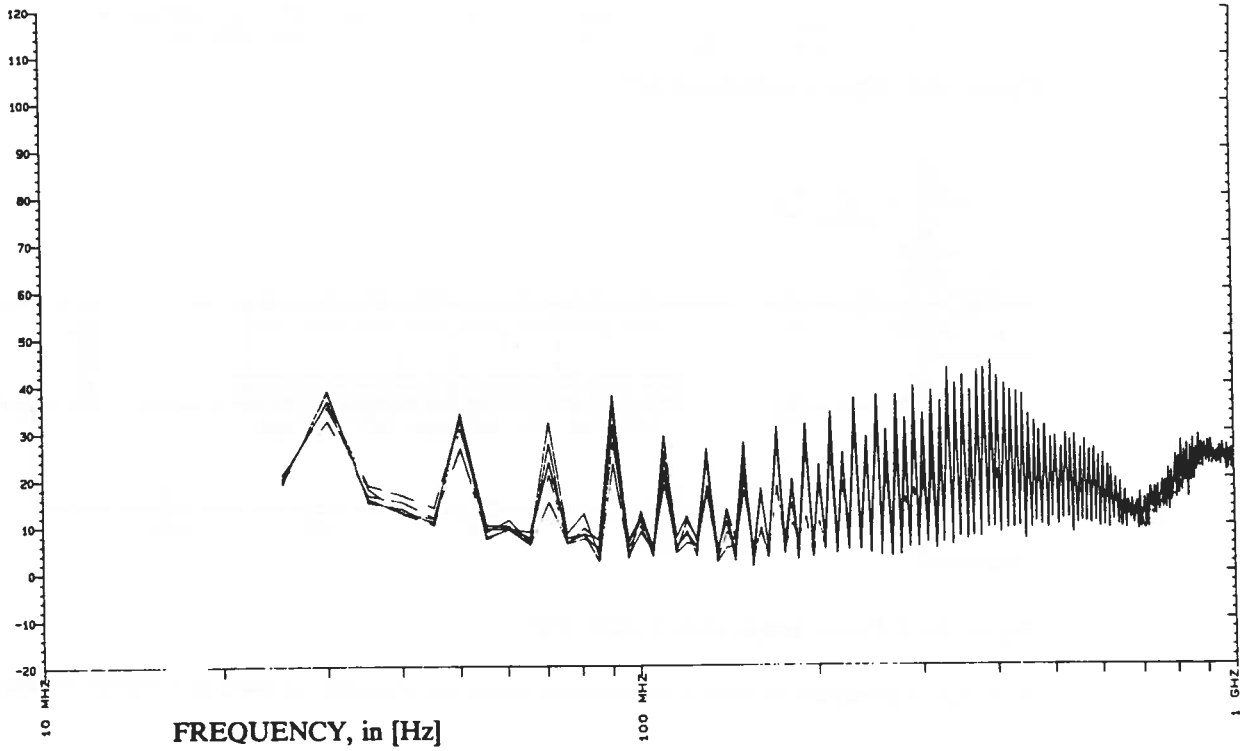

APPENDIX 6: SIMULATION RESULTS CGIC.

In the figures below the complete circuit as used in the simulation is given. Due to convergence problems and a new version, which did not function, of the software, the simulation results cannot be given.

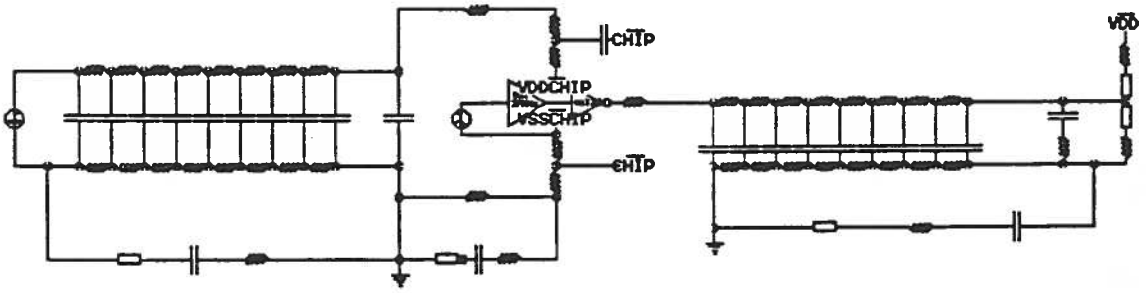

Figure A6.1: Complete circuit; The IC is modeled via a macro.

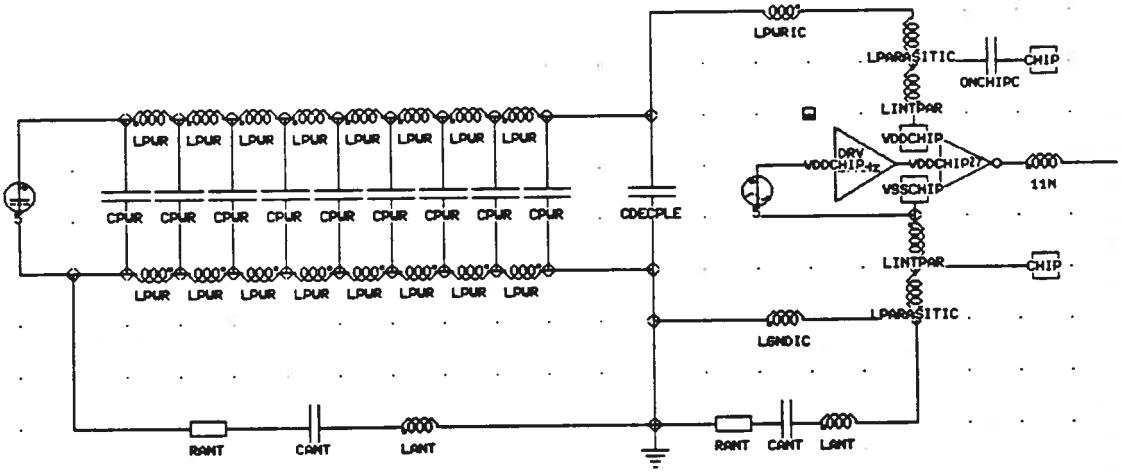

Figure A6.2: Signal transmission line.

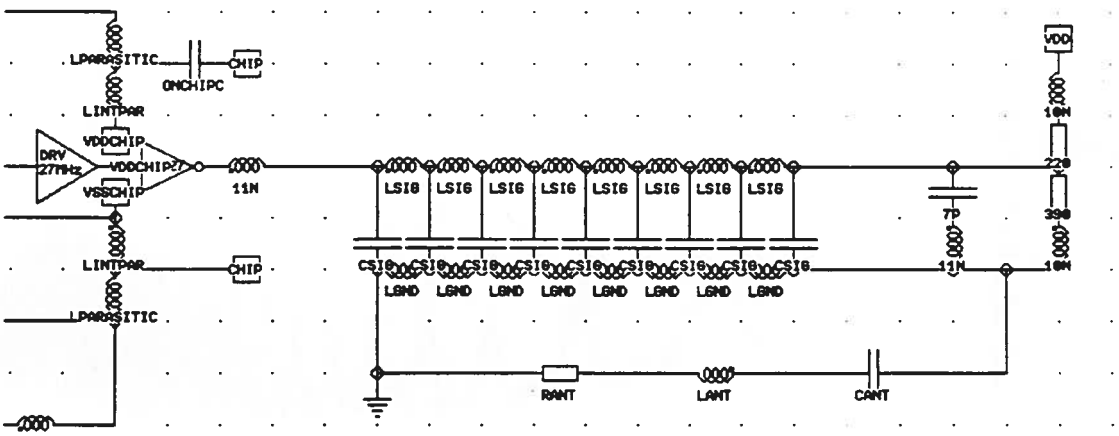

Figure A6.2: Power supply transmission line.

APPENDIX 7: EMI DESIGN RULES.

The design rules (DR) mentioned in this paragraph are collected during my career as EMI engineer. These DR's are for preventing radiated emission only, and are taken from several sources.

* Use the lowest possible clockfrequency needed for the application.
* Use the lowest possible rise-times needed for the application.
* Use the slowest logic family suitable for the function.
* Reduce all current loops.
* Give each high-frequency signal its own return, for instance by creating a ground plane.
* Each part of the circuit must be supplied and decoupled locally.
* Prevent supply short-currents via the PMOS-NMOS path.
* Use the lowest possible load capacitance.
* Apply separated power supply pins when using large IC's with several output drivers.
* Be aware that every conductor is inductive for frequencies above approximately 1 MHz.
* Analog and digital power supply must always be separated.
* Forget star-point grounds and replace this idea with the one-ground-plane ground.
* Use a large asymmetry for the signal tracks/leads with respect to the return- or ground track/lead.
* Use a large asymmetry for the power supply tracks/leads with respect to the return- or ground track/lead.
* Every IC must be decoupled locally. Eventually use ferrite beads to separate the IC's for high frequencies via the power supply, and also create more asymmetry with these beads.
* Clock signals leads and power supply decoupling loops are the greatest radiators. Tackle these parts first.
* Any interconnection cable must be connected to the reference of the circuit to prevent any antenna effect.
* All interconnection cable must be connected at one side of the product to prevent disturbing currents flowing through the product.
* Of course, all shielded cables used with digital logic, should have the shield grounded at both ends.
* Ground terminations of cable shields should provide a 360° contact with the shield.
* All cables entering or leaving the product require treatment to control radiated emission.
* I/O drivers should be near the connector.
* Clock ciruitry and leads should be away from the I/O area.
* The following techniques can be used to control the common mode currents. They should be used in the following order:
  - reduce the ground lift voltage,
  - use common mode ferrite chokes over I/O cables,
  - use cable shielding.
* The most important action in preventing common mode radiation is to lower the ground inductance with respect to the signal inductance.
* Every conductor is resonant at $\lambda/4$, $\lambda/2$ etc.
* Reduce the current on long lines; Use buffers to decrease currents.
* When conductive areas are available then I/O cables must be laid nearby.
* Use a 'chinese' power supply, i.e. feed the product with the power supply leads at the points where most current is needed.
* Prevent large currents to flow through the reference.

APPENDIX 8: BIBLIOGRAPHY AND CONSULTED WORKS.

* H.B. Bakoglu, Circuits, interconnects and packaging for VLSI, Addison-Wesley, 1990.

* B.D. Berman, The mutual inductance of a current source and a non-coplanar parallel, rectangular loop, IEEE Symposium on EMC, pages 309-314, 1989.

* T. Braxton, Effect of bus driver devices on transmission line emissions, IEEE Symposium on EMC, pages 317-321, 1988.

* C. Brench, Effects of cable and pheripheral placement on radiated emissions, IEEE Symposium on EMC, pages 351-356, 1989.

* A.C. Brombacher, Integrating reliability analysis in the design process of electronic circuits and systems, Enschede, 1990.

* D.R. Bush, Radiated emission of printed circuit board clock circuits, 6th International Sympiosium on EMC, pages 121-126, 1985.

* S. Cannigia, Models for circuit simulators to analyse crosstalk and radiation into wires, IEEE Symposium on EMC, pages 304-310, 1988.

* I. Catt, M.F. Davidson, D.S. Walton, Displacement current- and how to get rid of it, Wireless World, dec. 1978, pages 51-52.

* V. Costa, S. Canniggia, L. Catello, On the computation of electromagnetic field components from a transmission line: Theory and applications, IEEE Symposium on EMC, pages 651-656, 1990

* G. Costache, M. Radojicic, A model to predict radiated emissions from electric circuits, IEEE Symposium on EMC, pages 54-57, 1991.

* J.P. Charles, Electromagnetic interference control in logic circuits, 6th International Symposium on EMC, pages 145-150, 1985.

[Chatterton, 1992] P.A. Chatterton, M.A. Houlden, EMC, electromagnetic theory to practical design, Wiley, Chicester, 1992.

[Coenen, 1989] M. Coenen, EMC and PCB constraints, Philips Components Eindhoven, Lab. report ESG 89001, 1989.

* M. Coenen, An evaluation method to characterize the EMC performance of PCB's containing IC's, Philips Components Eindhoven, Lab. report ESG 8801, 1988.

* M. Coenen, Comparison between corner and center supply octal driver logic families, 9th International Symposium on EMC, pages 707-711, 1991.

* B. Danker, New measures to decrease radiation from printed circuit boards, 6th International Symposium on EMC, pages 115-120, 1985.

* B. Danker, EMC and loop inductances on printed wiring boards, 7th International Symposium on EMC, pages 583-588, 1987.

* S. Daijavad, J. Janak, H. Heeb, A. Ruehli, D. McBride, A fast method for computing radiation from a printed circuit board, IEEE Symposium on EMC, pages 300-304, 1990.

* S. Daijavad, B.J. Rubin, Modelling common-mode radiation of 3-D structures, IEEE transactions on EMC, vol. 34, no. 1, 1992.

* B. Demoulin, C. Lardé, P. Degauque, Interference effects in CMOS and TTL IC's, 8th International Symposium on EMC, pages 543-546, 1989.

L. Diaz-Olavarneta, Ground bounce in ASIC's: Model and test results, IEEE Symposium on EMC, pages 387-392, 1991.

[Durcansky, 1991] G. Durcansky, EMV-gerechtiges Gerätedesign, Franzis, Munchen, 1991.

* R. Dutschke, Praktische probleme beim Erstellen eines EMV-gerechten CAD-Layouts, EMV '92, Karlsruhe, pages 521-527, 1992.

* L. Dworsky, Modern transmission line theory and applications, Wiley, 1979.

* T. Edwards, Foundations for microstrip circuit design, Wiley, 1992.

[Fischer, 1992] R. Fischer, Anwendung des Prinzips der Virtuellen Masse zur Reduzierung der HF-Abstrahlung von Leitungen und Kabelbäumen, EMV '92, Karlsruhe, pages 433-440, 1992.

* F. Gardiol, Radiation from high frequency printed circuit boards, 9th International Symposium on EMC, pages 625-630, 1991.

* R.F. German, Use of a ground grid to reduce printed circuit board radiation, 6th International Symposium on EMC, pages 133-138, 1985.

* R.F. German, H.W. Ott, C.R. Paul, Effect of an image plane on printed circuit board radiation, IEEE Symposium on EMC, pages 284-291, 1990.

* J.J. Goedbloed, Electromagnetische compatibiliteit, Kluwer, Deventer, 1990.

* D.V. Gonshor, Wire radiation impact on system level EMC, IEEE Symposium on EMC, pages 667-670, 1990.

* H. Grabinski, Theorie und Simulation von Leiterbahnen, Springer, Berlin, 1990.

* L.B. Gravelle, P.F. Wilson, EMI/EMC in printed circuit boards, a literature review, IEEE transactions on EMC, vol. 34, no. 2, pages 109-116, 1992.

[Grivet, 1970] P. Grivet, The physics of transmission lines at high and very high frequencies, vol. 1, Academic Press, London, 1970.

[Grover, 1946] H.W. Grover, Inductance calculations, Dover publications, 1946.

[Hardin, 1991] K.B. Hardin, C.R. Paul, K. Naishadham, Direct prediction of common-mode currents, IEEE Symposium on EMC, pages 67-71, 1991.

* J.B. Hatfield, Reciprocity and moments method applied to predicting radiated emissions, 9th International Symposium on EMC, pages 65-69, 1991.

* T.H. Hubing, J.F. Kaufman, Modelling the electromagnetic radiation from electrically small table-top products, IEEE transactions on EMC, vol. 31, pages 74-84, 1989.

* T. Hsu, The validity of using image plane theory to predict board radiation, IEEE Symposium on EMC, pages 58-60, 1991.

[Jasik, 1961] H. Jasik (editor), Antenna engineering handbook, McGraw-Hill, New York, 1961.

* W. John, Bemerkungen zur behandlung von EMV probleme auf PCB mit expert-system unterstutzung, EMV '88, Karlsruhe, pages 499-510, 1988.

* W. John, Unterstützung des Leiterplattenentwurfs mit Hilfe einer integrierten EMV-Analyse-Workbench, EMV '92, Karlsruhe, pages 477-504, 1992.

* J.W.E. Jones, Achieving compatibility in inter-unit wiring, 6th International Symposim on EMC, pages 139-144, 1985.

[Ref. data, 1988] E.C. Jordan (editor), Reference data for engineers, Sams & Co, Indianapolis, 1988.

[Kaden, 1959] H. Kaden, Wirbelströme und Schirmung in der Nachrichtentechnik, Springer, Berlin, 1959.

* Y. Kami, Radiation from a transmission line carrying current of an arbitrarily waveform, IEEE Symposium on EMC, page 124-129, 1988.

* Y. Kami, R. Sato, Coupling and radiation problems for pair-line above a conducting plane, IEEE Symposium on EMC, page 662-666, 1990.

* B. Keiser, Principles of electromagnetic compatibility, Artech House, Norwood, 1987.

* R.L. Khan, G.I. Costache, Finite element method applied to modelling crosstalk problems on PCB's, IEEE transactions on EMC, vol. 31, pages 5-15, 1989.

* J. Kiang, On resonance and shielding of printed traces on a circuit board, IEEE transactions on EMC, vol. 32, pages 269-276, 1990.

* T.H. Kneath, Electromagnetic modelling methods for EMC design, IEEE Symposium on EMC, pages 489-495, 1987.

* D.N. Ladd, G.I. Costache, Considerations of using VIAS as a crosstalk reduction technique, 9th International Symposium on EMC, pages 631-634, 1991.

* C.F. Lee, K. Li, S.Y. Poh, R.T. Shin, L.A. Kong, Electromagnetic radiation from a VLSI package and heatsink configuration, IEEE Symposium on EMC, pages 393-398, 1991.

[Leferink, 1989] F.B.J. Leferink, P.A. Suringa, The use of near-field probes for EMI-diagnosis, Philips EMC-market, 1989.

[Mardiguian, 1988] M. Mardiguian, Electromagnetic control in components and devices, volume 5 of Handbook series on electromagnetic interference and compatibility, Interference Control Technologies, Gainesville, 1988.

* H. Meinke, F.W. Gundlach, Taschenbuch der Hochfrequenztechnik, Springer, Berlin, 1968, 3th edition.

[Meinke&Gundlach,'86] H. Meinke, F.W. Gundlach, Taschenbuch der Hochfrequenztechnik, Springer, Berlin, 1986, 4th edition.

* M.I. Montrose, Overview on design techniques for printed circuit board layout used in high technology products, IEEE Symposium on EMC, pages 61-66, 1991.

* B.L. Michielsen, Analysis of electromagnetic interference problems for 3-D wire structures and screens, 8th International Symposium on EMC, pages 73-78, 1989.

* R.F. Milsom, K.J. Scott, G. Clark, Electrical simulation of multi-layer PCB with non-parallel tracks and printed components, 8th International Symposium on EMC, pages 63-68, 1989.

* J.P. Muccioli, S.E. Ashley, Radiated emissions of very large scale integrated circuits, IEEE Symposium on EMC, pages 292-299, 1990.

* K. Naishadhan, A rigorous model to compute the radiation from printed circuit boards, IEEE Symposium on EMC, pages 127-130, 1989.

[Ott, 1988] H.W. Ott, Noise reduction techniques in electronic systems, John Wiley and sons, New York, 1988.

* H.W. Ott, Controlling EMI by proper printed wiring board layout, 6th International Symposium on EMC, pages 127-132, 1985.

* J. Poltz, Cross talk and ringing on a multilayer PCB, IEEE Symposium on EMC, pages 347-350, 1989.

* C.R. Paul, Printed ciruit board EMC, 6th International Symposium on EMC, pages 107-114, 1985.

* C.R. Paul, D.R. Bush, Radiated emissions from common mode currents, IEEE Symposium on EMC, pages 197-203, 1987.

[Paul, 1988] C.R. Paul, Diagnosis and reduction of conducted noise emissions, IEEE transactions on EMC, vol. 30, pages 553-560, 1988.

* C.R. Paul, A simple Spice model for coupled transmission lines, IEEE Symposium on EMC, pages 327-333, 1988.

[Paul, 1988] C.R. Paul, Diagnosis and reduction of conducted noise emissions, IEEE Symposium on EMC, pages 19-23, 1988.

* C.R. Paul, A comparison of the contributions of CM and DM currents in radiated emissions, IEEE transactions on EMC, vol. 31, pages 189-193, 1989.

[Paul, 1989] C.R. Paul, Modelling electromagnetic properties of printed circuit boards, IBM Journal Research and Development, vol. 33, no. 1, pages 33-49, 1989.

* C.R. Paul, effectiveness of multiple decoupling capacitors, IEEE transactions on EMC, vol. 34, no. 2, 1992

* A. Rainal, Computing inductive noise of chip packages, AT&T Bell Labs Technical Journal, vol. 63, no. 1, 1984.

* R. Raut, W.J. Steenaart, G.I. Costache, A note on the optimum laypout of electronic circuits to minimize the radiated electric fieldstrength, IEEE transactions on EMC,vol. 30, pages 88-89, 1988.

* R. Raut, On the computation of EM field components from a practical PCB, IEEE Symposium on EMC, pages 161-165, 1986.

* K. Riemens, Crosstalk and resonance effects in printed circuit boards, Philips Research Laboratories, Eindhoven, Nat.Lab. report 6370, 1989.

[Schibuya, 1987] N. Schibuya, H. Takagi, K. Ito, Analysis of PCB crosstalk using a circuit simulator, 7th International Symposium on EMC, pages 589-594, 1987.

[Schibuya, 1991] N. Schibuya, T. Takahashi, K. Ito, Measurement of radiated emission from printed wiring board and estimation of radiation due to current, 9th International symposium on EMC, pages 719-724, 1991.

* J. Simpson, Radiation from microstrip transmission line, IEEE Symposium on EMC, pages 340-343, 1988.

* A.J. Sistino, Radiation from a printed ciruit board: theory and application, 8th International Symposium on EMC, pages 57-62, 1989.

* K.P. Slattery, G. Fuller, The effect of the intrinsic impedances of logic families on the predicted radiated emission from PCB's, IEEE Symposium on EMC, pages 280-283, 1990.

* A. Smith, Coupling of external electromagnetic fields to transmission line, Wiley, New York, 1977.

* T.S. Smith, C.R. Paul, Effect of grid spacing on the inductance of ground grids, IEEE Symposium on EMC, pages 72-77, 1991.

[Sperling, 1992] D. Sperling, M. Richter, Aktiv und Passiv gekoppelte Mehrfachleitungen, EMV '92, Karlsruhe, pages 799-812, 1992.

[Stutzman, 1981] W.L. Stutzman, Antenna theory for engineering applications, Wiley, New York, 1981.

* M. Terrien, Mathematical models used for the estimation of radiated electric field amplitudes from close field measurements, IEEE Symposium on EMC, pages 204-208, 1987

* V. Ungvichian, R. Perez, A refined mathematical model applied to a multilayer board, 8th International Symposium on EMC, pages 69-71, 1989.

* C. Val, High performance surface mounting VHSIC packages, 4th International microelectronics conference, Kobe, Japan, pages 98-107, 1986.

* E.F. Vance, Comparison of electro and magnetic coupling through braided-wire cables, Technical report no. AFWL-TR-73-71.

* E.F. Vance, Shielding effectiveness of braided-wire shields, IEEE transactions on EMC, vol. 17, no 2, 1975.

* E.F. Vance, Coupling to shielded cables, Wiley, New York, 1978.

[Walker, 1990] C. Walker, Capacitance, inductance and crosstalk analysis, Artech House, Norwood, 1990.

* W.L. Weeks, Electromagnetic theory for engineering applivcations, Wiley, New York, 1964.

[Wheeler, 1975] H.A. Wheeler, Fundamental limitations of small antennas, Proceedings IRE, vol. 35, pages 1479-1484, 1947.

* H.A. Wheeler, Small antennas, IEEE transactions on Antennas and Propagation, vol. ap 23, pages 462-469, 1975.

* C.B. White, A comparison of simplified methods for predicting radiated emissions, IEEE Symposium on EMC, pages 646-650, 1990.

* J. Wilhelm, Electromagnetisch Verträglichkeit, Expert Verlag, 1981.

* Whalen, Determining EMI in micro electronics; A review of the past decade, 6th International Symposium on EMC, pages 337-344, 1985.